

THE MEASUREMENT OF THE THERMODYNAMIC PARAMETERS OF THE HYDRATE
STRUCTURE AND THE APPLICATION OF THEM IN THE PREDICTION OF THE
PROPERTIES OF NATURAL GAS HYDRATES

BY

P. B. Dharmawardhana

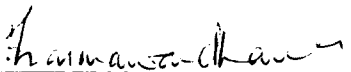
CLOSED RESERVE


ARTHUR LAKES LIBRARY
COLORADO SCHOOL of MINES
GOLDEN COLORADO 80401


A thesis submitted to the Faculty and the Board of Trustees of the Colorado School of Mines in partial fulfillment of the Degree of Doctor of Philosophy in Chemical and Petroleum Refining Engineering.

Golden, Colorado

Date: 5th Dec., 1980

Signed: 
P.B. Dharmawardhana

Approved: 
E.D. Sloan
Thesis Advisor


P.F. Dickson
Head of Department

Golden, Colorado

Date: Dec 4, 1980

T 2218

TO MY PARENTS

ACKNOWLEDGMENTS

The author wishes to express his sincere appreciation to the following persons who helped him during the course of his research:

Prof. E. D. Sloan Jr. and Dr. W. R. Parrish of Phillips Petroleum Co., Bartlesville, Oklahoma for their patience, guidance, encouragments, probing questions and stimulating discussions,

Professors R. E. D. Woolsey, A. J. Kidnay, R. D. Witters and V. F. Yesavage for their participation as the doctoral committee members and

my parents for their patience, guidance and encouragments.

Finally, the author gratefully acknowledges support from NSF grant No. ENG 76-18850.

ABSTRACT

The natural gas hydrates are quickly becoming a major energy resource in the world. Presently the van der Waals and Platteeuw model and the Parrish and Prausnitz model are in use in predicting the properties of natural gas. Parrish and Prausnitz utilized the volume difference, enthalpy difference and chemical potential difference between the empty hydrate and ice at 0° C and zero absolute pressure in their model. Out of the three parameters that were mentioned above only the volume difference between the empty hydrate lattice and ice has been previously measured with greater accuracy. This work experimentally determined the chemical potential difference and the enthalpy difference between the empty hydrate lattice and ice. These three fundamental parameters were used in optimizing the Kihara parameters σ and ϵ/k that described the enclathrated gas molecule and hydrate lattice molecule interactions. Finally the chemical potential difference, enthalpy difference and volume difference between the empty hydrate lattice and ice, and the Kihara parameters were used in predicting the properties of natural gas hydrates in two, three and four phase equilibria.

CONTENTS

CHAPTER 1	-	INTRODUCTION	1
CHAPTER 2	-	LITERATURE REVIEW	7
CHAPTER 3	-	STRUCTURE OF HYDRATE I AND II	11
CHAPTER 4	-	THE THERMODYNAMIC MODELS OF HYDRATES	15
CHAPTER 5	-	THE EXPERIMENTAL APPARATUS AND PROCEDURE	36
CHAPTER 6	-	RESULTS	52
CHAPTER 7	-	DATA ANALYSIS	55
CHAPTER 8	-	DATA REDUCTION AND CORRELATION	60
CHAPTER 9	-	DISCUSSION, CONCLUSION AND RECOMMENDATIONS	91
LITERATURE CITED			98
APPENDIX A	-	EXPERIMENTAL DATA FOR THE FILLING OF THE HYDRATE	103
APPENDIX B	-	THE LISTING OF THE SOURCES OF DATA THAT WERE USED IN HYDRATE CORRELATIONS	105
APPENDIX C	-	THE LISTING OF THE NUMERICAL VALUES FOR THE CONSTANTS "A" AND "B" IN EQUATION(8.22) FOR NATURAL GAS COMPONENTS	106
NOMENCLATURE			107
DOCUMENTATION OF THE COMPUTER PROGRAMS			110

LIST OF FIGURES

FIGURE 1	- Hydrate Lattice Of Structure I	12
FIGURE 2	- Hydrate Lattice Of Structure II	13
FIGURE 3	- Experimental Apparatus	38
FIGURE 4	- The Equilibrium Cell	39
FIGURE 5	- Schematic Drawing Of The Equilibrium Cell Windows	40
FIGURE 6	- Graph to Show The Effect Of Ultrasonic Agitation On The Experimentally Determined Values Of $\Delta\mu_{0,0}^{\beta-\alpha}$ Of Structure I Hydrate	48
FIGURE 7	- Graphical Representation Showing The Effect Of Ultrasonic Agitation On The Experimentally Determined Values Of $\Delta\mu_{0,0}^{\beta-\alpha}$ Of Structure II	49
FIGURE 8	- The Plot Of The Reciprocal Temperature Vs. $\ln P_{\frac{\beta}{W}}$ Of Structure I	66
FIGURE 9	- The Plot Of The Reciprocal Temperature Vs. $\ln P_{\frac{\beta}{W}}$ Of Structure II	67
FIGURE 10	- Comparison Of Experimental And Calculated Dissociation Pressures Of Vapor-Aq. Liquid- Hydrate Curves Of Methane-Ethane Mixed Hydrate Equilibria	79

LIST OF TABLES

TABLE 1	- Comparison Of Values For $\Delta\mu_{0,0}^{\beta-\alpha}$ and $\Delta h_{0,0}^{\beta-\alpha}$	4
TABLE 2	- Physical Properties Of Hydrate Lattice	14
TABLE 3	- Results Of The Sensitivity And Error Analysis	59
TABLE 4	- The Prediction Of The Water Content In Vapor Phase In Equilibrium With The Hydrate Phase	71
TABLE 5	- The Kihara Parameters Obtained Using The Peng And Robinson Equation Of State	75
TABLE 6	- The Kihara Parameters Obtained Using The Soave Redlich Kwong Equation Of State	76
TABLE 7	- The Prediction Of The Dissociation Pressure Of Hydrates Formed By Methane-Ethane Binary Mixtures In Vapor Aq. Liquid-Hydrate Equilibria	78
TABLE 8	- The Prediction Of The Dissociation Pressures Of Hydrates Formed By Carbon Dioxide-Methane Binary Mixtures In Vapor Aq. Liquid-Hydrate Equilibria	80
TABLE 9	- The Predicted Dissociation Pressures Of Hydrates Formed By Methane-Carbon Dioxide-Hydrogen Sulfide Ternary Mixtures In Vapor Aq. Liquid-Hydrate Equilibria	82

TABLE 10	-	The Prediction Of The Dissociation Conditions Of Hydrates Formed By Methane-Propane Binary Mixture In Vapor Aq. Liquid- Hydrocarbon Rich Liquid-Hydrate Equilibria	85
TABLE 11	-	The Prediction Of The Dissociation Conditions Of Hydrates Formed By Ethane-Propane Binary Mixture In Vapor Aq. Liquid-Hydrocarbon Rich Liquid-Hydrate Equilibria	86
TABLE 12	-	The Prediction Of The Dissociation Conditions Of Hydrates Formed By Methane-Ethane-Propane Ternary Mixtures In Vapor Aq. Liquid-Hydrocarbon Rich Liquid-Hydrate Equilibria	87
TABLE 13	-	The Prediction Of The Dissociation Conditions Of Hydrates Formed By Methane-Ethane-Propane Nitrogen-Carbon dioxide Mixture In Vapor-Aq. Liquid - Hydrate Equilibria	89
TABLE 14	-	Vapor-Hydrocarbon Rich Liquid Aq. Liquid-Hydrate Equilibria Of Natural Gas Mixtures	90

CHAPTER 1
INTRODUCTION

The modern world has entered into an era where economical and abundant supply of energy is of cardinal importance for healthy existence of industry. Natural gas was able to meet a substantial portion of the world's increasing energy demand for the past few decades. Ever increasing demand for energy due to steady growth of population, modernization and industrialization causes the investigations of the controlling factors in the production, transmission and utilization of natural gas. The main controlling factors are

- a. limited resources and
- b. production and transmission difficulties.

The exploration studies on natural gas have shown that there are vast amounts of natural gas reserves in the form of hydrates in the arctic area (1) and in deep sea formation (2). A recent study by U.S. Geological Survey has revealed that there is considerable amount of natural gas trapped under the seal of gas hydrates in continental slopes and rises off North and South Carolina. High pressure and low temperature insitu have transformed natural gas from the gas phase to the solid phase gas hydrates. Hence the existence of natural gas in substantial quantities has initiated extensive research to

explore various aspects of its existence and related topics.

The main research areas that are of chemical engineering importance are

- a. the determination of the conditions under which the hydrates could exist,
- b. prevention of the natural gas hydrate formation in the transmission lines and
- c. the recovery of natural gas from solid natural gas hydrates.

Hence an accurate method of predicting the thermodynamic properties of hydrates is necessary for preventing the hydrate formation in pipe lines, for determining the feasibility of producing the gas hydrate reserves and for understanding the conditions under which the gas hydrates exist.

Natural gas hydrates are non stoichiometric compounds which form in either of two structures. Each structure is composed of cavities of different sizes where the gas molecule is encaged. The structure that forms will depend on the the composition of the gas and the temperature of the system. The natural gas mixtures that contain propane and/or iso-butane normally form Structure II where as the mixtures that do not have these components normally form in Structure I; Holder (3) has indicated exceptions. Therefore, any accurate method for describing hydrate phase behavior must include

properties of both structures.

Currently, the gas industry uses the work of Parrish and Prausnitz (4) to predict the hydrate phase behavior. This method uses the statistical thermodynamic model of van der Waals and Platteeuw (5). This model requires properties of hydrate lattice along with the difference in chemical potential $\Delta\mu_{0,0}^{\beta-\alpha}$, enthalpy $\Delta h_{0,0}^{\beta-\alpha}$ and volume $\Delta v_{0,0}^{\beta-\alpha}$ between the empty hydrate lattice and coexisting phase, water or ice, at the ice point. These three parameters $\Delta\mu_{0,0}^{\beta-\alpha}$, $\Delta h_{0,0}^{\beta-\alpha}$ and $\Delta v_{0,0}^{\beta-\alpha}$ at 0°C and zero absolute pressure are common parameters for all hydrates in a given hydrate structure and may be considered as standard bases for prediction of the hydrate formation conditions. The necessary geometric properties and volume difference for both structures were measured by von Stackelberg and Müller (6) using X-ray crystallography. This work presents new values for $\Delta\mu_{0,0}^{\beta-\alpha}$ and $\Delta h_{0,0}^{\beta-\alpha}$ for both Structures I and II based upon cyclopropane hydrate.

The empty hydrate lattice does not exist in nature but attains stability by encagement of gas molecules in the cavities. Therefore, the empty hydrate lattice properties must be determined indirectly by obtaining the filled hydrate composition or by numerical estimation. Table 1 lists the various

TABLE 1. COMPARISON OF VALUE FOR $\Delta\mu_{0,0}^{\beta-\alpha}$ AND $\Delta h_{0,0}^{\beta-\alpha}$

<u>Investigator</u>	<u>Basis</u>	$\Delta\mu_{0,0}^{\beta-\alpha}$ cal./gm. mole		$\Delta h_{0,0}^{\beta-\alpha}$ cal./gm. mole	
		St. I	St. II	St. I	St. II
van der Waals and Platteeuw (1959)	Expt.	167	200	0	0
Barrer and Ruzicka (1962)	Expt.	-	88/128	-	-
Sortland and Robinson (1964)	Expt.	-	211	-	-
Child (1964)	Estimate	300	190	-	190
Parrish and Prausnitz (1972)	"	302		275	193
Holder (1976)	"	276	-	91	0
Holder & Corbin (1979)	"	305/309	-	225/529	-

reported values for $\Delta\mu_{0,0}^{\beta-\alpha}$ and $\Delta h_{0,0}^{\beta-\alpha}$. The value of $\Delta\mu_{0,0}^{\beta-\alpha}$ that was used by van der Waals and Platteeuw (5) was based on bromine hydrate which was later shown by Allen and Jeffrey (7) to form neither Structure I nor II. Sortland and Robinson estimated $\Delta\mu_{0,0}^{\beta-\alpha}$ for hydrate II by differentiating the P-T dissociation data of sulfur hexafluoride hydrate to obtain the heat of formation and then the hydrate composition. The values of $\Delta\mu_{0,0}^{\beta-\alpha}$ reported by Barrer and Ruzica (9) are approximately one half the other values reported in the literature. This is probably due to the occlusion of mother liquor in the hydrate and/or meta stability of the hydrate. Childs (10) estimated $\Delta\mu_{0,0}^{\beta-\alpha}$ and $\Delta h_{0,0}^{\beta-\alpha}$ for both hydrate structures by comparing entropies of formation of hydrates with those of other clathrates. Parrish and Prausnitz (4), Holder (3), and Holder and Corbin (11) numerically optimized for the two structures to obtain better fits of the statistical mechanical model to existing hydrate data. The values for $\Delta\mu_{0,0}^{\beta-\alpha}$ and $\Delta v_{0,0}^{\beta-\alpha}$ indicate the problem of occlusion of mother liquor and accurate measurement of the gas-to-water ratio. One objective of this work was to obtain experimental values for $\Delta\mu_{0,0}^{\beta-\alpha}$ and better estimates for $\Delta h_{0,0}^{\beta-\alpha}$.

A knowledge of the water content of natural gas in equilibrium with the hydrate phase is of great importance to natural gas industry to prevent the hydrate formation during

gas transportation. Sloan et. al.(12) and Ayoyagi et.al. (13) have shown that the water content of natural gas at the incipient hydrate formation conditions at hydrate/gas two phase region is much lower than that obtained by extrapolating the data given in the Gas Processors Association Engineering Data Book (14). Sloan et. al. (12) have adopted a new method to calculate the water content in the gas phase in equilibrium with the hydrate phase. This method utilized the vapor pressure data of the empty hydrate of Structures I and II. This work presents the empty hydrate vapor pressures of both Structures I and II which enable the calculation of water content in the vapor phase that is in equilibrium with the hydrate. In addition this work also introduces a new method to determine the water content in the vapor phase that is in equilibrium with the hydrate phase.

CHAPTER 2

LITERATURE REVIEW

The knowledge of the structure of water and ice at the molecular level is of fundamental importance in understanding the structure of hydrates because the basic building block, the water molecule, is common to all of them.

Extensive studies on the structure of ice (15,16,17,18, 19) and liquid water (20,21,22,23,24) were available in the literature during the time when there was active research in the determination of the hydrate structure. The structure of ice that was proposed by Pauling (24) gained much acceptance due to the agreement with neutron diffraction studies and residual entropy calculations. Pauling's conclusions could be listed as follows;

- a. In ice each oxygen atom is bonded to two hydrogen atoms forming an O-H covalent bond of 0.95 \AA with a H-O-H bond angle of 105° similar to that of the gaseous water molecule.
- b. Each water molecule in the ice lattice is oriented in such a manner that its two hydrogen atoms are directed towards two of the four oxygen atoms that surround it tetrahedrally forming hydrogen bonds.

- c. The water molecules are oriented in such a manner that only one hydrogen atom lies approximately on the O-O axis.
- d. The ice crystal can exist in one of many configurations of the water molecules (24).

Ice that has been cooled to absolute zero temperature shows non zero entropy, i.e. it shows a residual entropy, which indicates that the ice lacks regularity at the freezing point. Even with its irregular arrangement the oxygen loci are fairly well defined. The neutron defraction studies (25) are in agreement with Pauling's partial ordering of the water molecules in the ice lattice.

One would expect a higher heat of fusion of ice at its melting point due to the increase of the randomness of the water molecules. But, the fact that the heat of fusion of ice is small compared to its heat of sublimation indicates that there is no complete rupture of the oxygen-hydrogen bonds between adjacent molecules. In other words the tetrahedral structure of the ice lattice breaks down progressively with the increase in the temperature until the water molecules enter the gaseous phase. Thus the water molecules in the liquid state exhibit a dynamic equilibrium between partially disrupted tetrahedral structures. At any moment depending on the temperature, a water molecule in the liquid medium is

bonded to less than four neighbouring water molecules, having other neighbours at a continuous variety of distance. The hydrogen bonds thus mentioned are weak and last only fraction of a second. Morgan and Warren (24) describe this phenomenon as "broken down ice structure". In a similar manner liquid water in the vicinity of the structure which might be stabilized by the intrusion of other molecules of the right size and shape gets converted to hydrates by enclathrating the hydrate-forming molecules.

The knowledge of the structure of the liquid water and ice, and X-ray diffraction data of von Stackelberg and Müller helped Claussen (26) to elucidate the structure of hydrates based on following hypothesis;

- a. The crystal lattice of the hydrate is formed by the water molecules with the hydrate-forming molecules occupying the void spaces within the lattice.
- b. The resulting water framework should be ice like because of the high heats of formation of the hydrates (27).
- c. No free hydroxyl groups are present.

By trial and error it was found that the pentagonal dodecahedra lattice provided a plausible closed structure for "hydrate building block". The tetrahedral angle between the oxygen molecules was modified from 109.5° to 108.0° ,

introducing a slight, but probably not excessive strain between molecules. The packing of the pentagonal dodecahedron into three dimensional arrays produced,

- a. the body centered pentagonal dodecahedron (26,28,29,30) commonly called Structure I and
- b. the diamond pentagonal dodecahedron (26,28), commonly called Structure II.

CHAPTER 3

STRUCTURE OF HYDRATE I AND II

Each unit cell of Structures I and II was formed by forty six and one hundred and thirty six molecules of water respectively. The water molecules that form the host lattice of the hydrate structures were arranged in such a manner to form two small and six large cavities or cages per unit cell for Structure I and sixteen small and eight large cavities or cages per unit cell for Structure II. The arrangement of the water molecules that form the small and large cavities of Structures I and II is illustrated in Figures 1 and 2. Each water molecule in the hydrate lattice is bonded to four neighbouring water molecules in the lattice by hydrogen bonds. In other words there are four hydrogen bonds that extend from each water molecule in the hydrate lattice. These hydrogen bonds form the edge of the polyhedron.

The geometric properties of the Structures I and II are given in Table 2.

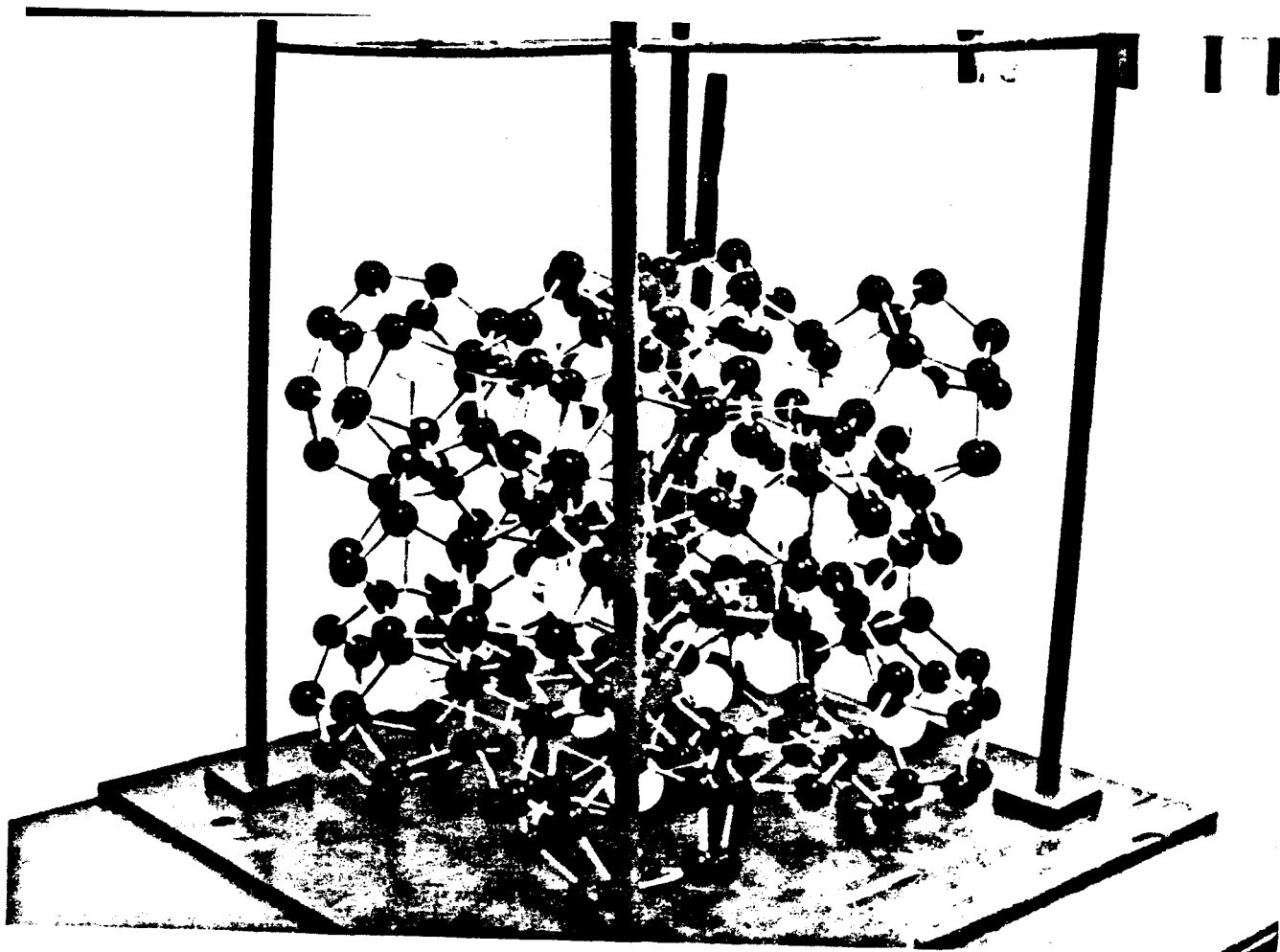


Figure 1 Hydrate Lattice of Structure 1

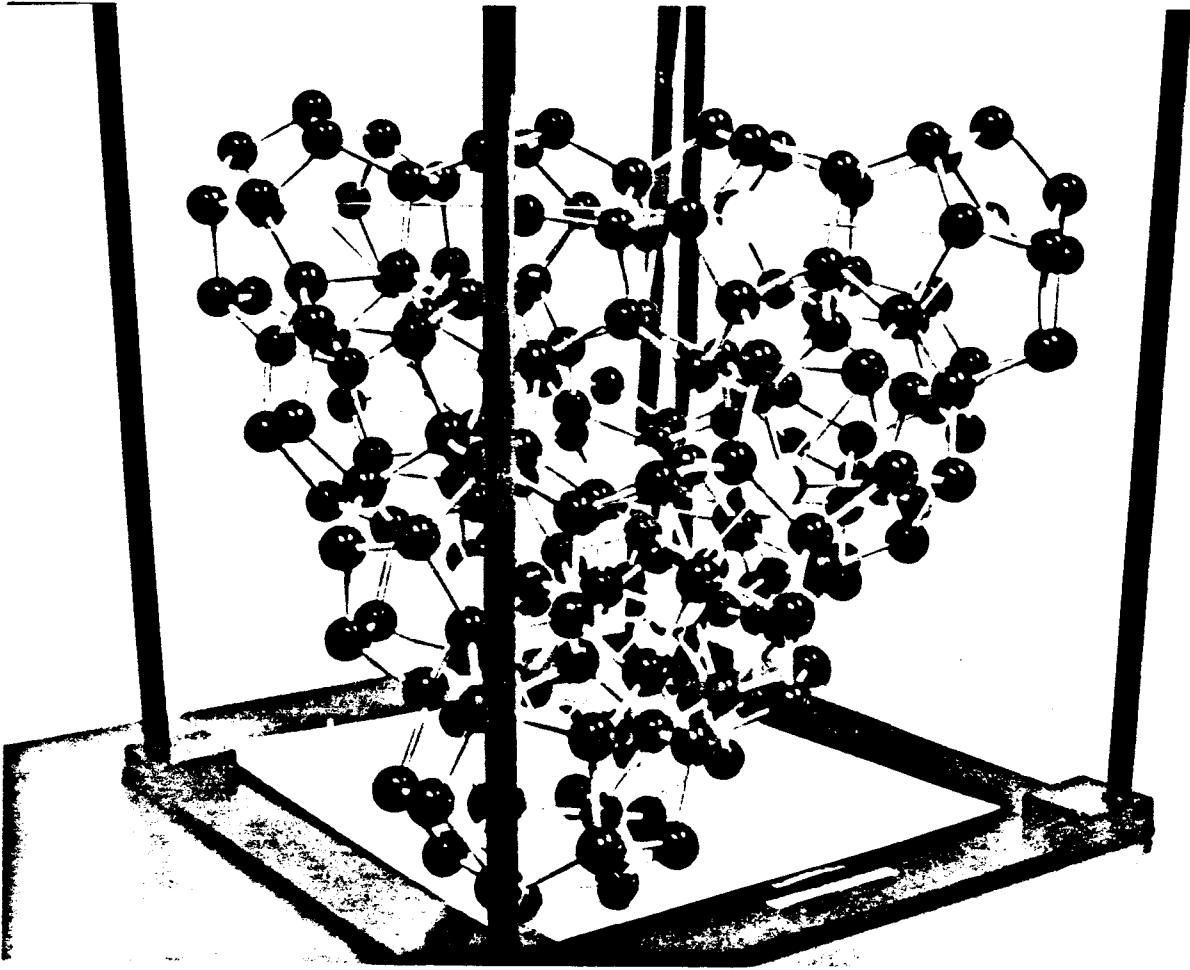


Figure 2 Hydrate Lattice of Structure II

TABLE 2. PHYSICAL PROPERTIES OF THE HYDRATE LATTICE

	Structure I		Structure II	
	Small	Large	Small	Large
No. of water molecules per unit cell	46		136	
No. of cavities per unit cell	2	6	16	8
Cell diameter Å	7.95	8.60	7.82	9.46
Coordination no.	20	24	20	28

CHAPTER 4THE THERMODYNAMIC MODELS OF HYDRATES

The discovery of the cause of the "freezing of the line" in the natural gas industry by Hammerschmidt (33) initiated an extensive investigation into the properties and behavior of the natural gas hydrates by the Bureau of Mines from 1935 to 1941 under the guidance of Deaton and Frost (16).

In 1941 Wilcox, Carson and Katz (31) showed that the hydrate-forming conditions could be predicted using vapor-solid equilibrium constant analogous to that of vapor liquid equilibria.

$$\begin{array}{l}
 \text{Equilibrium} \\
 \text{constant between} \\
 \text{vapor \& solid} \\
 K_{v-s}
 \end{array}
 = \frac{\text{mole fraction of hydrocarbon in the} \\
 \text{vapor phase}}{\text{mole fraction of hydrocarbon in the} \\
 \text{hydrate phase}} \quad (4.1)$$

Wilcox et. al. (32) also correlated the dissociation pressure of series of natural gas mixtures with the gas gravity. This model was an excellent start and illustrates the tremendous intuition characteristic of Professor Katz when he had no access to the molecular structure of hydrates. One drawback

in the treatment of Wilcox et. al. was that all the constants that they published, such as K_{v-s} and the constants in the hydrate dissociation pressure-gas gravity correlations, are functions of temperature and pressure but independent of the gas composition. Also the correlation gives no idea of the structure being formed, primarily because it is a macroscopic method without foundation on a molecular basis. With the determination of the microscopic structure for hydrates the next logical development was to formulate a method to predict the properties of hydrates with a molecular foundation.

The statistical mechanical model of van der Waals and Platteeuw (5) relates the equilibrium pressure and temperature to the chemical potential difference between the empty and filled hydrate lattice. The basic assumptions in the model are as follows;

- a. The host molecule contribution to the free energy of the lattice is independent of the mode of occupancy of the cavities by the solute molecules. In other words, the model assumes either the host lattice distortion or interference by the solute molecules to be zero.
- b. Multiple occupancy of the cages is impossible.
- c. There is no interaction between the encaged solute molecules.

d. Classical statistics are valid under all conditions.

McKoy and Sinanoglu (34) have shown that small molecules like argon are not further than 1 \AA from the centre of the cavity so that the end of the guest molecule is never closer than 2.5 to 3 \AA from the wall of the cavity. This situation does not exist for large molecules like isobutane and n-butane. Hence the solute molecules do not push the host lattice permanently from its equilibrium position. Hence the assumption "a" is excellent for the smaller molecules.

The second assumption is justified by analytical methods. As far as the third assumption is concerned, numerical calculations have shown that the contribution of the solute-solute interaction to the configurational energy is at most few percent of the binding energy of the solute molecules in the cage. This could be related to the distance between the centers of the cages which is considerably large. According to Davidson (35) the third assumption is a reasonable approximation for the clathrate hydrates, but strong polarity of the guest molecules and larger molecular size of the guest molecules may be expected to affect the validity of both assumptions "a" and "c".

The thermodynamic model that was proposed by van der Waals and Platteeuw (5) was based on the regular crystal

structure of hydrates. The enclathration of the guest molecule by water molecules could be compared to a case of a sphere being kept in a three dimensional box. Since there are two types of cavities per unit cell the probability of occupancy could be obtained through classical statistics. Further more van der Waals and Platteeuw (5) noticed the analogy between the enclathration of the guest molecule and three dimensional adsorption.

The essential features in the development of van der Waals and Platteeuw's model is that the property of the hydrates were obtained through the grand partition function. The grand partition function with respect to the solvent was obtained through ordinary partition function with respect to the solvent. The ordinary partition function was derived by classical statistics by identifying the similarity of the probability of occupancy of N_i balls in N_i boxes, where the geometry of the cavities were known and the particles were assumed to be spherical. The grand partition function with respect to the solvent that was derived by van der Waals and Platteeuw is given below.

$$\Xi = \exp\left[-\frac{F}{kT}\right] \sum_{N_{ji}} \pi_i \left\{ \frac{(v_i N_Q)!}{(v_i N_Q - \sum_j N_{ji})! \pi_j N_{ji}!} \pi_j^{N_{ji}} \lambda_j^{N_{ji}} \right\} \quad (4.2)$$

where Ξ = grand partition function
 v = no. of cavities per mole of water in a unit cell
 N = no. of molecules
 F = free energy of the empty lattice and
 h = molecular partition function.

Subscripts

J, K = molecular identification
 i = type of cavities
 Q = molecules in the clathrate host lattice

Equation (4.2) is similar to the partition function that describes the ideal localized adsorption of N_{Mi} molecules on N_i sites, which is given by Hill(36) as

$$\Xi = \sum_{N_{Mi}} \frac{N_i^{N_{Mi}}}{(N_i - N_{Mi})! N_{Mi}!} (b_{Mi} \lambda_M)^{N_{Mi}} \quad (4.3)$$

where λ is the absolute activity. Equation (4.2) could be simplified using the multinomial theorem as follows;

$$\Xi = \exp[-F/(kT)] \pi_i \left(1 + \sum_J h_{Ji} \lambda_J\right)^{v_i N_Q} \quad (4.4)$$

The grand partition function gives the means by which one can relate the microscopic properties to macroscopic thermodynamic properties.

One could relate Ξ to the chemical potential difference as follows;

$$kT d \ln \Xi = (u/T) dT + Pdv + \sum_K kTN_K \frac{d\lambda_K}{\lambda_K} - \mu_Q dN_Q \quad (4.5)$$

Hence at constant T, v, N, λ_J

$$\lambda_K \left(\frac{\partial \ln \Xi}{\partial \lambda_K} \right) = \sum_K N_{Ki} = N_K \quad (4.6)$$

$$= \sum_i v_i N_Q \frac{h_{Ki} \lambda_K}{(1 + \sum_J h_{Ji} \lambda_J)} \quad (4.7)$$

$$N_{Ki} = v_i N_Q \frac{h_{Ki} \lambda_K}{(1 + \sum_J h_{Ji} \lambda_J)} \quad (4.8)$$

Since y_{Ki} is the probability of finding a molecule in a cavity type i ,

$$y_{Ki} = \frac{h_{Ki} \lambda_K}{(1 + \sum_J h_{Ji} \lambda_J)} \quad (4.9)$$

also,

$$y_{Ki} = \frac{N_{Ki}}{(v_i N_Q)} \quad (4.10)$$

The chemical potential of water in the hydrate phase is given as

$$\mu_W^H = -RT \left(\frac{\partial \ln \epsilon / \partial N_Q}{T, v, \lambda_J} \right) \quad (4.11)$$

$$= \mu_W^\beta - RT \sum_i v_i \ln \left(1 + \sum_J h_{Ji} \lambda_J \right) \quad (4.12)$$

The equation (4.12) could be further simplified as

$$\mu_W^H = \mu_W^\beta + RT \sum_i v_i \ln \left(1 - \sum_K y_{Ki} \right) \quad (4.13)$$

The equation (4.13) could be compared with a most familiar equation of classical thermodynamics, such as

$$\mu_i = \mu_i^0 + RT \ln a_i \quad (4.14)$$

where,

μ_i = chemical potential of the mixture, and

μ_i^0 = chemical potential of the pure components.

Hence $RT \ln a_i$ is the contribution due to the interaction between solvent and solute molecules. μ_W^β in the equation (4.13) could be compared with μ_i^0 in the equation (4.14), and $\ln a_i$, the contribution due to the solute-solvent interaction, could be compared with $\sum_i v_i \ln \left(1 - \sum_K y_{Ki} \right)$ which is the contribution due to the occupancy of the cavities formed by the host molecules.

The probability of finding a molecule type K in a cavity type i, y_{iK} , is the same as the fraction of type i cavities occupied by the gas component K, hence

$$y_{iK} = \frac{C_{Ki} f_K}{1 + \sum_K C_{Ki} f_K} \quad (4.15)$$

where f_K is the fugacity of the component type K and C_{Ki} is the Langmuir constant of the component K in type i cavities. The Langmuir constant accounts for the gas-water interaction in the cavities. Using Lennard-Jones-Devonshire cell theory van der Waals and Platteeuw showed that the Langmuir constant may be determined by

$$C_{Ki} = \frac{4 \pi}{k T} \int_0^{\infty} \exp[-\omega(r)/(kT)] r^2 dr \quad (4.16)$$

where

T = absolute temperature and

k = Boltzmann's constant and

$\omega(r)$ = spherically symmetrical cell potential function.

$\omega(r)$ is a function of the cell radius, the coordination number, Z, and the nature of the gas-water interaction.

The predicted values of equilibrium properties of pure hydrates by van der Waals and Platteeuw showed large deviation from the experimental data, primarily due to two reasons;

a. The numerical values used in the calculations were obtained from bromine hydrate which was later shown (7) to form neither Structure I nor Structure II.

b. The Lennard-Jones parameters for water that were used in the calculations were estimated based on argon hydrate.

Both the reasons "a" and "b" are interrelated. In other words $\Delta\mu_{T,P}^{\beta-\alpha}$ for argon hydrate was obtained on the basis of bromine hydrate.

Nagata and Kobayashi (37) used the same type of approach as van der Waals and Platteeuw but instead of using estimated Lennard-Jones parameters for water-host molecule, and mixing rules, Lennard Jones parameters which describe the interaction between host and guest molecule, $(\epsilon/k)_{AB}$ and δ_{AB} , were fitted directly to the V-L-H equilibrium data.

McKoy and Sinanoglu (34) used the Kihara potential function with a spherical core in calculating the Langmuir constant and obtained better predictions for pure gas hydrates as compared to that by Nagata and Kobayashi.

McKoy and Sinanoglu's model assumed the core diameter of the lattice molecule to be zero and utilized estimated values of ϵ/k and δ for water. The estimated values of ϵ/k and δ for the lattice molecules are then used in the calculations on the gas hydrates along with the combination rules for parameters, such as;

the hard sphere $\delta_{AB} = (\delta_A + \delta_B)/2$ and
 geometric mean $\epsilon_{AB} = \sqrt{(\epsilon_A \epsilon_B)}$ approximations.

The present work follows basically Parrish and Prausnitz's approach that showed an improvement over McKoy and Sinnanoglu, i.e. $(\epsilon/k)_{AB}$ and δ_{AB} that describe the host and guest molecule interactions were directly calculated from the equilibrium data along the ice-vapor-hydrate and liquid water-vapor-hydrate equilibrium lines. Parrish and Prausnitz used the Kihara potential which are slightly more accurate than the Lennard-Jones potential used by Nagata and Kobayashi.

In analyzing the equations (4.13) and (4.15) which could be rewritten in the combined form as

$$\Delta \mu_{T,P}^{\beta-\alpha} = RT \sum_i v_i \ln(1 + \sum_K C_{iK} f_K) \quad (4.17)$$

where

$$\Delta \mu_{T,P}^{\beta-\alpha} = \mu_W^\beta - \mu_W^\alpha$$

It is evident that there are two unknowns $\Delta \mu_{T,P}^{\beta-\alpha}$ and f_K assuming C_{iK} , the Langmuir constant is known.

The effect of temperature and pressure on the chemical potential difference could be calculated by using the total differential

$$d \Delta \mu = \left(\frac{\partial \Delta \mu}{\partial T} \right)_P dT + \left(\frac{\partial \Delta \mu}{\partial P} \right)_T dP. \quad (4.18)$$

This could be further simplified as,

$$d \Delta \mu = -\Delta H/T dT + \Delta v dP \quad (4.19)$$

Dividing both sides by RT

$$d(\Delta \mu/RT) = -\left(\frac{\Delta H/RT^2} \right)_P dT + \left(\frac{\Delta v/RT} \right)_T dP \quad (4.20)$$

where ΔH and Δv are the molar enthalpy and molar volume difference between hydrate and the coexisting phase ice or water as the case may be.

If ice coexists with the hydrate

$$\Delta H = \Delta h_{0,0}^{\beta-\alpha} \quad (4.21)$$

$$\Delta v = \Delta v_{0,0}^{\beta-\alpha} \quad (4.22)$$

$$\mu_{T,P}^H = \mu_{T,P}^{\beta} \quad (4.23)$$

$$\text{and } \mu_{T,P}^{\beta-\alpha} = \mu_{T,P}^{\beta} - \mu_{T,P}^{\alpha} \quad (4.24)$$

where $\Delta h_{0,0}^{\beta-\alpha}$ and $\Delta v_{0,0}^{\beta-\alpha}$ are the molar enthalpy and molar volume difference between empty hydrate and ice. $\mu_{T,P}^H$, $\mu_{T,P}^\beta$ and $\mu_{T,P}^\alpha$ are the chemical potential of hydrate (filled), empty hydrate and ice at a specific temperature T and pressure P.

If liquid water is in equilibrium with the hydrate,

$$\Delta H = \Delta h_{0,0}^{\beta-\alpha} + \Delta h_W^f \quad (4.25)$$

$$\Delta V = \Delta v_{0,0}^{\beta-\alpha} + \Delta v_W^f \quad (4.26)$$

$$\mu_{T,P}^H = \mu_{T,P}^L \quad (4.27)$$

$$\Delta \mu_{T,P}^{\beta-L} = \mu_{T,P}^\beta - \mu_{T,P}^L \quad (4.28)$$

where Δh_W^f and Δv_W^f are the difference of molar enthalpy and molar volume between ice and liquid water. $\mu_{T,P}^L$ is the chemical potential of water at a temperature T and pressure P.

With $\Delta \mu_{0,0}^{\beta-\alpha}$ known, $\Delta \mu_{T,P}^{\beta-\alpha}$ at 0°C and at equilibrium pressure, which is denoted by $\Delta \mu_{0,P}^{\beta-\alpha}$, could be obtained by integrating the equation (4.20) between the limits of equilibrium pressure at 0°C and zero absolute pressure, keeping the temperature constant.

If ice is in equilibrium with the hydrate

$$\Delta\mu_{0,P}^{\beta-\alpha} = \Delta\mu_{0,0}^{\beta-\alpha} + \Delta v_{0,0}^{\beta-\alpha} P \quad (4.29)$$

and if liquid water is in equilibrium

$$\Delta\mu_{0,P}^{\beta-\alpha} = \left(\Delta v_{0,0}^{\beta-\alpha} + \Delta v_{W}^f \right) P + \Delta\mu_{0,0}^{\beta-L} \quad (4.30)$$

The next step is to integrate equation (4.20) along the three phase line between the limits T and 0°C. The upper and lower limits of the last integral correspond to the equilibrium pressures at temperatures T and 0°C

$$\int_{0^{\circ}\text{C}}^T d\Delta\mu = \int_{0^{\circ}\text{C}}^T (-\Delta H/T) dT + \int_{P \text{ at } 0^{\circ}\text{C}}^{P \text{ at temp. } T} \Delta v dP \quad (4.31)$$

By taking into consideration that the integration is carried out along the three phase equilibrium line which is univariant, equation (4.31) could be rewritten as

$$\int_{0^{\circ}\text{C}}^T d(\Delta\mu/RT) = \int_{0^{\circ}\text{C}}^T (-\Delta H/RT) dT + \int_{0^{\circ}\text{C}}^T (\Delta v/RT)(dP/dT)dT \quad (4.32)$$

It should be noted that one needs equilibrium data from zero degrees centigrade to the temperature of interest in solving equation (4.32). This difficulty was overcome by

Nagata and Kobayashi (37) by introducing a reference hydrate in the classical thermodynamic model. The reference hydrate is the one whose phase equilibrium loci are known throughout the temperature range.

Nagata and Kobayashi calculated the chemical potential difference of argon hydrate using methane hydrate as the reference. This concept of reference hydrate was further extended to both hydrate Structures I and II by Parrish and Prausnitz by selecting reference hydrates whose three-phase equilibrium data are accurately known. The introduction of the reference hydrate made it easier for one to calculate the chemical potential difference of a given hydrate along its three phase line without knowing the three-phase line through a wide temperature range.

With the introduction of the reference hydrate equations (4.29) and (4.30) become

$$\Delta\mu_{0,Pr}^{\beta-\alpha} = \Delta v_{0,0}^{\beta-\alpha} Pr + \Delta\mu_{0,0}^{\beta-\alpha} \quad (4.33)$$

and

$$\Delta\mu_{0,Pr}^{\beta-L} = \left(\Delta v_{0,0}^{\beta-\alpha} + \Delta v_W^f \right) Pr + \Delta\mu_{0,0}^{\beta-\alpha} \quad (4.34)$$

respectively. Equation (4.32) could be further simplified

for the reference hydrate, if ice and hydrate coexist:

$$\Delta\mu_{T,Pr}^{\beta-\alpha}/RT = \Delta\mu_{0,Pr}^{\beta-\alpha}/(273.15 R) - \int_{0^{\circ}C}^T \frac{\Delta h_{0,0}^{\beta-\alpha}}{(RT)^2} dT + \int_{0^{\circ}C}^T \Delta v_{0,0}^{\beta-\alpha} (dP/dT)_r dT \quad (4.35)$$

where P_r is the equilibrium pressure of the reference hydrate at the ice point. The subscript $(0,Pr)$ refers to the temperature and pressure of the reference hydrate. (note. 0 means $0^{\circ}C$)

If liquid water and hydrate coexist:

$$\Delta\mu_{T,Pr}^{\beta-L}/RT = \Delta\mu_{0,Pr}^{\beta-L}/(273.15 R) - \int_{0^{\circ}C}^T \frac{(\Delta h_{0,0}^{\beta-\alpha} + \Delta h_W^f)}{(RT)^2} dT + \int_{0^{\circ}C}^T (\Delta v_{0,0}^{\beta-\alpha} + \Delta v_W^f) (dP/dT)_r dT \quad (4.36)$$

The last step in this transformation is to translate the $\Delta\mu_{T,Pr}^{\beta-\alpha}$ or $\Delta\mu_{T,Pr}^{\beta-L}$ to $\Delta\mu_{T,p}^{\beta-H}$ by taking into consideration the difference in pressure between the reference hydrate dissociation pressure and the dissociation pressure of the hydrate of interest at the temperature of interest. This could be done by integrating equation (4.19) within limits of hydrate equilibrium pressure and the reference hydrate pressure at a constant temperature T .

When ice is in equilibrium,

$$\Delta \mu_{T,P}^{\beta-\alpha} = \mu_{T,Pr}^{\beta-\alpha} + \Delta v_{0,0}^{\beta-\alpha} (P-Pr) \quad (4.37)$$

and when liquid water is in equilibrium,

$$\Delta \mu_{T,P}^{\beta-\alpha} = \mu_{T,Pr}^{\beta-L} + \left(\Delta v_{0,0}^{\beta-\alpha} + \Delta v_W^f \right) (P-Pr) \quad (4.38)$$

Parrish and Prausnitz have expressed the reference hydrate pressure as a function of temperature as follows;

$$\ln Pr = Ar + Br/T + Cr \ln T \quad (4.39)$$

The same reference hydrates that were used by Parrish and Prausnitz (4) were used in the present work, where Ar, Br and Cr are constants.

Ng and Robinson used the same model of Parrish and Prausnitz in predicting the hydrate dissociation pressure, but modified van der Waals and Platteeuw's model by adding an empirical function without any theoretical foundation. Ng and Robinson's (38) modification is given below.

$$\Delta \mu_{T,P}^{\beta-\alpha} = \left(\pi_J \left[1 + 3(\alpha_J - 1)y_J^2 - 2(\alpha_J - 1)y_J^3 \right] \right) \left\{ \left[\sum_i v_i \right] \ln \left(1 + \sum_J C_{iJ} f_J \right) \right\} \quad (4.40)$$

Where α_j is the interaction parameter between the least and each of the other more volatile hydrate-forming molecules of type J and Y_j is the mole fraction of component J. The other difference is that Ng and Robinson used Peng and Robinson equation of state in evaluating the fugacities of different components. Hence the improved dissociation predictions are mainly due to both the Peng and Robinson equation of state and the empirical function of Y_j and α_j that was added to the van der Waals and Platteeuw's model. It should be noted that Parrish and Prausnitz used a less accurate equation of state (but the best available at that time) to obtain the fugacity.

Four-Phase Equilibria.

Parrish and Prausnitz's model (4) was designed for three-phase equilibria such as vapor-aqueous liquid-hydrate and vapor-ice-hydrate. Ng and Robinson introduced a computational method and extended Parrish and Prausnitz's model to four phase equilibria. The three and four-phase lines represent univariant and invariant lines respectively. Ng and Robinson's method of evaluating four phase loci could be explained as follows.

The bubble point pressure of liquid hydrocarbon mixture of known composition was evaluated at an assumed temperature. The pressure and individual component fugacities were checked for the hydrate dissociation pressure using Parrish and Prausnitz's model. The procedure was repeated until the bubble point temperature and pressure became equal to the hydrate dissociation temperature and pressure.

Two-Phase Equilibria

Sloan et. al. (12) extended the van der Waals and Platteeuw model for two-phase region, vapor-hydrate with the introduction of empty hydrate vapor pressure P_W^β .

The empty hydrate structure does not exist in nature. Hence the empty hydrate vapor pressure has no physical reality. But the empty hydrate vapor pressure is very useful from a thermodynamic stand point because it links the fugacity of water in the hydrate lattice to the fugacity of water in any other coexisting phases that are in equilibrium with the hydrates. The van der Waals and Platteeuw model could be rewritten as follows;

$$\mu_{T,P}^\beta - \mu_{T,P}^H = RT \sum_i v_i \ln \left(1 + \sum_J C_{iJ} f_J \right) \quad (4.41)$$

One could define the activity of water in the filled hydrate lattice a_W^H in an analogous manner to equation (4.41) using the empty hydrate lattice as the reference.

$$\mu_{T,P}^H - \mu_{T,P}^\beta = RT \sum_i v_i \ln a_W^H \quad (4.42)$$

The fugacity of water in the filled hydrate lattice is related to the chemical potential between filled and empty hydrate as follows.

$$\mu_{T,P}^H - \mu_{T,P}^\beta = RT \ln (f_W^H / f_W^\beta) \quad (4.43)$$

where f_W^H and f_W^β are the fugacities of water in the filled and empty hydrate lattice respectively. The fugacity of water in the empty hydrate lattice could be expressed as follows;

$$f_W^\beta = P_W^\beta \phi_W^\beta \exp \int_{P_W^\beta}^P (v_W^\beta / RT) dP \quad (4.44)$$

If hydrate and vapor coexist, at equilibrium the fugacity of water in the filled hydrate lattice is equal to the fugacity of water in the vapor phase. Therefore,

$$f_W^H = P_W^\beta \phi_W^\beta \exp \left[-\mu_{T,P}^\beta / RT + \int_{P_W^\beta}^P (v_W^\beta / RT) dP \right] \quad (4.45)$$

where v_W^β is the molar volume of empty hydrate lattice.

Since the empty hydrate vapor pressure is quite low as shown in the later calculations, the fugacity coefficient of the empty hydrate vapor pressure ϕ_W^B is considered to be unity.

Sloan et. al. used the Virial Equation of State in calculating the fugacity of water in the vapor phase in equilibrium with the hydrate phase. Next, Sloan et. al (12) used equation (4.45) in optimizing the virial coefficients and the empty hydrate vapor pressure. Since the second pure and cross virials were known, optimization was carried out on the third virial coefficients and P_W^B .

Ng and Robinson (38) followed a similar approach as Sloan et. al. but used the Peng and Robinson equation of state to evaluate the fugacity of water from the experimental data. By this procedure Ng and Robinson were able to optimize only the empty hydrate vapor pressure without the involvement of the virial coefficients.

Ng and Robinson expressed the vapor fugacity of empty hydrate Structures I and II as follows:

$$\ln f_W^B = C_1 - C_2/T + (C_3T - C_4)P \quad (4.46)$$

where C_1 , C_2 , C_3 and C_4 are constants that were calculated using the water content in the vapor phase in equilibrium with hydrates in two-phase region. In the present work f_W^B was calculated using the Poynting correction and P_W^B (see Equation 4.44).

It is worthwhile to mention that the data that were used by Ng and Robinson in optimizing the empty hydrate fugacity of the Structure II were obtained by Kobayashi and coworkers who are currently re-evaluating the data. It should be noted that the method of Sloan et. al. cannot be extended for the determination of the water content in equilibrium with hydrates in multi-component mixtures due to lack of third virial coefficients.

CHAPTER 5

THE EXPERIMENTAL APPARATUS AND PROCEDURE

General Description

The amount of hydrate that was formed was determined by carrying out a mass balance on the hydrate. In this work the amount of water that was converted to hydrates was determined by the variation of the electrical conductivity of a weak potassium chloride solution. .01N potassium chloride solution was used in the experiment as the hydrating medium, and its initial and final electrical conductivity were measured with the help of an accurate Wheatstone Bridge. Since potassium chloride does not enter into the hydrate structure, the difference between the initial and final specific conductivity of the medium gives the amount of water that was converted to hydrates. The amount of gas that was enclathrated was calculated from the initial and final pressure of the system.

Cyclopropane was used as the hydrate-forming gas due to the fact that it forms both Structures I and II under different conditions of temperature and pressure. In performing this experiment the main experimental difficulty one has to overcome is to prevent the occlusion of the mother liquor within

the hydrate mass. In the present work this difficulty was overcome by the use of an ultrasonic agitation device that breaks the hydrate mass and prevents the trapping of the mother liquor (occlusion of the mother liquor) between the growing hydrate mass.

Experimental Apparatus

The schematic diagram of the experimental system is shown in Figure 3. The description of the individual components are presented under the following subsections.

- a. The equilibrium cell.
- b. The pressure measuring system.
- c. The temperature measuring system and the associated control system.
- d. System for the measurement of the electrical conductivity.
- e. The agitation and vacuum systems.
- f. The gas charging system.

a. The Equilibrium Cell

The equilibrium cell as illustrated in Figures 4 and 5, is cylindrical and had an internal diameter of 2 inches and length

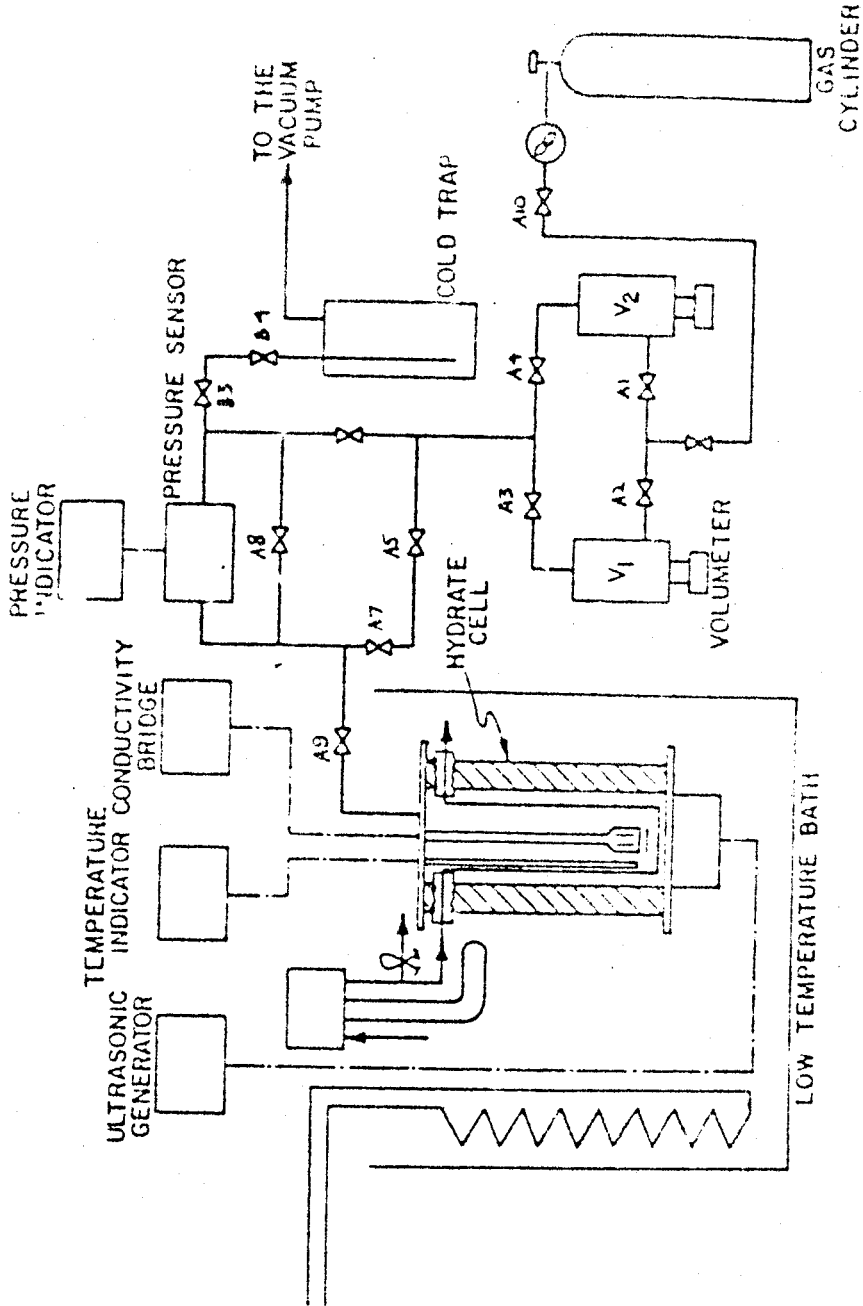


FIGURE 3. Experimental Apparatus.

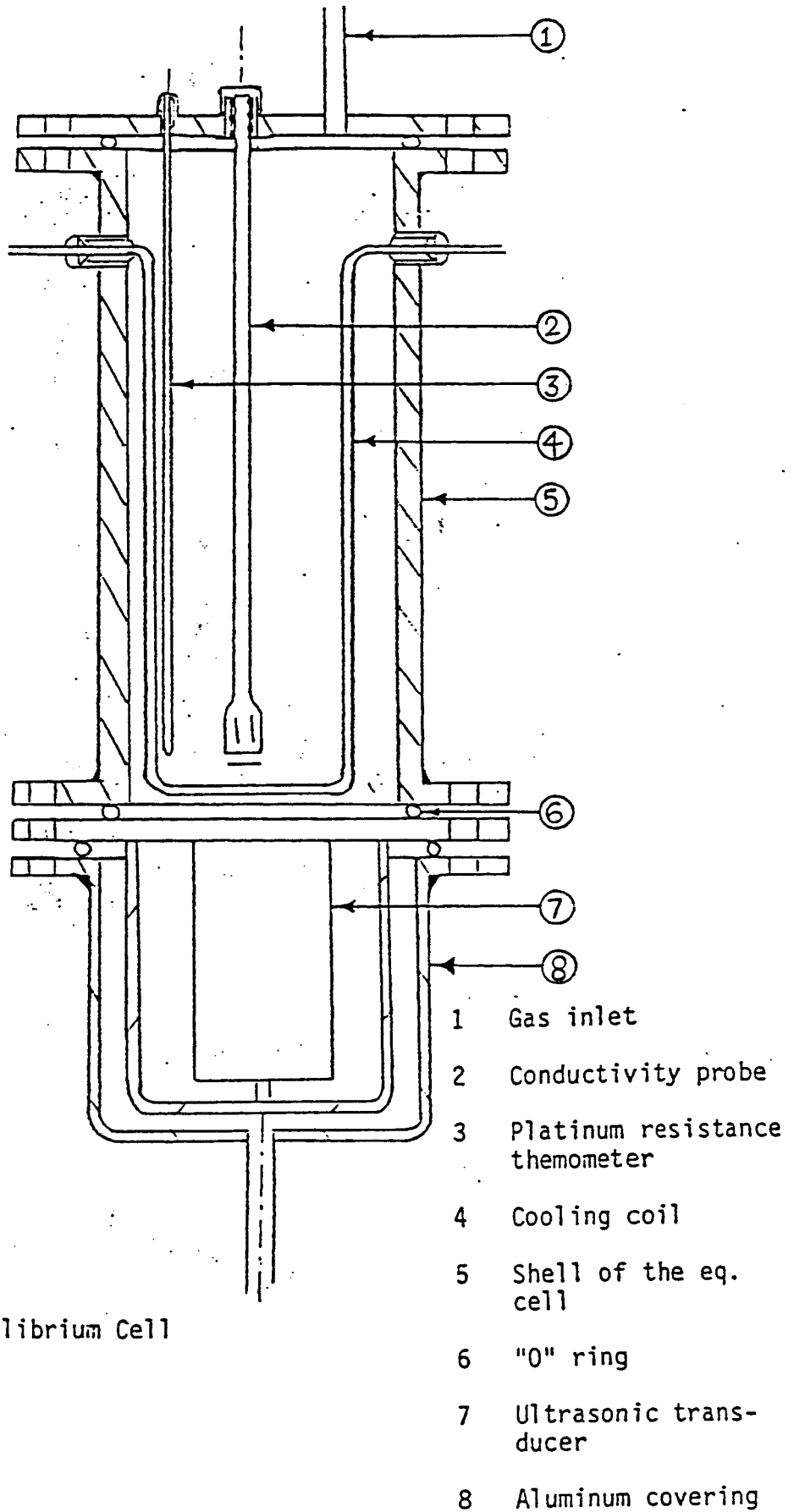


Fig. 4 The Equilibrium Cell

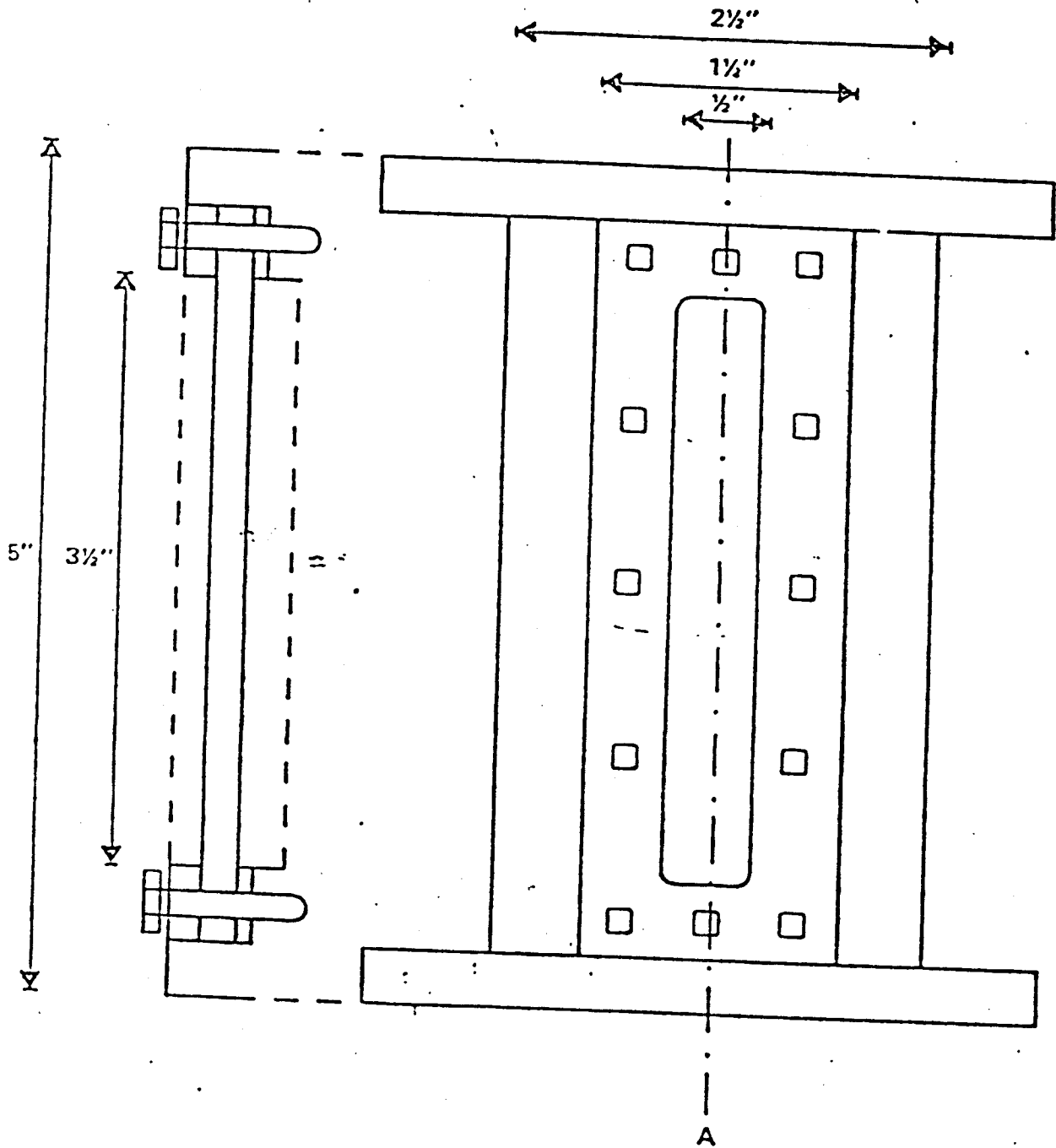


FIGURE 5 SCHEMATIC DRAWING OF THE EQUILIBRIUM CELL WINDOWS

of 5 inches. It was constructed of bronze alloy with a tensile strength of 40,000 psia. The top and bottom of the cell plates were made of 410 stainless steel. Each cell plate was removable and was kept in place by four bolts. Rubber "O" rings were used as seals for the top and bottom closures. Two sight glass windows were built on opposite sides of the cell in order to observe the hydrate formation. The windows were made of $\frac{1}{4}$ inch plexi-glas with Teflon seals. Each window was kept in place by twelve $\frac{1}{8}$ inch bolts. The ultrasonic transducer that produced agitation in the liquid column in the cell was bolted to the outside of the bottom plate. Except for the side where the transducer was in contact with the bottom plate, all the other sides of the transducer were protected by a cylindrical covering of aluminum with an internal diameter of three inches. The cell was connected to the gas charging system through a $\frac{1}{4}$ inch tube attached to the top plate. The platinum resistance thermometer was attached to the top plate by an "Omegalock" compression fitting. The top plate also supported the "Beckman" conductivity cell. Rubber "O" rings were used with the fittings that held the conductivity cell to the top plate to provide a better seal. The equilibrium cell was supported by three legs of 4.5 inches long, inside a 127 cubic inch rectangular box.

T 2218

b. The Pressure Measuring System.

The pressure measuring system consists of a Barocel pressure sensor and an electric manometer. The pressure sensor was a Barocel capacitance manometer, type 570 D-2000 T-2A1 designed to sense either differential or absolute pressure. The sensor consists of a sealed diaphragm which is opened on one side to the system whose pressure was to be measured, and the other side was kept under vacuum or opened to a source whose pressure is known. The mechanism was such that the diaphragm moves with the variation of the pressure of the system. The movement of the diaphragm was translated to an electrical signal. The sensor was mounted on a thermal base that prevented any condensation of gases and aided in degasing. The temperature of the thermal base could be stabilizes either at 105° F or 180° F. The electrical output of the pressure sensor was sent to a Barocel electrical manometer Model 1173 constructed by Datametrix Inc..

c. The Temperature Measuring System And The Associated Control Systems.

The temperature in the cell was sensed by a 6.5 inch long Omega, type PR-11 platinum resistance temperature probe. The

temperature indicator was a Doric Digiral read out Model DS-100-T5. The temperature range was from -10°C to 80°C . The temperature measuring and readout systems were calibrated against a Leeds and Northrup platinum resistance thermometer traceable to the National Bureau of Standards.

The temperature bath was constructed of $\frac{1}{2}$ inch Plexi-glas sheets. The dimensions of the bath were as follows; 13 inch in length, 7.5 inches in width, 17 inches in height with an overall capacity of $5\frac{1}{2}$ gallons. The outer wall of the bath was insulated with 1 inch thick Amoflex Foam Sheets. The bath fluid was Dow-Corning 200 Silicon fluid with a freezing point of -40°F and viscosity of 5 centistokes at 0°C . This fluid was selected mainly because of its good dielectric properties.

The refrigeration system was model PCC-24A-3 Blue M Hermetic refrigerator with a $\frac{1}{2}$ HP compressos. The refrigeration system has an overall heat removable capacity of 3500 BTU/hr. The temperature range was -23°C to room temperature with the temperature control within $\pm .15^{\circ}\text{C}$. The refrigerant Freon-12 emerged through a thermostatic expansion valve and flowed through a stainless steel coil of $7/16$ inch O.D. wound on a 7 inch mandrel. The refrigerator was equipped with a hot gas by-pass system to minimize undershooting and to allow better control of the cooling. The temperature of the bath was further controlled by a Model 1440-GKU Thermomix controller

from VWR Scientific with a built-in immersed thermostat of 750 watt capacity and a 10 liter/min. capacity pump. With the Thermomix controller and Blue M refrigerator the temperature of the bath was controlled within $\pm .005^{\circ}$ C at a temperature range of 0° C to 10° C.

d. The System For The Measurement Of The Electrical Conductivity.

The electrical conductivity of the salt solution was sensed by Beckman electrical conductivity cell of cell constant .01. The electrical conductivity was measured by Beckman Conductivity Bridge, Model No. RC19. The conductivity cell was attached to the top plate of the equilibrium cell by means of a specially machined Swagelock connector with two "O" ring seals.

e. The Agitation And Vacuum Systems

The ultrasonic agitation system consisted of an ultrasonic transducer attached to the bottom plate of the equilibrium cell and connected to an ultrasonic generator with a 25 foot leak proof cable. The transducer assembly consisted of a steel back block, a pair of lead zirconate titanate ferroelectric elements with a connector tab and an aluminum front block. These were held together by a center bolt under high tension.

The ultrasonic generator was solid-state module which operated from a commercial 120 V, 60 Hz electrical outlet. The generator allowed the resonant frequency of the dynamic unit to control the generator and it is usually operated at about 24.5 KHz. The maximum power output was 75 watts. The power input to the ultrasonic system was regulated by a Variac. The ultrasonic unit was assembled by Bliss Sonic Company in Fayetteville, Pennsylvania. The ultrasonic system was designed for an optimum efficiency with 2.5 inches of liquid in the cell.

The vacuum system consisted of a Welch-Duo-Seal Vacuum pump, Model 1399, rated at .0015 mm Hg ultimate pressure which was connected to the system via $\frac{1}{4}$ inch copper tubing and a 7/16 inch I.D. rubber vacuum hose. The vacuum pump served two purposes. Such as,

- a. to maintain vacuum in reference compartment of the pressure sensor and
- b. to evacuate the system.

The liquid nitrogen trap was used upstream of the pump to prevent any condensibles from entering the pump and back diffusion of the pump oil. The outlet of the pump was vented to the atmosphere outside the building.

f. The Gas Charging System.

The gas charging system consists of a size D cyclopropane cylinder, two Volumetric volumeters and an assembly of valves and tubing connected to the equilibrium cell.

Purity Of Cyclopropane Used In The Experiment.

Carbon dioxide	1 ppm
Air	50 ppm
Propylene	1230 ppm
Allene	100 ppm
Cyclopropane	balance.

Procedure

Initially the electrical conductivity of potassium chloride solutions of concentrations .01 to .02 N were determined at different temperatures. As mentioned under the general description the whole success of the experiment lies in preventing the occlusion of mother liquor in the hydrate mass by using ultrasonic agitation. Hence the level of ultrasonic agitation that totally eliminated the occlusion of the mother liquor was determined by the experiment at different agitation levels. Since the ultrasonic agitation is a function of the power input which is determined by the variac setting, the optimum variac setting is determined graphically by plotting the variac setting against $\Delta\mu_{0,0}^{\beta-\alpha}$. The two graphs that illustrate the effect of the variac setting on the chemical potential difference are given in Figures 6 and 7.

The Procedure Followed In Obtaining Data.

1. The equilibrium cell was thoroughly cleaned and dried.
2. The bottom part of the equilibrium cell, i.e. the ultrasonic system, bottom cell plate and the legs were connected to the shell of the equilibrium cell.
3. The valves A5 and A6 were kept closed. The valves A1, A2, A3, A4 and A6 were opened and the system was evacuated

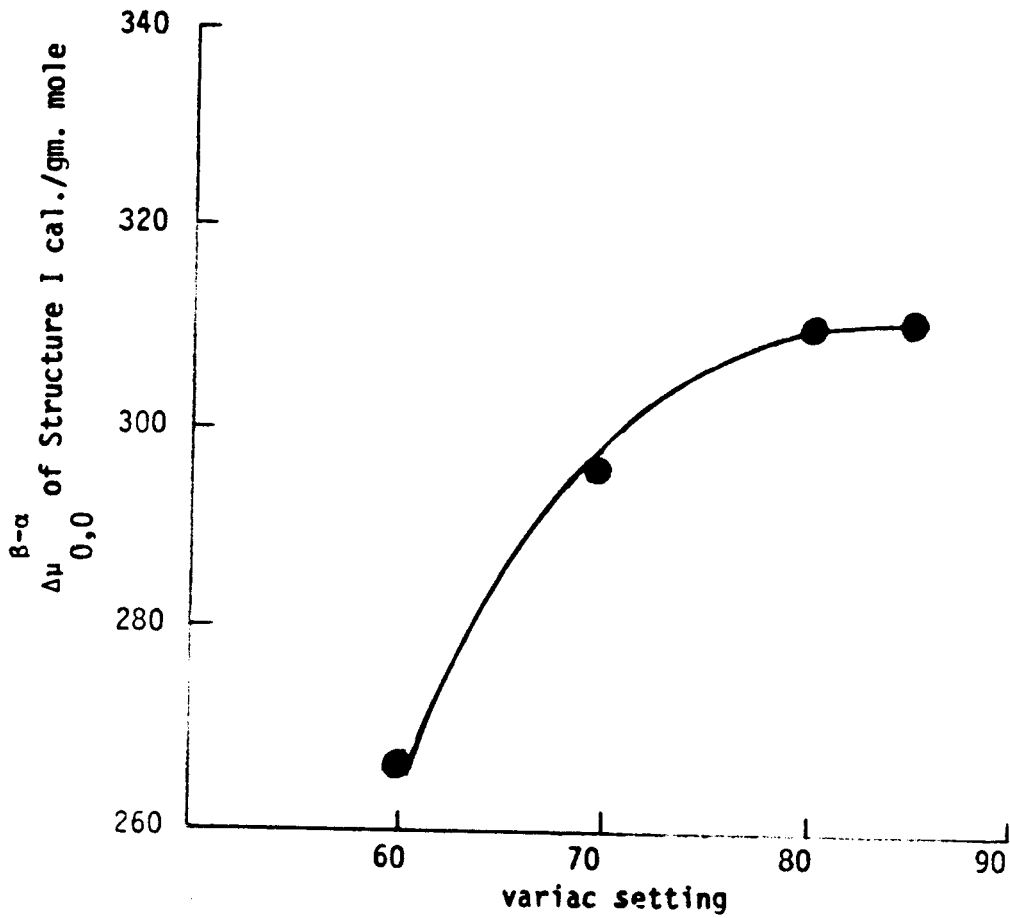


Figure 6. Graph to show the effect of ultrasonic agitation on the experimentally determined values of $\Delta\mu_{0,0}^{\beta-\alpha}$ of Structure I hydrate.

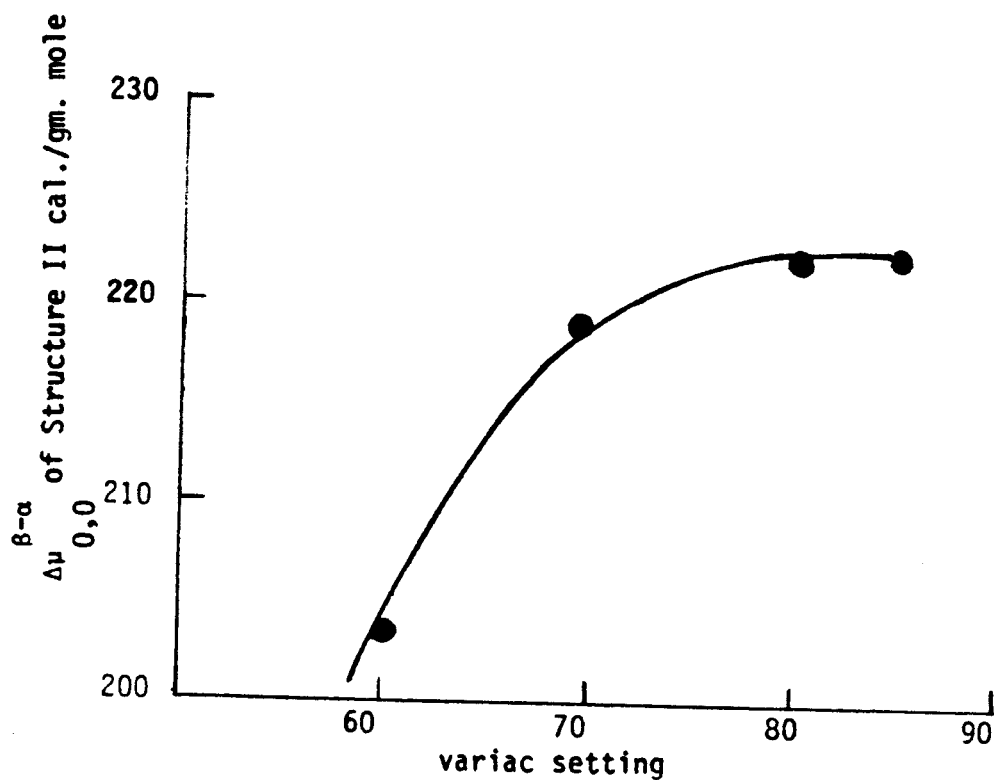


Figure 7. Graphical representation showing the effect of ultrasonic agitation on the experimentally determined values of $\Delta\mu_{0,0}^{\beta-\alpha}$ of Structure II.

over night.

4. Approximately .01N potassium chloride solution was made from deionized double distilled water.
5. A known weight of potassium chloride solution was placed in the equilibrium cell and the top closure of the equilibrium cell was fitted to the rest of the equilibrium cell.
6. The equilibrium cell was very slowly evacuated to prevent any splashing of the potassium chloride solution for 10 minutes. The rate of deaeration was controlled by a monitoring valve B4. Any water vapor leaving the cell was condensed and measured in the cold trap. (liquid nitrogen was used as the coolant).
7. The valve A9 was closed. A8, A6, B3 and B4 were kept open. A1, A2, A3, A4 and A10 were opened to load the volumeters with cyclopropane. The volumeters were brought to zero position, and the volumeters were shut off from the gas supply by closing the valve A10, and the system was allowed to reach equilibrium. The pressure and the ambient temperature were recorded. The equilibrium cell was transferred to the low temperature bath and the conductivity was measured. The valve A9 was opened. The ultrasonic agitation was started and the gas hydrates were allowed to form. When the equilibrium was reached the system was recharged with cyclopropane to cause more

hydrate to form.

8. When an acceptable amount of hydrate was formed and the system had reached equilibrium, the ultrasonic agitation was gradually reduced and turned off while maintaining a constant cell temperature.
9. The cell temperature, equilibrium pressure and the electrical conductivity of the hydrating medium were measured.

CHAPTER 6RESULTS

The main aim in the present work is to determine the thermodynamic parameters that describe the hydrate structure such as $\Delta\mu_{0,0}^{\beta-\alpha}$ and $\Delta h_{0,0}^{\beta-\alpha}$. The third parameter $\Delta v_{0,0}^{\beta-\alpha}$ has been measured by von Stackelberg by spectroscopy.

It is obvious that $\Delta\mu_{0,0}^{\beta-\alpha}$ and $h_{0,0}^{\beta-\alpha}$ cannot be measured directly by experimental means. What one could measure is the chemical potential difference between the empty and filled hydrate lattice at a given temperature and pressure. This could be done by using the van der Waals and Platteeuw model that is given in equation (4.13). y_{iK} the degree of filling of the cavities was measured by using a dilute solution of potassium chloride solution. Potassium chloride does not enter in to the hydrate structure. Hence by measuring the variation of the potassium chloride concentration in the liquid medium one could determine the amount of hydrates that was formed. Similarly by noting the initial and final pressure of the system one could obtain the amount of gas molecules that was converted to hydrates.

Cyclopropane was used as the hydrate-forming gas due to the fact it forms both the structures depending on the tempera-

ture and pressure. $\Delta\mu_{0,0}^{\beta-\alpha}$ and $\Delta h_{0,0}^{\beta-\alpha}$ were calculated from the experimentally obtained $\Delta\mu_{T,p}^{\beta-\alpha}$ by the method that is explained in the data reduction section. It is clear that $\Delta\mu_{0,0}^{\beta-\alpha}$ and $\Delta h_{0,0}^{\beta-\alpha}$ could be obtained by using two data points. The procedure of calculating $\Delta\mu_{0,0}^{\beta-\alpha}$ and $\Delta h_{0,0}^{\beta-\alpha}$ was repeated several times using fifteen different data points to determine the repeatability of the numerical values obtained for $\Delta\mu_{0,0}^{\beta-\alpha}$ and $\Delta h_{0,0}^{\beta-\alpha}$. The numerical values thus obtained agreed to within 2-4%. The $\Delta\mu_{0,0}^{\beta-\alpha}$ and $\Delta h_{0,0}^{\beta-\alpha}$ were next utilized in obtaining the Kihara parameters ϵ/k and δ for different hydrate-forming gases and the empty hydrate vapor pressure.

The chemical potential difference and enthalpy difference between the empty hydrate lattice and ice, the Kihara parameters ϵ/k and σ , and the empty hydrate vapor pressures for Structures I and II are given below.

	Structure I	Structure II
	Cal./gm. mole	Cal./gm.mole
$\Delta\mu_{0,0}^{\beta-\alpha}$	310 \pm 6	224 \pm 7
$\Delta h_{0,0}^{\beta-\alpha}$	332 \pm 12	245 \pm 10

The Empty Hydrate Vapor Pressures For St. I & II.

Structure I.

$$\ln P_W^{\beta} = 17.440 - 6003.925/T$$

Structure II.

$$\ln P_W^{\beta} = 17.332 - 6017.635 /T$$

where P_W^{β} in atm. and T in K.

The error of P_W^{β} is within $\pm 2\%$ with a confidence level of 99%.

The Kihara Parameters Obtained Using Peng And Robinson

Equation of State

Component	$\epsilon/k \text{ \AA}^{\circ}$	$\sigma \text{ \AA}$	$a \text{ \AA}$
Methane	156.72	3.2000	.3834
Ethane	177.01	3.2444	.5651
Propane	208.45	3.3111	.6502
Nitrogen	135.58	2.8964	.3526
Carbon dioxide	168.48	2.9716	.6805
Hydrogen sulfide	203.30	3.2001	.3600

CHAPTER 7

DATA ANALYSIS

The experimental data were analysed for the

- a. errors due to measured variables,
- b. sensitivity of the errors of the measured variables and
- c. repeatability of the calculated variables.

Error Analysis

The error analysis is a means by which one could determine the error attached to the dependent variable due to the errors in the independent variables.

Hence there are two main advantages in conducting an error analysis :

- a. To determine the effect of errors of measured variables on the dependent variable. In other words the error analysis gives the error margin of the dependent variable.
- b. To obtain the probability of the error distribution. This will provide one with the confidence level and the upper and lower bounds of the dependent variable. The most widely used method of error analysis is illustrated below. If the dependent variable is z where

$$z = f(x_1, x_2, x_3, \dots, x_i) \quad i = 1, n \quad (7.1)$$

then, the error of the dependent variable,

$$\text{error of } z = \sum_{i=1}^n (\partial f / \partial x_i) dx_i \quad (7.2)$$

This method provides one with the range of the error of the dependent variable but it does not give the error distribution of the dependent variable. Hence the present work utilized the Monte Carlo method of error analysis that is illustrated below.

If R_1 and R_2 are a pair of uniform random variables whose mean and variance are m and V respectively then a pair of random variates $S1$ and $S2$ could be obtained (40) assuming the normal distribution with mean m and variance V . Where,

$$S1 = V(-2 \ln R_1)^{.5} \cos (6.28 R_2) + m \quad (7.3)$$

$$S2 = V(-2 \ln R_1)^{.5} \sin (6.28 R_2) + m \quad (7.4)$$

On the first entry to the routine, the uniform variates R_1 and R_2 are computed and retained and the normal variate $S1$ is returned to the user. On the second entry the previously

computed R_1 and R_2 are used to compute S_2 . All the subsequent entries alternate between these two steps.

Hence, in conducting the Monte Carlo technique of error analysis a large number of times one could obtain the probability distribution of the dependent variable. The probability distribution will enable one to evaluate the $\pm 3\sigma$ error.

Sensitivity Analysis

The sensitivity analysis is a way to determine the effect of the errors of each independent variable on the dependent variable. In other words the sensitivity analysis is used in determining as to the error of which independent variable that should be minimized in order to improve the value of the dependent variable.

The sensitivity analysis could be conducted by using the same Monte Carlo technique as mentioned before, but the simulation was conducted only on one independent variable. In other words one assumes the variance of all the other independent variables except the one under study to be zero. Hence the sensitivity analysis is quite an important tool

in planning and designing of the experiment because it gives an accurate indication as to where the experimentalist should concentrate in order to minimize the error of the dependent variables.

Repeatability of the Dependent Variable

The repeatability of a dependent variable was tested by carrying out the experiment several times and repeating the calculation for each data point to determine the numerical value of the dependent variable. The numerical values thus obtained will enable one to determine within what range the dependent variable will lie under the existing experimental conditions.

The results of the error and sensitivity analysis are given in Table 3.

Table 3. Results Of The Sensitivity And Error Analysis

	Parameter under investigation	Standard deviation	$\pm 3 \sigma$ error cal./gm. mole	
			Structure I	Structure II
SENSITIVITY ANALYSIS	Bath temp.	.03 °C	1.12	1.91
	Ambient temp.	.03 °C	2.87	3.82
	System pressure	26.39 Pa	4.00	2.87
	Volume of the system	.15 cm ³	4.53	2.15
	Specific resistance	1 * 10 ⁻⁴	9.56	14.81
ERROR ANALYSIS	$\beta - \alpha$ $\Delta \mu$ 0,0		23.41	26.78

CHAPTER 8

DATA REDUCTION AND DATA CORRELATION

Since the liquid water is in equilibrium with the hydrate phase at a temperature above its ice point,

$$\mu_{T,P}^H = \mu_{T,P}^L + RT \ln a_W \quad (8.1)$$

where $\mu_{T,P}^H$, $\mu_{T,P}^L$ are the chemical potential of hydrate and pure liquid water at a given temperature and pressure. a_W is the activity of water in the salt solution. Hence equation (8.1) could be rewritten for cyclopropane hydrate when vapor, liquid water and hydrate coexist.

$$\Delta\mu_{T,P}^{\beta-H} = -RT \nu \ln(1-y) + RT \ln a_W \quad (8.2)$$

Equation (8.2) was used in computing $\Delta\mu_{T,P}^{\beta-H}$ for both Structures I and II taking into consideration that cyclopropane occupies the large cavities. The activity of water in the potassium chloride solution that is in equilibrium with the hydrate phase was calculated from tabulated freezing point depression data

(CRC Hand Book 1977/1978, page D244). The effect of cyclopropane on the activity of the solution was neglected due to its low solubility ($x_{\text{cyclopropane}} < .00025$) in water as measured by Zerpa et. al.(41).

With $\Delta\mu_{T,P}^{\beta-L}$ in hand the next step is to calculate $\Delta h_{0,0}^{\beta-L}$ and $\Delta\mu_{0,0}^{\beta-\alpha}$ from $\Delta\mu_{T,P}^{\beta-L}$. Using the Parrish and Prausnitz's one could express $\Delta\mu_{T,P}^{\beta-\alpha}$ as a function of $\Delta h_{0,0}^{\beta-\alpha}$ and $\Delta\mu_{0,0}^{\beta-L}$. In other words by combining equations (4.34), (4.36) and (4.38) one could obtain a mathematical expression for $\Delta\mu_{T,P}^{\beta-L}$ with two unknowns $\Delta\mu_{0,0}^{\beta-\alpha}$ and $\Delta h_{0,0}^{\beta-\alpha}$ that are linearly related to the dependent variable $\Delta\mu_{T,P}^{\beta-L}$ as shown below.

$$\frac{\Delta\mu_{T,P}^{\beta-L}}{RT} = \frac{\Delta\mu_{0,0}^{\beta-\alpha}}{273.15 R} + \frac{(\Delta v_{0,0}^{\beta-\alpha} + \Delta v_{0,0}^f) Pr}{273.15 R} + \int_{273.15}^T \frac{(\Delta h_{0,0}^{\beta-\alpha} + \Delta h_{0,0}^f) dT}{RT^2}$$

$$\int_{273.15}^T \frac{(\Delta v_{0,0}^{\beta-\alpha} + \Delta v_{0,0}^f) (dp/dT)_r dT}{RT} + \frac{(\Delta v_{0,0}^{\beta-\alpha} + \Delta v_{0,0}^f) (P-Pr)}{RT} \quad (8.3)$$

Since there are only two unknowns, $\Delta h_{0,0}^{\beta-\alpha}$ and $\Delta\mu_{0,0}^{\beta-\alpha}$, in equation (8.3) their numerical values could be obtained by using two data points that belong to the same hydrate Structure.

The values $\Delta\mu_{0,0}^{\beta-\alpha}$ and $\Delta h_{0,0}^{\beta-\alpha}$ for Structure I were obtained directly by the method mentioned above. The temperature range

for cyclo-propane hydrate prevented using the above mentioned method directly to evaluate $\Delta\mu_{0,0}^{\beta-\alpha}$ and $\Delta h_{0,0}^{\beta-\alpha}$ for Structure II. Therefore the following procedure was adopted.

For cyclo-propane hydrate van der Waals and Platteeuw's model could be rewritten as follows;

$$\Delta\mu_{T,P}^{\beta-L} = RT \sum_i v_i \ln(1 + C_i f_i) \quad (8.4)$$

Where f and C_i are the fugacity of cyclo-propane and the Langmuir constant for cyclo-propane in large cavities respectively. The Langmuir constant could be best described by the equation (4.16) using the Kihara potential function with a spherical core.

The theoretical work of McKoy and Sinanoglu (34) have shown that $\omega(r)$ derived using the Kihara potential function gives better predictions for the hydrate properties as opposed to that derived using Lennard-Jones potential function.

McKoy and Sinanoglu expressed $\omega(r)$, using the Kihara potential function as follows

$$\omega(r) = 2Z_m \epsilon \left[\sigma^{12} \left(\delta + a/R \right) / (R-r) - \sigma^{11} \left(\delta + a\delta/R \right) / (R-r) - \sigma^6 \left(\delta + a\delta/R \right) / (R-r) - \sigma^4 \left(\delta + a\delta/R \right) / (R-r) - \sigma^5 \left(\delta + a\delta/R \right) / (R-r) \right] \quad (8.5)$$

$$\delta^N = \left[\left(1-r/R-a/R \right)^{-N} - \left(1+r/R-a/R \right)^{-N} \right] / N \quad (8.6)$$

For Structure I, the Kihara parameters for cyclo-propane were found using the values obtained for $\Delta\mu_{\beta-\alpha}$ and $\Delta h_{\beta-\alpha}$ for Structure II below the ice point was calculated using equations (8.6), (8.5), (4.16) and (8.4). The dissociation fugacity for equation (8.4) was taken from the work of Hafemann and Miller (68).

$\Delta\mu_{\beta-\alpha}$ and $\Delta h_{\beta-\alpha}$ for Structure II were calculated similarly to Structure I, from the two sets of values for $\Delta\mu_{\beta-L}$ such as:

- $\Delta\mu_{\beta-L}$ obtained using Langmuir constant (calculated using the Kihara parameters) and dissociation fugacities of cyclo-propane, and
- $\Delta\mu_{\beta-L}$ obtained experimentally.

The $\Delta\mu_{\beta-\alpha}$ and $\Delta h_{\beta-\alpha}$ thus obtained for Structure II from the two sets of values showed a difference of less than 4%.

Determination of the Water Content in the Vapor Phase in Equilibrium with the Hydrate Phase

It was mentioned in the literature review section that it is difficult to extend the method proposed by Sloan et.al.(12) to multicomponent mixtures directly. The present work proposes two methods in order to overcome this difficulty.

Method A

As mentioned in the literature review Sloan et. al. calculated the empty hydrate vapor pressure from the experimental data obtained from the two phase (vapor-hydrate) region. The present work follows the same principle but the empty hydrate vapor pressure P_w^β was calculated using three phase equilibrium line below the ice point. Since ice-vapor-hydrate coexist,

$$f_w^H = f_w^{\text{ice}} \quad (8.7)$$

where f_w^{ice} and f_w^H are the fugacities of water in ice and hydrate respectively. But,

$$f_w^{\text{ice}} = P_w^{\text{ice}} \phi_w^{\text{ice}} \int_{P_w^\beta}^P \exp \left[\frac{v_w^{\text{ice}}}{RT} \right] dP \quad (8.8)$$

Assuming that the ice is incompressible, P_w^β could be obtained by equalizing equations (4.45) and (8.8) as follows ;

$$P_w^\beta = \frac{\phi_w^{\text{ice}} \exp \left[\frac{v_w^{\text{ice}} (P - P_w^\beta)}{RT} \right]}{\phi_w^\beta \exp \left[- \frac{\Delta \mu_{T,P}^{\beta-\alpha}}{RT} + \int_{P_w^\beta}^P \frac{v_w^\beta}{RT} dP \right]} \quad (8.9)$$

P_w^β was calculated by using all the available hydrate dissociation data along the three phase line below the ice point for both the hydrate Structures I and II. The empty hydrate vapor pressure thus obtained could be expressed within an error of $\pm 2\%$, as an arbitrary function of temperature, as follows;

For Structure I hydrate,

$$\ln P_w^\beta = 17.440 - 6003.925/T \quad \text{and} \quad (8.10)$$

for Structure II

$$\ln P_w^\beta = 17.332 - 6017.6351/T \quad (8.11)$$

with a confidence level of 99%. The temperature and pressure of equations (8.10) and (8.11) are expressed in K and Atm. respectively. The data sources that were used in the determination of the empty hydrate vapor pressure is given in the Appendix B. The plots of the inverse absolute temperature versus $\ln P_w^\beta$ for Structures I and II are given in Figures 8 and 9.

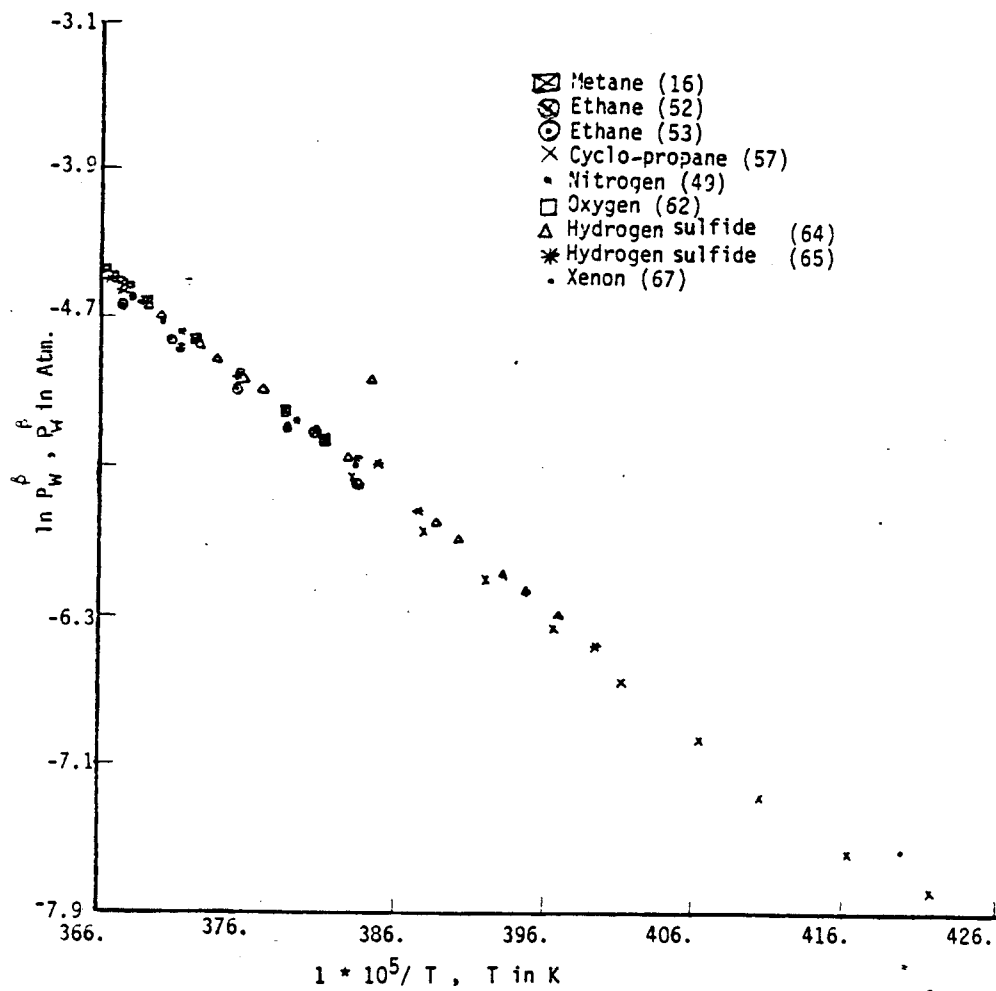


Fig. 8 The plot of the reciprocal temperature vs. $\ln \frac{P_v}{P_a}$ of Structure I

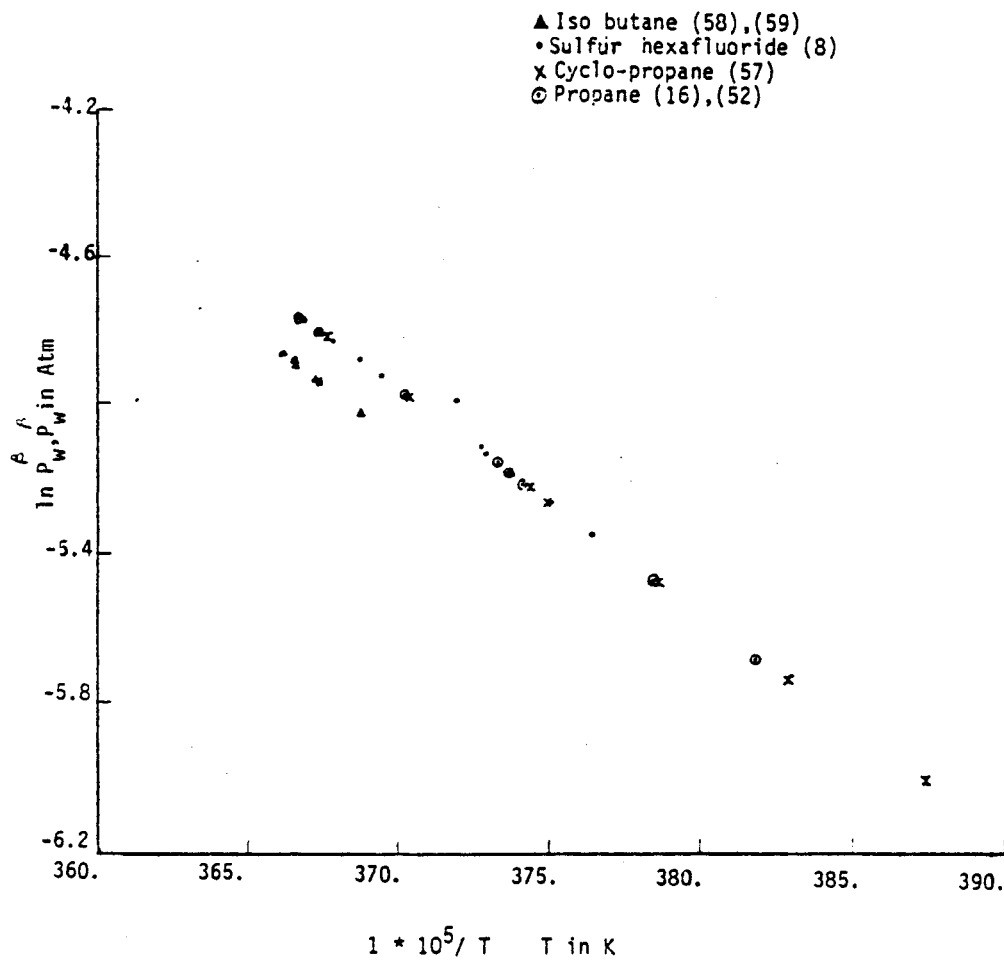


Fig. 9 The plot of the reciprocal temperature vs. $\ln P_w^B / P_w^A$ of Structure II

The empty hydrate vapor pressure thus obtained was used with equation (4.45) in predicting the water content in the in the vapor phase in equilibrium with the hydrates in the two phase region as follows;

$$f_{W}^V = Y_{W} P \phi_{W} \quad (8.12)$$

where Y_{W}^V = mole fraction of water vapor in the vapor phase and

ϕ_{W} = fugacity coefficient of water in the vapor phase.

At equilibrium equations (8.12) and (4.45) could be equalized as follows;

$$Y_{W}^V P \phi_{W} = P_{W}^{\beta} \phi_{W}^{\beta} \exp \left[\frac{-\Delta\mu_{T,P}^{\beta-H}}{(RT)} + v_{0,0}^{\beta} \frac{(P-P_{W}^{\beta})}{(RT)} \right] \quad (8.13)$$

The fugacity coefficient of the empty hydrate ϕ_{W}^{β} , could be considered to be unity (the numerical value of P_{W}^{β} falls in the region of the vapor pressure of ice).

$$Y_{W}^V = \frac{P_{W}^{\beta} \exp \left[\frac{-\Delta\mu_{T,P}^{\beta-H}}{(RT)} + v_{0,0}^{\beta} \frac{(P-P_{W}^{\beta})}{(RT)} \right]}{P \phi_{W}} \quad (8.14)$$

Method B

The van der Waals and Platteau model could be rewritten as follows;

$$\mu_{T,P}^{\beta} - \mu_{T,P}^{\alpha} = RT \sum_i v_i \ln \left(1 + \sum_J C_{iJ} \frac{f_J}{f_i} \right) \quad (8.15)$$

By adding and subtracting $\mu_{T,P}^{\beta}$ from the left hand side of equation (8.15),

$$\mu_{T,P}^{\beta} - \mu_{T,P}^{\alpha} + \mu_{T,P}^{\alpha} - \mu_{T,P}^{\alpha} = RT \sum_i v_i \ln \left(1 + \sum_J C_{iJ} \frac{f_J}{f_i} \right) \quad (8.16)$$

$$\text{But } \mu_{T,P}^{\beta} - \mu_{T,P}^{\alpha} = \Delta \mu_{T,P}^{\beta-\alpha} \quad (8.17)$$

$$\Delta \mu_{T,P}^{\beta-\alpha} = \Delta \mu_{0,0}^{\beta-\alpha} - \int_{0^{\circ}\text{C}}^T (\Delta h_{0,0}^{\beta-\alpha} / RT) dT + \int_0^P \Delta v_{0,0}^{\beta-\alpha} dP \quad (8.18)$$

From equation (4.33)

$$\mu_{T,P}^{\beta} - \mu_{T,P}^{\alpha} = RT \ln \left(\frac{f_W^{\beta}}{f_W^{\alpha}} \right) \quad (8.19)$$

By combining equations (8.18), (8.16) and (8.19)

$$RT \ln\left(\frac{f_W^H}{f_W^{\text{ice}}}\right) = -RT \sum_i v_i \ln\left(1 + \sum_J C_{iJ} f_J\right) + \Delta\mu_{0,0}^{\beta-\alpha} - \int_{0^\circ\text{C}}^T (\Delta h_{0,0}^{\beta-\alpha} / T) dT + \int_0^P \Delta v_{0,0}^{\beta-\alpha} dP \quad (8.20)$$

Therefore

$$Y_W = \frac{f_W^\alpha}{f_W^{\text{ice}}} \exp\left[-\sum_i v_i \ln\left(1 + \sum_J C_{iJ} f_J\right) + \Delta\mu_{0,0}^{\beta-\alpha} / (RT) - \int_{0^\circ\text{C}}^T \Delta h_{0,0}^{\beta-\alpha} / (RT^2) dT + \int_0^P \Delta v_{0,0}^{\beta-\alpha} / (RT) dP\right] / (P\phi_W) \quad (8.21)$$

The main advantage in the method B is that it has eliminated the empty hydrate vapor pressure from the calculations. The main disadvantage is that it cannot be used under conditions where liquid water and hydrate, or ice and hydrate coexist. Under such conditions the left hand side of equation (8.20) becomes zero. The predicted values for the water content in the vapor phase in equilibrium with methane hydrate by the two methods that are given in Table 4 show the validity of the present treatment.

It should be noted that the predictions of the water content in equilibrium with the hydrate phase in two phase region

Table 4. The Prediction of The Water Content In The Vapor Phase In Equilibrium With The Hydrate Phase

SYSTEM		-				Methane-water.
PHASE IDENTIFICATION		-				Hydrate phase(methane hydrate) and vapor phase (methane and water)
Temp. ° F	Pressure psia	Exp. data	Correlat- ed valu- es by Ng & Robin- son.	Predicted values by equations (8.21) (8.14)		
		ppm	ppm	ppm	ppm	
water content in the vapor phase						
26.33	500.	178.09	176.89	144.99	150.38	
26.33	1000.	94.43	95.28	77.11	82.42	
26.33	1500.	64.22	65.48	57.44	63.28	
8.33	500.	78.24	79.23	57.09	60.54	
8.33	1000.	39.56	38.51	31.09	34.01	
8.33	1500.	24.23	23.95	23.80	26.87	
-9.67	500.	32.17	33.67	20.88	22.68	
-9.67	1000.	15.45	14.83	11.71	13.14	
-9.67	1500.	8.46	8.40	9.29	10.77	
-27.67	500.	12.30	13.45	7.04	7.84	
-27.67	1000.	5.60	5.42	4.10	4.72	
-27.67	1500.	2.72	2.82	3.41	4.06	
Mean absolute deviation			1	9	7	

published by Ng and Robinson are really the correlated values rather than predictions because they used the same set of data in obtaining the vapor fugacity of the empty hydrate lattice. Unfortunately there is no reliable experimental data to demonstrate the applicability of the two methods that were proposed in the present work for hydrate Structure II.

Optimization of the Kihara Parameters

It is clear from the literature review that the $\Delta\mu_{T,P}^{\beta-\alpha}$ along the three-phase line, could be evaluated in two independent routs. Such as,

- by knowing $\Delta\mu_{0,0}^{\beta-\alpha}$, $\Delta h_{0,0}^{\beta-\alpha}$, $\Delta v_{0,0}^{\beta-\alpha}$, equilibrium temperature and pressure one could evaluate $\Delta\mu_{T,P}^{\beta-H}$ using the thermodynamic model of Parrish and Prausnitz.
- by knowing the Kihara parameters, equilibrium temperature and pressure one could evaluate $\Delta\mu_{T,P}^{\beta-H}$ using the van der Waals and Platteeuw's model.

Therefore with the right set of Kihara parameters, $\Delta\mu_{T,P}^{\beta-H}$ calculated from the two routes a. and b. should coincide.

This concept was used in optimizing the Kihara parameters.

The core diameters of the guest molecules were obtained from the work of Tee et. al. (42). Hence the optimization was done on ϵ_{AB}/k and σ_{AB} .

For those components that form Structure II in the pure form (referring to pure gas hydrates), except for isobutane, the value ϵ_{AB}/k and σ_{AB} were selected to give the minimum absolute deviation between $\Delta\mu_{T,P}^{\beta-H}$ calculated from the routes "a" and "b".

This treatment could not be extended to Structure I formers because there were multiple numbers of pairs of ϵ_{AB}/k

and σ_{AB} that fall into the same range of mean absolute deviation of the chemical potential difference calculated from the routes "a" and "b" along the three-phase line of pure hydrates. Out of these multiple pairs of ϵ_{AB}/k and σ_{AB} the best pair was selected based on Structure II hydrate. This procedure could be explained using methane hydrate and methane-propane hydrate data as examples.

First, pure methane hydrate data were used in obtaining ϵ_{AB}/k and σ_{AB} values with methane hydrate. The best pair of ϵ_{AB}/k and σ_{AB} for methane hydrate was selected using the mixed hydrate dissociation pressure data of methane-propane. For isobutane, due to the narrow temperature range where isobutane hydrate data were available and the fact that the data below 0°C were inconsistent, methane-isobutane hydrate data were used in obtaining the Langmuir constant for isobutane. Since pure n-butane does not form hydrates C_{ij} for n-butane was calculated from n-butane-methane hydrate (46) data. The sources of data that were used in the correlations are given in Appendix B.

According to the assumptions made in formulating the van der Waals and Platteeuw's model, the Langmuir constant for n-butane and isobutane cannot be derived from their model. Hence the Langmuir constant was given as an arbitrary function of the temperature, such as

$$C_{ij} = (A/T) \exp (B/T). \quad (8.22)$$

TABLE 5. The Kihara Parameters Obtained Using The
Peng And Robinson Equation Of State

Component	ϵ/k K	σ Å	a Å
Methane	156.72	3.2000	0.3834
Ethane	177.01	3.2444	0.5651
Propane	208.45	3.3111	0.6502
Nitrogen	135.58	2.8964	0.3526
Carbon dioxide	168.48	2.9716	0.6805
Hydrogen sulfide	203.30	3.2000	0.3600

TABLE 6. The Kihara Parameters Obtained Using The
Soave Modified Redlich Kwong Equation Of State

Component	ϵ/k K	σ $\overset{\circ}{\text{A}}$	a $\overset{\circ}{\text{A}}$
Methane	154.54	3.1710	0.3834
Ethane	176.91	3.2541	0.5651
Propane	208.96	3.3074	0.6502
Nitrogen	136.01	2.8950	0.3526
Carbon dioxide	168.27	2.9718	0.6805
Hydrogen sulfide	203.00	3.1989	0.3600

Since there are two equations of state widely used in hydrate work,

- a. the Peng and Robinson equation of state and
- b. the Soave modified Redlich Kwong equation of state

the Kihara parameters were obtained using both equations of state. Thus the accuracy of each equation of state in predicting the component fugacities was considered. The Kihara parameters obtained by using the Peng and Robinson, and Soave modified Redlich Kwong equations of state are given in Tables 5 and 6 respectively.

The applicability of the Kihara parameters thus obtained was demonstrated by applying them in the prediction of mixed hydrate properties. In Table 7 and Figure 10 the predicted values for methane-ethane mixed hydrate three-phase dissociation pressures show sufficient improvement over that predicted by Ng and Robinson, and Holder (3). It should be noted that Holder used the same set of data in his computer program in optimizing the Kihara parameters for methane and ethane hydrates. Ng and Robinson used the same set of data in optimizing α_j . The predicted dissociation pressures for methane-carbon dioxide(45) mixed hydrate also showed a similar improvement (see Table 8). For methane-carbon dioxide-hydrogen sulfide mixture Ng and Robinson used the initial composition of the gas mixture rather than the equilibrium composition in predicting the dissociation pressures (based on the sample calculations in the Ng and Robinson computer program). The resulting

Table 7. The Prediction Of The Dissociation Pressures Of Hydrates Formed By Methane-Ethane Binary Mixtures In Vapor- Aq. Liquid - Hydrate Equilibria.

EXPERIMENTAL DATA (16)

Vapor phase mole fraction		Temp.	Press.	Predicted dissociation pressures. psi.			
CH ₄	C ₂ H ₆	°F	psia	Mtd 1*	Mtd. 2 ⁺	Mtd. 3 [#]	Holder(3)
.95	.05	36.	283.	333.2	391.2	396.9	348
.95	.05	40.	363.	415.8	488.6	496.6	444
.95	.05	44.	469.	520.5	612.7	624.7	569
.95	.05	50.	687.	741.8	879.1	904.5	840
.95	.05	56.	1005.	1073.7	1278.6	1335.4	1280.
.904	.096	32.	184.	218.3	245.7	252.7	224.
.904	.096	36.	238.	283.5	319.3	328.6	287
.904	.096	40.	303.	355.3	400.5	412.8	367
.904	.096	44.	391.	446.9	504.3	521.4	473
.904	.096	50.	512.	643.6	728.0	758.6	702
.904	.096	56.	832.	940.5	1071.5	1133.2	1082
.564	.436	35.	137.	137.0	140.3	149.8	129
.564	.436	40.	187.	184.6	188.8	202.0	176
.564	.436	45.	255.	250.1	255.0	273.9	246
.564	.436	50.	353.	342.2	348.2	376.2	342
Mean absolute deviation				47.6	109.0	120.4	81

- * using the Kihara parameters in Table 5 with the Peng & Robinson equation of state
 + using the Kihara parameters in Table 6 with SRK equation of state
 # using the method of Ng and Robinson with their Kihara Parameters

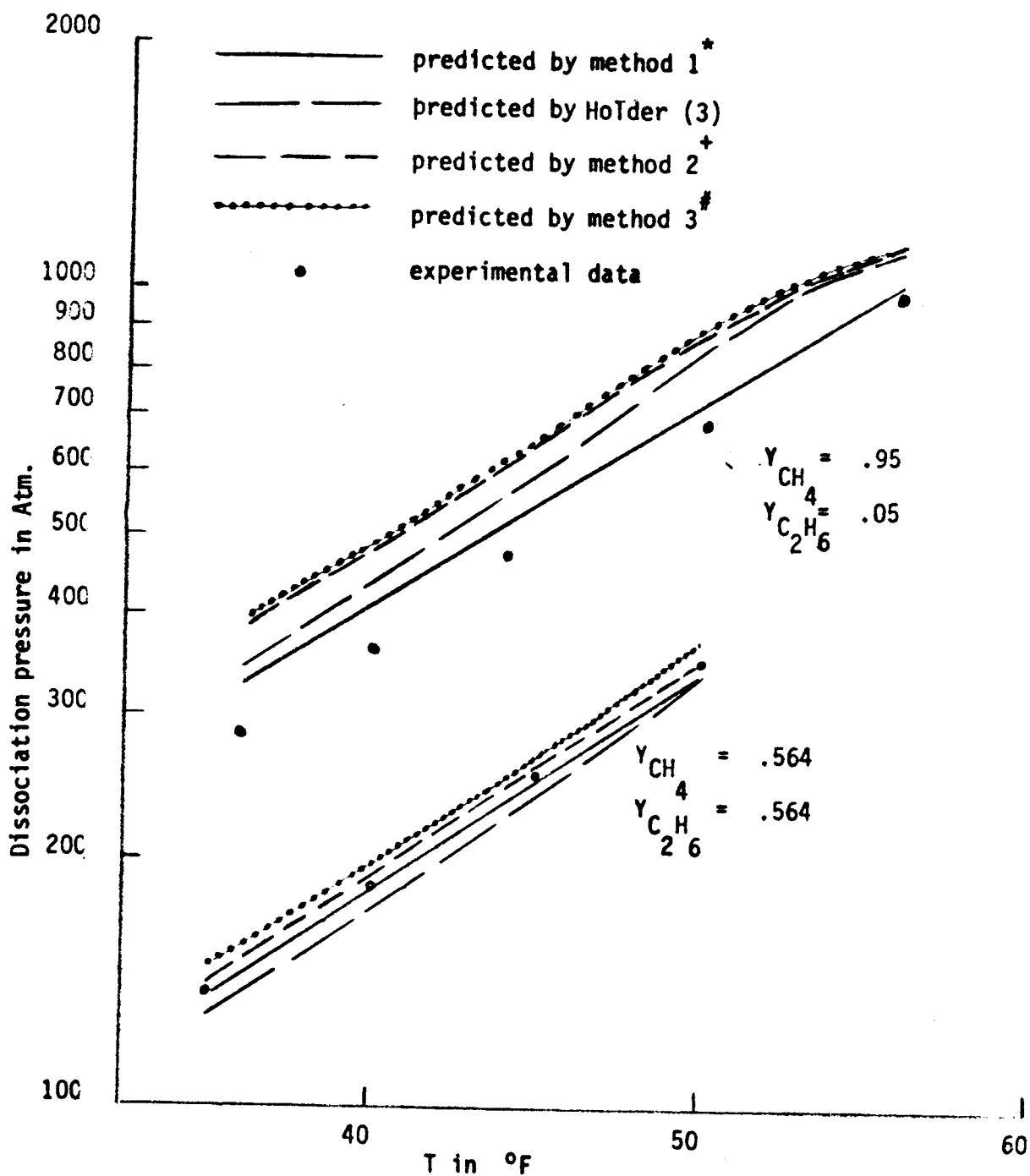


Figure 10. Comparison of Experimental and Calculated Dissociation Pressures of Vapor-Aq. Liquid-Hydrate Curves of Methane-Ethane Mixed Hydrate Equilibria.

*,+,# see foot note in Table 7

Table 8. The Prediction Of The Dissociation Pressures Of Hydrates Formed By Carbon Dioxide-Methane Binary Mixtures In Vapor- Aq. Liquid-Hydrate Equilibria.

EXPERIMENTAL DATA (45)		PREDICTED DISSOCIATION PRESSURE (psia)				
Vapor Composition (mole fraction)		Temp.	Press.	Mtd. 1 [*]	Mtd. 2 ⁺	Mtd. 3 [#]
CH ₄	CO ₂	°F	psia			
.378	.622	49.2	652.0	644.4	680.5	652.0
.379	.621	45.7	517.0	517.0	546.0	520.2
.374	.626	42.1	405.0	416.3	438.5	416.2
.367	.633	36.9	293.0	307.4	325.2	305.6
.359	.641	33.9	240.0	259.1	274.4	256.5
Mean Absolute Deviation				10.5	31.5	8.7

* using the Kihara parameters in Table 5 with the Peng and Robinson equation of state.

+ using the Kihara parameters in Table 6 with the SRK equation of state.

using the modification of Ng and Robinson with their Kihara parameters.

predictions are given in Table 9. The applicability of the newly obtained Kihara parameters in the four-phase region was demonstrated by using methane-propane(43), ethane-propane (3) and methane-ethane-propane (3) mixtures. The resulting predictions are given in Tables 10, 11 and 12 respectively. The applicability of the Kihara parameters obtained in the present work to multicomponent mixtures of industrial importance was shown by using the

- a. multicomponent data of Deaton and Frost in the three phase region (see Table 13) and
- b. laboratory mixture data of Ng and Robinson (69) in the four phase region (see Table 14).

McLeod and Campbell's data were not used in the present work because it was the pseudo composition and not the absolute composition that was recorded in their work.

In all the above calculations the Langmuir constant was calculated using equations (8.6), (8.5) and (4.16) but the Langmuir constant within the temperature range of 260 to 300 K could be expressed by an empirical relationship as in equation (8.22). The numerical values of A and B are given in Appendix C. Within the temperature range 260 to 300 K the maximum deviation for C_{ij} calculated from equations (8.22) and (4.16) is .3% or less for each gas.

Table 9. The Predicted Dissociation Pressure Of Hydrates
 Formed By Methane-Carbon Dioxide-Hydrogen Sulphide
 Ternary Mixtures In Vapor-Aq. Liquid-Hydrate Equilibria.

EXPERIMENTAL DATA (45)			Predicted dissociation pressure (psia)				
Vapor Composition (mole fraction)			Temp. °F	Press. psia	Method	Method	Method
CH ₄	CO ₂	H ₂ S			1*	2 ⁺	3 [#]
.686	.249	.065	42.8	214.	235.0	253.2	256.0
.699	.241	.060	48.0	295.	328.9	355.7	360.3
.705	.235	.060	51.5	402.	404.1	435.7	445.0
.715	.228	.057	55.8	543.	543.0	590.0	606.9
.725	.220	.055	59.5	715.	706.9	769.7	799.0
.725	.220	.055	62.3	897.	840.1	923.0	960.5
.725	.220	.055	64.0	1095.	955.7	1045.6	1104.3
.810	.130	.060	56.2	516.	553.8	553.8	641.1
.820	.126	.054	57.5	661.	644.1	644.1	752.4
.820	.126	.054	61.3	854.	825.4	825.4	981.8
.820	.126	.054	63.7	998.	966.1	966.1	1168.5
.820	.125	.055	66.3	1255.	1190.0	1190.0	1488.8
.820	.126	.054	67.5	1397.	1275.8	1275.8	1624.7
.820	.126	.056	68.8	1565.	1410.2	1410.2	1836.0
.825	.121	.054	70.8	1790.	1735.0	1735.0	2342.7
.820	.126	.054	72.3	2042.	2042.0	2042.0	2848.8

Table 9 continued

Vapor composition			Experimental data		Predicted dissociation pressure (psia)		
CH ₄	CO ₂	H ₂ S	°F	psia	Method 1 [*]	Method 2 ⁺	Method 3 [#]
.820	.126	.054	73.8	2278.0	2445.0	2793.3	3460.6
.699	.127	.174	57.7	293.0	283.0	298.1	313.8
.700	.123	.167	62.2	384.0	378.6	398.4	422.7
.720	.120	.160	65.0	483.0	469.6	495.7	526.2
.720	.120	.160	68.3	637.0	580.8	616.2	662.4
.720	.120	.160	70.7	743.0	675.7	711.9	772.2
.720	.223	.057	67.7	1628.0	1245.4	1383.9	1497.1
.723	.222	.055	69.0	1742.0	1464.6	1621.7	1817.1
.789	.136	.075	35.2	102.0	145.5	157.8	163.3
.810	.118	.072	51.8	276.0	384.9	419.3	440.0
.810	.118	.072	54.0	401.0	436.0	478.2	501.3
.800	.120	.080	60.7	617.0	607.8	659.6	703.0
.800	.120	.080	63.0	722.0	722.0	781.7	841.8
.800	.120	.080	66.0	862.0	862.0	940.5	1027.0
.816	.111	.073	67.8	1013.0	1055.8	1168.7	1294.5
.839	.094	.067	69.5	1092.0	1294.5	1450.4	1664.7
.850	.087	.063	75.8	2416.0	2626.0	2998.5	3793.9
.785	.139	.076	46.2	243.0	265.0	288.8	299.6
.803	.130	.067	48.8	330.0	335.6	366.8	381.2

Table 9 continued

Vapor composition(mole fraction)			Experimental data		Predicted dissociation pressure (psia)		
CH ₄	CO ₂	H ₂ S	°F	psia	Method 1*	Method 2 ⁺	Method 3 [#]
.711	.119	.170	72.0	942.0	710.2	747.1	816.0
.708	.121	.171	74.0	1071.0	811.1	852.7	942.2
.725	.119	.156	76.0	1219.0	1043.8	1101.8	1255.4
.688	.136	.176	76.0	1161.0	908.3	953.3	1064.7
Mean absolute deviation					85.9	117.2	203.8

* using the Kihara parameters in Table 5 with the Peng and Robinson equation of state.

+ using the Kihara parameters in Table 6 with the SRK equation of state.

using the modification by Ng and Robinson with their Kihara parameters.

Table 10. The Prediction Of The Dissociation Conditions Of Hydrates
Formed By Methane-Propane Binary Mixtures In Vapor-
Aq. Liquid-Hydrocarbon Liquid-Hydrate Equilibria.

EXPERIMENTAL DATA (43)				Predicted dissociation conditions			
Liquid phase, mole fraction		Temp.	Press.	Method 1*	Method 3 #		
CH ₄	C ₃ H ₈	°F	psia	Temp. °F	Press. psia	Temp. °F	Press. psia
.0000	1.0000	41.38	81.5	41.38	81.38	37.08	75.85
.0071	.9929	43.65	96.00	43.65	98.33	36.39	88.52
.0092	.9908	45.03	107.00	44.38	103.50	40.36	97.86
.0220	.9780	48.32	138.00	47.47	133.60	43.74	127.81
.0343	.9657	51.55	173.00	49.83	162.30	46.30	156.38
.0446	.9554	52.82	189.00	51.31	185.93	47.83	179.75
.0780	.9220	58.66	295.00	55.59	263.77	52.61	257.57
.1302	.8698	62.64	398.00	60.12	386.11	57.24	378.95
.1370	.8630	62.67	401.00	58.94	397.98	54.55	386.96
.2570	.7430	69.86	710.00	66.21	686.30	63.80	678.60
.4823	.5177	75.02	1175.00	70.27	1191.85	67.05	1182.28
.5635	.4365	75.98	1329.00	68.28	1327.17	63.87	1318.60
Mean absolute deviation				2.51	9.39	6.40	14.83

* using the Kihara parameters in Table 5 with the Peng and Robinson equation of state.

using the modification of Ng and Robinson with their Kihara parameters

Table 11. The Prediction Of The Dissociation Conditions Of Hydrates
Formed By Ethane-Propane Binary Mixtures In Vapor-
Aq. Liquid-Hydrocarbon Rich Liquid-Hydrate
Equilibria

EXPERIMENTAL DATA (3)			Predicted dissociation conditions				
Liquid phase		Temp.	Press.	Method 1 *		Method 3 #	
Mole fraction		F	psia	Temp.	Press.	Temp.	press.
C ₂ H ₆	C ₃ H ₈			F	psia	F	psia
.435	.565	44.2	214.	41.56	200.93	39.72	196.17
.523	.477	47.6	252.	45.09	237.95	43.29	232.56
.689	.311	52.0	324.	50.47	313.48	48.68	306.67
.689	.311	41.7	189.	56.32	336.40	53.30	324.41
.689	.311	43.2	207.	54.98	331.06	51.98	319.26
.689	.311	45.1	226.	53.66	325.81	50.90	315.10
.689	.311	45.4	234.	60.79	354.66	55.45	332.90
.689	.311	46.3	236.	53.39	324.75	50.42	313.26
.168	.832	40.9	130.	39.77	122.50	35.46	115.11
.168	.832	40.8	140.	39.78	122.52	35.43	115.07
.280	.720	40.4	156.	38.45	149.88	34.20	141.34
.280	.720	41.2	102.	37.97	148.91	33.15	139.27
Mean absolute deviation				4.43	48.40	6.42	46.94

* using the Kihara parameters in Table 5 with the Peng & Robinson equation of state

using the modification of Ng and Robinson with their Kihara parameters

Table 12. The Prediction Of Dissociation Conditions Of Hydrates
 Formed By Methane-Ethane-Propane Ternary Mixtures In
 Vapor-Aq. Liquid-Hydrocarbon Rich Liquid-Hydrate
 Equilibria

EXPERIMENTAL DATA (3)			Predicted dissociation conditions					
Liquid phase mole fraction			Temp. Press.		Method 1*		Method 3#	
CH ₄	C ₂ H ₆	C ₃ H ₈	°F	psia	°F	psia	°F	psia
.0255	.0000	.9745	49.4	150.	48.2	141.7	44.6	136.0
.0207	.1890	.7903	47.5	180.	44.0	177.2	38.8	166.7
.0175	.3140	.6685	44.5	229.	42.9	204.1	39.3	195.6
.0468	.0820	.8712	53.1	218.	48.3	208.3	40.8	193.8
.0418	.1810	.7772	51.8	234.	48.5	227.5	44.6	218.7
.0392	.2310	.7298	50.6	244.	48.1	236.3	44.8	228.5
.0870	.0540	.8590	57.7	307.	55.9	300.2	53.0	293.6
.0784	.1480	.7736	56.7	315.	54.0	306.9	51.1	299.6
.0725	.2120	.7155	54.6	320.	52.6	311.2	49.8	303.7
.0584	.3650	.5766	53.2	331.	48.9	319.8	45.8	310.8
.0123	.5170	.4707	49.3	293.	46.7	266.4	44.9	260.8
.0072	.7162	.2766	53.0	337.	51.6	343.5	48.4	330.8
.0051	.7990	.1959	55.2	396.	54.0	382.8	52.3	374.9
.0230	.5490	.4280	50.9	317.	49.2	307.5	47.3	301.2
.0140	.7260	.2600	54.6	396.	53.4	369.5	51.6	362.1
.0454	.5060	.4486	51.1	345.	49.8	342.0	47.5	334.3

Table 12 continued.

EXPERIMENTAL DATA (3)			Hydrate dissociation conditions					
Liquid phase mole fraction CH ₄			Temp.	Press.	Method 1 *		Method 3 #	
			°F	psia	°F	psia	°F	psia
.0353	.6160	.3487	53.5	373.0	51.7	366.5	48.3	353.6
.0297	.6770	.2933	54.9	409.0	53.6	384.9	51.7	377.4
Mean absolute deviation					2.2	11.7	5.3	19.5

* using the Kihara parameters in table 5 with the Peng & Robinson equation of state.

using the modification by Ng and Robinson with their Kihara parameters.

Table 13. The prediction of the dissociation conditions of hydrate formed by methane-ethane-propane-nitrogen-carbon dioxide mixture in vapor-aq. liquid-hydrate equilibria.

Vapor phase composition of the mixture (mole fraction)

methane = .965 propane = .018 carbon dioxide = .006
ethane = .09 nitrogen = .002

EXPERIMENTAL DATA (16)

Temp. F	Press. psia	Predicted dissociation press. psia	
		Method 1*	Method 3#
33.0	183.0	191.2	209.2
35.0	207.0	217.9	237.6
40.0	294.0	303.7	327.4
45.0	414.0	426.1	455.1
50.0	587.0	607.9	643.7
58.2	1077.0	1169.5	1223.9
62.0	1506.0	1725.8	1764.3
Mean absolute deviation		53.4	84.7

* using the Kihara parameters in Table 5 with the Peng and Robinson equation of state.

using the modification of Ng and Robinson with their Kihara parameters.

Table 14. Vapor-Hydrocarbon Rich Liquid-Aq. Liquid-Hydrate
Equilibria Of Natural Gas Mixtures

EXPERIMENTAL DATA (38)

Mixture identification no.	Composition of the liquid(hydrocarbon rich) phase(mole fraction)						
	N ₂	CH ₄	C ₂ H ₆	C ₃ H ₈	i C ₄ H ₁₀	nC ₄ H ₁₀	CO ₂
1	.003		.313	.515	.169	.	
2	.002	.022	.306	.508	.162		
3	.002	.219	.247	.408	.124		
4			.234	.304	.196	.266	
5			.215	.489	.238		.058
6			.170	.386	.189		.255

Mixture identification no.	EXPERIMENTAL DATA		Predicted dissociation conditions			
	Temp. °F	Press. psia	Method 1 * Temp. °F	Press. psia	Method 3 # Temp. °F	Press. psia
1	40.2	168.0	40.2	171.06	38.9	165.
2	46.5	227.0	45.38	218.04	45.5	223.
3	65.3	696.0	62.97	679.55	64.9	694.
4	35.0	100.0	35.00	99.35	34.9	99.
5	44.4	175.0	45.70	179.29	42.1	172.
6	51.4	340.0	56.13	363.06	49.5	334.
Mean absolute deviation			1.58	9.4	1.2	3.2

* using the Kihara parameters in Table 5 with the Peng & Robinson equation of state

using the modification of Ng and Robinson with their Kihara parameters

CHAPTER 9

Discussion, Conclusion and RecommendationsDiscussion

The main aim of the present work is to find better values for $\Delta\mu_{0,0}^{\beta-\alpha}$ and $\Delta h_{0,0}^{\beta-\alpha}$ and obtain better Kihara parameters based on the experimental data. The Kihara parameters ϵ_{AB}/k and σ_{AB} that are currently available were based on estimated values of $\Delta\mu_{T,P}^{\beta-\alpha}$ and $\Delta h_{T,P}^{\beta-\alpha}$. As mentioned earlier present work adopted a different route in optimizing the Kihara parameters from that of Parrish and Prausnitz. Parrish and Prausnitz related the Kihara parameters ϵ_{AB}/k and σ_{AB} to the critical temperature and acentric factor of the enclathrated molecular species respectively. Hence one could conclude that the contribution by the lattice molecules towards the ϵ_{AB}/k and σ_{AB} is independent of the nature of the enclathrated molecule which is questionable. The other inaccuracy that crept into the Kihara parameters of Parrish and Prausnitz was caused by the usage of less accurate core diameters for the enclathrated molecular species which were considerably different from the most recent values of Tee et. al. (42). The third draw back was that Parrish and Prausnitz assumed that n-butane does not enter into the hydrate lattice which was later shown to be untrue.

In spite of these shortcomings the thermodynamic model perfected by Parrish and Prausnitz could be considered to be a major achievement in hydrate research.

Holder and co-workers (3,11) used the arithmetic mean approximation and geometric mean approximation for σ_{AB} and ϵ_{AB}/k respectively. Since Kihara parameters for water were not accurately determined and the arithmetic mean and geometric mean approximations are not quite accurate, the Kihara parameters that were reported by them are less accurate. The present method that directly optimized ϵ_{AB}/k and σ_{AB} overcame the geometric mean and arithmetic mean approximations.

The next modification that followed the Parrish and Prausnitz model was by Ng and Robinson (38). They used the same core diameters of Parrish and Prausnitz, but used α_J an arbitrary adjustable parameter with the van der Waal's and Platteeuw's model. Hence one could infer that the additional parameter α_J introduced by Ng and Robinson overcomes the inaccuracy introduced by the numerical values of the Kihara parameters. The predicted dissociation pressures by the present method that fell within the same range as that of Ng and Robinson's justifies the above statement.

It was shown that the Peng and Robinson equation of state is much superior to that of the Soave modified Redlich Kwong equation state in the prediction of the hydrate properties.

Hence one could also relate the less accurate predictions of hydrate properties by Parrish and Prausnitz (4), and Holder (3) to the equation of state that was used.

In using an equation of state for the prediction of thermodynamic properties in VLE it always occurs that there is a possibility of error washout if one adheres to the same equation of state throughout the procedure. But in hydrate models what one does is to equalize a statistical mechanical model to classical thermodynamic model that in no way allows the possibility of error washout. Hence hydrate models could provide one with a better method of comparing the equations of state.

In determining the water content in the vapor phase in equilibrium with the hydrate phase Ng and Robinson followed the same fundamental equation as Sloan et. al. (12) but used their modified form of the van der Waals and Platteeuw model Peng and Robinson equation of state, and calculated the empty hydrate vapor phase fugacity from the experimental data of the water content content in equilibrium with the hydrate phase in the two-phase region hydrate-water. Unfortunately Ng and Robinson could not demonstrate the applicability of this method for other systems due to lack of experimental data. It was later known (39) that the data that were used for Structure II were inaccurate. The present work calculated the empty hydrate

vapor pressure in a manner quite unrelated to that of Peng and Robinson, but used the experimentally obtained values to demonstrate the applicability for the determination of the equilibrium water content with the hydrate phase. The second method that was proposed overcomes the usage of the empty hydrate vapor pressure values, but provides one with the same range of accuracy. As mentioned earlier the second method cannot be used in the three-phase region where ice or liquid water co-exists. It should be noticed in Figure 9 the empty hydrate vapor pressure of isobutane falls below that of the others. This could be due to the lattice distortion and the restricted rotation of the isobutane molecule. Due to the larger molecular size isobutane hydrate cannot be described by van der Waals and Platteeuw's model. Inadequacy of the van der Waals and Platteeuw's model could account for the lower empty hydrate vapor pressure obtained by using isobutane hydrate.

In the prediction of the water content in the vapor phase in equilibrium with the hydrates Ng and Robinson followed a similar approach to Sloan et. al.. The main difference lies in the calculation of the fugacity of water in the empty hydrate lattice. Ng and Robinson have expressed the fugacity of water in the empty hydrate lattice as an arbitrary function of temperature and pressure whose constants were calculated from the

experimental data. The present work followed the same approach as Sloan et. al. and expressed the fugacity of water in the empty hydrate lattice as a function of the empty hydrate vapor pressure, fugacity coefficient and the Poynting correction. The fugacity coefficient of water in the empty hydrate lattice was assumed to be unity. This assumption was based on the fact that the empty hydrate vapor pressure is in the region of the vapor pressure of ice. The fact that the predicted vapor phase water content using the empty hydrate vapor pressure (method A) and the vapor pressure of ice (method B) are more or less the same, further confirms the validity of the assumption that the fugacity coefficient of water in the empty hydrate lattice is unity.

Conclusion

The author wishes to conclude the following;

- a. $\Delta\mu_{\beta-\alpha}^{0,0}$ and $\Delta h_{\beta-\alpha}^{0,0}$ were experimentally obtained.
- b. The Kihara parameters were obtained using both the Soave modified Redlich Kwong, and Peng and Robinson equations of state.
- c. The Peng and Robinson equation of state explains the behavior of hydrates better than the Soave modified Redlich Kwong equation of state.
- d. The present work demonstrated the applicability of the empty hydrate vapor pressure data for the determination of the water content in equilibrium with the hydrate phase.
- e. It is also possible to use the vapor pressure of ice in the determination of the water content in equilibrium with hydrates.

Recommendations

The author wishes to suggest the following for future investigations.

- a. The van der Waals and Platteeuw's, and Parrish and Prausnitz's models should be modified to accommodate the lattice distortion and restricted rotation of larger enclathrated molecules.
- b. The resulting model from "a" should be used in conjunction with isobutane mixtures such as isobutane and propane to test its applicability.
- c. Effort should be made to determine experimentally the water content in the vapor phase in equilibrium with Structure II hydrates.

LITERATURE CITED

1. Katz, L. K., J. Pet. Tech., 23, 419 (1971).
2. Katz, L. K., J. Pet. Tech., 557 (1972).
3. Holder, G. P., Ph. D. Thesis, Univ. of Michigan, Ann Arbor, Michigan (1976).
4. Parrish, W. R. and Prausnitz, J. M., Ind. Eng. Chem. Process. Des. Dev., 11, 26 (1972).
5. van der Waals and Platteeuw, S. C., Adv. Chem. Phys., vol.2, pp 1-55, Inter Science Publishers Inc., New York.
6. Von Stackelberg, M. and Muller, H. R., Electrochem, 58, 25 (1954)
7. Allen, K. W. and Jeffrey, G. A., J. Chem. Phys., 38 (1963).
8. Sortland, L. D. and Robinson, D. B., Can. J. Chem. Eng., 42, 38 (1964).
9. Barrer, R. M. and Ruzicka, D. J., Trans. Faraday Soc., 58, 2239, 2253, 2262 (1965).
10. Childs, W. C., J. Phys. Chem., 68, 1834 (1964).
11. Holder, G. P. and Cobin, G., 86th National AIChE Meeting, Houston, Texas, April 1-6 (1979).
12. Sloan, E. D., Khoury, F. M. and Kobayashi, R., Ind. Eng. Chem. Fundam., 15, 318 (1976).
13. Ayoyagi, K., Kyoo, Y. S., Sloan, E. D., Dharmawardhana, P. B., and Kobayashi, R., Proceedings 58th Annual G. P. A. Convension (1979).

14. Engineering Data Book, Gas Processors Association, Tulsa, Oklahoma (1977).
15. Pauling, L., J. Am. Chem. Soc., 57, 2680 (1935).
16. Deaton, W. M. and Frost, E. M., U. S. Bureau of Mines Monographs, 8, (1946).
17. Cole, R., Ph.D. Thesis, Univ. of Ill., (1952).
18. Bragg, W. H., Proc. Phys. Soc. (London), 34, 98 (1922).
19. Barnes, W. M., Proc. Roy. Soc., 125, 610 (1929).
20. Stewart, G. W., Phys. Rev., 37, 9 (1931).
21. Amaldi, J. Physik Zeits., 32, 914 (1931).
22. Meyer, H. H. Ann. d. Physik, 5, 701 (1930).
24. Morgan, J. and Warren, B. E., J. Chem. Phys., 6, 666 (1938).
25. Wollen, E. O. and Davidson, W. L. and Shell, C. G., Phys. Rev., 75, 1348 (1949).
26. Claussen, W. F., J. Chem. Phys., 19, 1425 (1951).
27. Schneder, W., Sammlung Chem. Und Chem. Tech. Vort XXIX, pp 1 (1926 - 27).
28. Clausen, W. F., J. Chem. Phys., 19, 259, 662 (1951).
29. Pauling, L. and Marsh, R. E. Proc. Natl. Acad. Sci. U. S., 38, 112 (1952).
30. Stackelberg, M. Von and Muller, H. G., J. Chem. Phys., 19, 1319 (1951).
31. Wilcox, W. I., Carson, D. B. and Katz, D. L., Ind. Eng. Chem., 33, 662 (1941).
32. Katz, D. L., Am. Inst. Mining and Metal. Eng., Tech. Publ.

No. 1748.

- 33 Hammerschmidt, E. G., I. & E. C., 26, 851, (1934).
34. McKoy, V. and Sinanoglu, O., J. Chem. Phys., 38, 2946 (1963).
35. Davidson, D. W., Water, vol. 2, 115, Plenum Press, New York (1973).
36. Hill, T. L., Introduction to Statistical Thermodynamics, Reading, Mass., Addison-Wesley Pub. Co. (1960).
37. Nagata, F. and Kobayashi, R., Ind. Eng. Chem. Fundam., 5, 344, 466 (1964).
38. Ng, H. and Robinson, D. B., Ind. Eng. Chem. Fundam., 15, 293, (1976).
39. Kobayashi, R., Personal Communication.
40. Mashman, J., Mathematical Methods of Digital Computers vol II, Edited by Ralston and Wilf, John Willey and Sons, 1967, pp 249 - 263.
41. Zerpa, C. O., Dharmawardhana, P. B., Parrish, W. R. and Sloan, E. D., Chem. Eng. Data, 24, 26 (1979).
42. Tee, L. S., Gotoh, S. and Steward, W. E., I. & E. C. Fundam., v 5, 3, 363 (1966).
43. Verma, V. K., Ph. D. Thesis, Univ. of Michigan, Ann Arbor (1974).
44. Ng, H. and Robinson, D. B., Ind. Eng. Chem. Fundam., v 15, 4, 293, (1976).
45. Hutton, J. M. and Robinson, D. B., M. S. Thesis, Univ. of Edmonton (1965).

46. Ng, H. and Robinson, D. B., AICHE J., v 22, 656 (1976).
47. Personal Communication, Exxon Production Research Company, (2-20-1980).
48. Ng, J. H. and Robinson, D. B., Fluid Phase Equilibria, 1, 4, 283 (1978).
49. Jhaveri, J. and Robinson, D. B., Can. J. Chem. Eng., 43, 75, (1965).
50. Marshall, D. R., Saito, S. and Kobayashi, R., AICHE J., 10, 202 (1964).
51. McLeod, H. O. and Campbell, J. H., Petrol. Trans. AIME., 222, 590 (1961).
52. Reamer, H. H., Selleck, F. T. and Sage, B. H., Petrol. Trans. AIME., 195, 197 (1952).
53. Roberts, O. L., Brownscombe, E. R., Howe, L. S. and Ramser, H., Petro. Eng., 12 (6), 56 (1941).
54. Diepen, G. A. M. and Scheffer, F. E. C., Rec. Trav. Chim., 69, 593 (1959).
55. Snell, L. E., Otto, F. D. and Robinson, D. B., AICHE. J., 7, 483 (1961).
56. van Cleef, A. and Diepen, G. A. M., Rec. Trav. Chem., 79, 582 (1960).
57. Hafemann, D. R. and Miller, L. J., J. Phys. Chem., 73, 1398 (1969).
58. Schneider, G. R. and Farrer, J., Office of Saline Water Res.

Progr. Rept. No. 292, Jan. 1968.

59. Rouher, O. S. and Barduhn, A. J., *Desalination*, 6, 57 (1969).
60. van Cleeff, A. and Diepen, G. A. M., *Rec. Trav. Chim.*, 79, 582 (1960).
61. van Cleeff, A. and Diepen, G. A. M., *ibid*, 84, 1085 (1965).
62. van Cleeff, A. and Diepen, G. A. M., *ibid*, 186, 83 (1949).
63. Unruh, C. H. and Katz, D. L., *Trans. AIME*, 186, 83 (1949).
64. Korvezee, A. E. and Scheffer, F. E. C., *Rec. Trav. Chim.*, 50, 256 (1931).
65. Noaker, L. J. and Katz, D. L., *Trans. AIME.*, 201, 237 (1954).
66. Selleck, F. T., Carmichael, L. T., and Sage, R. H., *Ind. Eng. Chem.*, 44, 2219 (1952).
67. Barrer, R. M. and Edge, A. V. J., *Proc. Roy. Soc. (London)*, A 300 (1460), 1 (1967).
68. Hafemann, D. R. and Miller, S. L., *J. Phys. Chem.*, 73, 1398, (1969).
69. Wilhelm, E., Rubin, B. and Robet, J. W., *Chem. Review*, 219, 77 (1977)

Appendix A.

Experimental Data For The Filling Of The Hydrate.

	T ° C	P KPa	Moles of cyclo prop- pane in hydrate	Moles of water in hydrate
St I	7.020	176.25	0.03482	0.26920
	5.307	142.39	0.04276	0.33099
	5.125	138.39	0.04602	0.35618
	5.000	135.99	0.03362	0.26032
	5.535	128.28	0.03118	0.24140
	4.275	124.02	0.02385	0.18471
	4.000	120.12	0.04658	0.36077
	3.750	115.75	0.04568	0.35372
	3.505	115.20	0.04156	0.32191
	3.000	101.24	0.05171	0.40055
	2.765	102.74	0.04922	0.38144
	2.540	99.35	0.06063	0.47004
	2.305	96.69	0.04182	0.32422
	2.205	95.35	0.04759	0.36889
	2.000	93.35	0.04964	0.38499
St II	1.120	81.01	0.01883	0.15052
	1.120	81.62	0.02221	0.17713
	1.100	81.09	0.02888	0.23042
	1.100	81.23	0.05051	0.40250
	1.025	79.87	0.02714	0.21694
	1.025	81.30	0.04017	0.32079

0.920	77.35	0.03831	0.30618
0.645	73.41	0.03058	0.24480
0.870	100.98	0.03921	0.31280
0.420	70.10	0.03725	0.29752
0.225	66.71	0.03296	0.26352
0.105	65.66	0.04372	0.35011
0.090	64.55	0.03004	0.24032
0.025	64.37	0.06310	0.50565
0.010	64.02	0.05872	0.46959

The Listing of the Sources of Data that were Used in Hydrate

	<u>Correlations</u>
COMPONENT	REFERENCE
methane	16, 49, 50, 51
ethane	52, 53
propane	16, 52
cyclo-propane	57
isobutane	58, 59
nitrogen	49, 50, 60, 62
oxygen	62
carbon dioxide	16, 63
hydrogen sulfide	64, 65, 66
xenon	6, 57, 67
sulfur hexafluoride	8
methane-ethane	16
methane-carbon di- oxide	45
methane-carbon di- oxide-hydrogen sulfide	45
methane-isobutane	44
carbon dioxide-propane	44
nitrogen-propane	48
methane-propane	16, 43
ethane-propane	3
n butane-methane	46
methane-propane- hydrogen sulfide	47



APPENDIX C

Parameters For Calculating Langmuir Constant
Between 260 K and 300 K

GAS	small cavities of St.I		large cavities of St.I	
	$A * 10^3$	B	$A * 10^2$	B
Methane	2.7711	2752.8047	1.4865	2878.0682
Ethane	0.0	0.0	0.4071	3820.7119
Propane	0.0	0.0	0.0	0.0
n-Butane	0.0	0.0	0.0	0.0
Iso-Butane	0.0	0.0	0.0	0.0
Nitrogen	17.7986	1931.5130	5.7883	1669.2292
Carbon dioxide	1.5227	2943.9948	1.0242	3172.6655
Hydrogen sulfide	2.3458	3701.3170	1.3532	3739.3355
	small cavities of St.II		large cavities of St.II	
Methane	2.1778	2713.4259	6.6777	2310.0682
Ethane	0.0	0.0	2.9157	3277.9254
Propane	0.0	0.0	1.3212	4506.9810
n-Butane	0.0	0.0	0.0404	2687.9744
Iso-Butane	0.0	0.0	0.0788	3083.9044
Nitrogen	14.8724	2002.6644	15.6182	1319.4734
Carbon dioxide	1.1620	2837.3018	5.3986	2478.0545
Hydrogen sulfide	1.8306	3671.9126	6.4567	2976.4243

Nomenclature

a	=	core radius, \AA
a_w	=	activity of water
C_{iJ}	=	Langmuir constant of the component J in cavity type i
F	=	free energy
f	=	fugacity
h_{iJ}	=	molecular partition function of molecule type J in cavity type i
h	=	enthalpy
N	=	no. of molecules
k	=	Boltzmann's constant
P	=	pressure, Atm.
P_r	=	dissociation pressure of the reference hydrate
r	=	radial coordinate, \AA
R	=	gas constant
T	=	temperature
v	=	molar volume, $\text{cm}^3/\text{gm. mole}$
y_{iJ}	=	probability of finding a molecule J in cavity type i
Y	=	vapor phase mole fraction
Z	=	coordinate number

Greek Letters

- ϵ = depth of intermolecular potential function
- μ = chemical potential difference, cal./gm. mole
- ν_i = no. of cavities of type i per mole of water in a unit cell
- σ = distance parameter when the Kihara potential is zero, A
- δ = polynomial defined in equation (8.6)
- λ = absolute activity
- Ξ = grand partition function

Superscript

- β = empty hydrate
- α = ice phase
- H = hydrate phase
- L = liquid phase
- $\beta-\alpha$ = difference between empty hydrate and ice
- $\beta-L$ = difference between empty hydrate and liquid water
- V = vapor phase

Subscript

0,0	=	property at 273.15 K and zero Atm. absolute pressure
J,K,M	=	component identification
i	=	cavity type
W	=	water
r	=	reference hydrate
Q	=	host molecule

DOCUMENTATION OF THE COMPUTER PROGRAMES

1. MYPEN.FOR
2. LIQE.FOR
3. W.FOR
4. WICE.FOR

THE COMPUTER PROGRAM MYPEN.FOR

The computer program MYPEN.FOR calculates the hydrate formation conditions for natural gas mixtures in three phase equilibria. The computer program is written in Fortran IV. The component identification numbers are given below.

1	=	methane			
2	=	ethane	6	=	pentane
3	=	propane	7	=	nitrogen
4	=	n-butane	8	=	carbon dioxide
5	=	isobutane	9	=	hydrogen sulfide

The Kihara parameters, the numbers to identify the cavities of Structures I and II that could be filled by the guest molecules, solubility data and the critical properties of the components are to be supplied to the main program through the data file FOR15.DAT. in the following sequence;

The data have to be entered in four sets with one line per component.

Set I = The Kihara parameters

$\epsilon/k, \sigma, a$ for component 1

. . .

. . .

. . .

. . .

$\epsilon/k, \sigma, a$ for component 9

Set II = Identification numbers to indicate the possibility of filling of the hydrate cavities of Structures i and II. Arbitrary numbers 20. and 0.0 were used by the author to indicate filled and empty cavities. The data sequence is illustrated below.

small cavity, large cavity, small cavity, large cavity . . . COMP. 1
 Structure I Structure I Structure II Structure II

. . . .

small cavity, large cavity, small cavity, large cavity . . . COMP. 9
 Structure I Structure I Structure II Structure II

SET III = The solubility data to calculate the solubility of each component in liquid water. The solubility was calculated by the equation

$$R \ln (\text{mole fraction of component } i \text{ in water}) = A + B/T + C \ln T + DT .$$

Where A, B, C and D are constants. The numerical values for the constants A, B, C and D for all the nine components were taken from the work of E. Wilhelm et. al. (69).

The data sequence is illustrated below.

A, B, C, D for component 1

. . . .

. . . .

. . . .

. . . .

A B C D for component 9

SET IV = The critical properties. The data sequence is given below.

critical, temp.	critical, pressure	critical, volume	acentric factor	COMPONENT 1
.	.	.	.	
.	.	.	.	
.	.	.	.	
.	.	.	.	
critical, temp.	critical, pressure	critical, volume	acentric factor	COMPONENT 9

The equilibrium data have to be supplied to the computer program through the data file FOR02.DAT in the following sequence.

Temperature ($^{\circ}$ F), first guess, for pressure (psi)	vapor phase mole fraction of components 1 to 9	DATA POINT 1
.	.	
.	.	
.	.	
.	.	DATA POINT n

Hydrate structure and the number of data points have to be supplied to the program at execution according to the FORMAT(2I).

THE COMPUTER PROGRAM LIQE.FOR

The computer program LIQE.FOR calculates the hydrate formation conditions for natural gas mixtures in four phase (hydrate-aq. liquid-hydrocarbon rich liquid-vapor) equilibria. LIQE.FOR computer program uses the same data file FOR15.DATA that has been already described under the computer program MYPEN.FOR. The equilibrium data have to be supplied to the computer program through the data file FOR02.DAT in the following sequence.

First guess for temperature of	, first guess for pressure psi	, liquid phase mole fraction of the components 1 to 9	DATA POINT 1
.	.	.	
.	.	.	
.	.	.	DATA POINT n

Hydrate structure and the number data points have to be supplied to the program at execution according to the FORMAT(2I).

THE COMPUTER PROGRAM W.FOR

The computer program W.FOR calculates the water content of methane in equilibrium with the hydrate phase by taking the empty hydrate vapor pressure as the basis. The critical temperature, critical pressure, critical volume and acentric factor should be supplied through the data file FOR02.DAT. The temperature in K, pressure in psi. and the preliminary guess for the water content in the vapor phase in lbs./MMcf have to be supplied to the program through the data file FOR01.DAT. The number of predictions needed should be supplied at the execution of the program.

THE COMPUTER PROGRAM WICE.FOR

The computer program WICE.FOR is similar to W.FOR but the program takes the vapor pressure of ice as the basis in the calculations.

C MYPEN.FOR

```

    DIMENSION CL(4,10),PHI(10),Y(10),DMU(2)
    DIMENSION EP(10),SIGP(10),CP(10),CB(4,10),SO1(10)
1,SO2(10),SO3(10),SO4(10),TC(10),PC(10),VC(10),W(10)
    DIMENSION D(2),VU(2),VL(2)
140  FORMAT(1X,4(F10.5,X))
    READ(4,10)NHY,NN
    NCOMP=9
    PINCX=.001
    DO 21 I=1,NCOMP
    READ(15,10) EP(I),SIGP(I),CP(I)
304  FORMAT(1X,4(F10.5,X))
21  CONTINUE
    DO 3 I=1,NCOMP
    READ(15,10)CB(1,I),CB(2,I),CB(3,I),CB(4,I)
3  CONTINUE
    DO 4 I=1,NCOMP
    READ(15,10) SO1(I),SO2(I),SO3(I),SO4(I)
4  CONTINUE
    DO 6 I=1,NCOMP
    READ(15,10)TC(I),PC(I),VC(I),W(I)
6  CONTINUE

    DD 1 IX=1,NN
    READ(02,10)T,P,Y(1),Y(2),Y(3),Y(4),Y(5),Y(6),Y(7),Y(8),Y(9)
    DS=.0
    NG=NG+1
    NSF=0
    NR=0
    NEWPT=0
    PEX=P
    P=P/14.696
    T=(T-32.)*5./9.+273.15
530  CONTINUE
    CALL LANG(T,CL,EP,SIGP,CP,NCOMP,CB)
25  FORMAT(1X,2(F10.5,X))
    CL(4,4)=4.040815/T*EXP(2587.9744/T)
    CL(4,5)=7.046619/T*EXP(3083.9044/T)
    CALL ACT(SO1,SO2,SO3,SO4,T,ACTI,NCOMP,Y)
111  CONTINUE
    DO 660 K=1,2
112  CALL PENG(T,P,NCOMP,Y,PHI,TC,PC,VC,W)
    CALL AMUC(T,P,NHY,AMU)
10  FORMAT(10G)
    IF(NHY.GT.1) GO TO 18
    DO 17 I=1,NCOMP
    IF(Y(I).EQ..0) GO TO 610
    CSML=CL(1,I)*PHI(I)
    CSMLS=CSMLS+CSML

```

```

        CLG=CL(2,I)*PHI(I)
        CLGS=CLG+CLGS
610    CONTINUE
17     CONTINUE
        AM1=2.*ALOG(1.+CSMLS)/46.
        AM2=6.*ALOG(1.+CLGS)/46.
        DMCAL=(AM1+AM2)*1.987*T+ACTI
        CSMLS=.0
        CLGS=.0
        GO TO 20
18     DO 19 I=1,NCOMP
        IF(Y(I).EQ..0) GO TO 620
        CSML=CL(3,I)*PHI(I)
        CSMLS=CSMLS+CSML
        CLG=CL(4,I)*PHI(I)
        CLGS=CLG+CLGS
620    CONTINUE
19     CONTINUE
        AM1=16.*ALOG(1.+CSMLS)/136.
        AM2=8.*ALOG(1.+CLGS)/136.
        DMCAL=(AM1+AM2)*1.987*T+ACTI
        CSMLS=.0
        CLGS=.0
20     DEL=AMU-DMCAL
        WRITE(03,711)P,DEL
711    FORMAT(1X,2(F10.4,X))
        WRITE(20,701)P,DEL,DPS,DS,AMU,NG,NR
701    FORMAT(1X,'P,DEL,DPS,DS,AMU,NORD,NSF',5(F10.3,X),2(13,X))
        IF(NR.EQ.1) GO TO 702
694    CONTINUE
        D(K)=DEL
662    DPS=ABS(DEL)*100./AMU
        IF(DPS.LT..1) GO TO 80
        P=P+PINCX
660    CONTINUE
        DPS=(DEL/AMU*100)
        IF(ABS(DPS).LT..1) GO TO 80
        NEWPT=NEWPT+1
        IF(NEWPT.EQ.1) GO TO 300
        NTEST=DS/ABS(DS)+DEL/ABS(DEL)
        IF(NTEST.EQ.0) GO TO 702
        IF(ABS(DEL).GT.ABS(DS)) GO TO 703
800    PS=P
        DS=DEL
        P=P-DEL/((D(2)-D(1))/PINCX)
        K=0
        GO TO 111
80     T=(T-273.15)*9./5.+32.
        P=P*14.696
        DPSUM=DPSUM+ABS(PEX-P)
        WRITE(10,43)Y(1),Y(8),T,PEX,P

```

```
7      K=0
      N=0
      NR=0
      NC1=0
      NU1=0
      NUM=0
      NU=0
      NRC=0
43     FORMAT(1X,2(F8.5,X),3(F7.1,X))
1      CONTINUE
      PDMN=DPSUM/MN
      WRITE(10,34)PDMN
34     FORMAI(1X,F10.2)
      STOP

702    CONTINUE
      DEL=AMU-DMCAL
      DPS=ABS(DEL)*100./AMU
      IF(NR.EQ.1) GO TO 51
51     IF(DPS.LT..1) GO TO 80
      DSAVE=DEL
52     FURMAT(1X,2(F10.3,X))
      NR=1
      NRC=1+NRC
      IF(NRC.GT.1) GO TO 668
      U1=DEL
      U2=DS
      U3=P
      U4=PS
44     FORMAT(1X,4(F10.5,X))
      GO TO 690
668    U2=DEL
      U4=P
      NUM=DEL/ABS(DEL)
      IF(NUM)670,672,676
670    U1=AMAX1(VU(1),VU(2))
      GO TO 675
676    U1=AMIN1(VU(1),VU(2))
      GO TO 675
672    WRITE(4,681)
681    FURMAT(1X,'CHECK CONVERGENCE')
      STOP
675    CONTINUE
      DO 682 II=1,2
      IF(U1.EQ.VU(II)) U3=VL(II)
682    CONTINUE
690    P=(U1*U4-U2*U3)/(U1-U2)
      VU(1)=U1
      VU(2)=U2
      VL(1)=U3
      VL(2)=U4
```



```
49  FORMAT(1X,'VU &VL',4(F10.4,X))  
    GO TO 111  
703  T=(T-273.15)*9./5.+32.  
     P=PS*14.696  
     WRITE(10,704)T,PEX,P  
704  FORMAT(23X,'*',3(F10.3),X)  
     GO TO 7  
     STOP  
     END
```

```

SUBROUTINE AMUC(T,P,NHY,DMU2)
PR(X)=EXP(AR+BR/X+CR*ALOG(X))
C INPUT T IN DEG K, P IN MM HG, DTF IN DEG K
VINT=0.0
VINT1=0.0
VINT2=0.0
10 FURMAT(3F)
IF(NHY.GT.1) GO TO 20
C CALCULATE STRUCTURE I PROPERTIES
V=6./46.
AML=.001449
BML=4579.6
GO TO 30
C CALCULATE STRUCTURE II PROPERTIES
20 V=8./136.
AML=.013136
BML=4653.4
30 CML=AML/T*EXP(BML/T)
TC=397.8
TR=T/TC
W=.127
PC=54.23
R=82.056
B=(.083-.422/(TR**1.6)+W*(.139-.172/(TR**4.2)))*
1R*TC/PC
PHI=EXP((P*B)/(R*T))
C CALCULATE LN OF ACTIVITY
A=(-1436.3*DTF)/(1.987*273.15**2)
IF(NHY.GT.1) GO TO 60
C CALCULATE STRUCTURE I PROPERTIES
AR=-1212.2
BR=44344.0
CR=187.719
DV=4.598
DH=332.
DM=310.
GO TO 70
C CALCULATE STRUCTURE II PROPERTIES
60 AR=-1023.14
BR=34984.3
CR=159.923
DV=4.998
DH=245.
DM=224.
70 TU=273.15
C CALCULATE MUO/RTO AT PO,TU
DMUO=(DM+DV*PR(TU)*.0242152)/(1.987*TO)
C CALCULATE ENTHALPY INTEGRAL
HINT=(1./1.987)*(DH*(1./T-1./TO)+2616.398*(1./T-
11./TO)+20.6166*ALOG(T/TO)-.021163*(T-TO))
IF(T.LT.273.15) HINT=1.*DH*(1./T-1./273.15)/1.987

```

```
C      CALCULATE VOLUME INTEGRAL
      N=ABS(273.15-T)
      DO 40 I=1,N+1
      DT=1.
      TI=TI+DT
      IF(I.EQ.1)TI=TO
      DPRDT=((-BR/TI+CR)/TI)*PR(TI)
      VINT1=(DPRDT/TI)*(DV/82.056)
      VINT=.5*(VINT1+VINT2)+DT*VINT
      VINT2=VINT1
40     CONTINUE
      DMPR=(DMUD+HINT+VINT)*1.987*T
115    FORMAT(1X,F15.2)
      DMU2=DMPR+DV*.0242152*(P-PR(T))
      RETURN
      END
```

```

SUBROUTINE LANG(T,CL,EP,SIGP,CP,NCOMP,CB)
DIMENSION A(4),Z(4),CB(4,10),KS(10),CL(4,10),
IX(20),WT(20),SIGP(10),EP(10),CP(10)

```

```

NPT=10

```

```

NP=5

```

```

DATA(X(J),WT(J),J=6,10)/.1488743389,.29552422147,
1.4333953941,.2692667193,.6794095683,.2190
2863625,.86506336627,.1494513492,.9739065285,
3.0666713443/

```

```

DATA (A(I),Z(I),I=1,4)/3.95,20.,4.3,24.,3.91,20.,4.73,
128./

```

```

DATA PI,BK/3.1416,1.3804E-16/

```

```

DO 22 J=1,NP

```

```

X(J)=-X(NPT-J+1)

```

```

WT(J)=WT(NPT-J+1)

```

22

```

CONTINUE

```

```

KBLDW=0

```

```

DO 5 J=1,NCOMP

```

```

DO 1 I=1,4

```

1

```

CL(I,J)=.0

```

```

C=CP(J)

```

```

EK=EP(J)

```

```

EC=EP(J)*BK

```

```

RC=SIGP(J)*1.122462

```

```

DO 5 I=1,4

```

```

IF (CB(I,J).LT.1.) GO TO 5

```

```

RCA=RC/A(I)

```

```

CA=C/A(I)

```

C

```

NEWTON RAPSON METHOD FOR FINDING LIMITS , YL

```

C

```

FIRST GUESS S=.4

```

```

S=.4

```

```

RCA6=RCA**6

```

```

RCA12=RCA**12

```

```

DO 2 N=1,20

```

```

IF (S.GT.1.0.OR.S.LE.0.0) GO TO 6

```

```

UM=1./(1.-S-CA)

```

```

UP=1./(1.+S-CA)

```

```

UM5=UM**5

```

```

UP5=UP**5

```

```

DA4=UM5+UP5

```

```

DA5=UM5*UM+UP5*UP

```

```

DB6=DA4+CA*DA5

```

```

UM11=UM**11

```

```

UP11=UP**11

```

```

DA10=UM11+UP11

```

```

DA11=UM11*UM+UP11*UP

```

```

DB12=DA10+CA*DA11

```

```

DB=RCA12*DB12-2.*RCA6*DB6

```

```

A10=UM11/UM-UP11/UP

```

```

A11=UM11-UP11
B12=(.1*A10+CA*A11/11.0)
A4=UM5/UM-UP5/UP
A5=UM5-UP5
B6=A4/4.+CA*A5/5.
B=RCA12*B12-2.*RCA6*B6
W=Z(I)*EK/(2.*S*T)*B
DWY=-W/S+Z(I)*EK*DB/(2.*S*T)
DS=S-(W-10.)/DWY
IF(ABS((DS-S)/DS).LT.0.01) GO TO 3
2  S=DS
3  YL=S
C  GAUSSIAN INTEGRATION
P=2.*PI*A(I)**3/(T*136.2)*YL
SQ=.0
DO 4 N=1,NPT
Y=YL*(X(N)+1.)/2.
UP=1./(1.+Y-CA)
UM=1./(1.-Y-CA)
UP5=UP**5
UM5=UM**5
A4=UM5/UM-UP5/UP
A5=UM5-UP5
B6=A4/4.+CA*A5/5.
UP11=UP**11
UM11=UM**11
A10=UM11/UM-UP11/UP
A11=UM11-UP11
B12=(.1*A10+CA*A11/11.)
B=RCA12*B12-2.*RCA6*B6
W=Z(I)*EK/(2.*Y*T)*B
4  SQ=SQ+EXP(-W)*Y**2*WT(N)
270 CL(I,J)=P*SQ
5  FORMAT(1X,4(F10.5,X))
CONTINUE
RETURN
6  KBLW=2
WRITE(4,7)
7  FORMAT(1X,'PROBLEM BLOW UP')
RETURN
END

```

```

SUBROUTINE PENG(T,P,NCOMP,Y,PHI,TC,PC,VC,W)
DIMENSION TC(10),PC(10),W(10),B(10),PHI(10),VC(10),AK(10)
1,A(100,100),Y(10),TR(10),PR(10),CG(100,100)
DATA CG(1,7),CG(1,8),CG(1,9),CG(2,7),CG(2,8),CG(2,9),
1CG(3,7),CG(3,8),CG(3,9),CG(4,7),CG(4,8),CG(4,9),
2CG(5,7),CG(5,8),CG(5,9),CG(6,7),CG(6,8),CG(6,9),
3CG(7,8),CG(7,9),CG(8,9)/.036,.1,.085,.05,.13,.084,
4.08,.135,.075,.09,.13,.06,.095,.13,.05,.095,.125,.065,
5-.02,.18,.1/
R=82.056
ID=-1
DO 97 I=1,NCOMP
DO 97 J=1,NCOMP
CG(J,I)=CG(I,J)
A(I,J)=.0
AM=.0
BM=.0
B(I)=.0
AK(I)=.0
97 CONTINUE
10 FORMAT(10G)
DO 1 I=1,NCOMP
TR(I)=T/TC(I)
IF(Y(I).EQ..0) GO TO 149
PR(I)=P/PC(I)
A(I,I)=.45724*(R*TC(I))**2/PC(I)
B(I)=.0778*R*TC(I)/PC(I)
103 FORMAT(1X,'I,A(I)',I2,X,F15.3)
AK(I)=.37464+1.54226*W(I)-.26992*W(I)**2
102 FORMAT(1X,'I,K',I2,X,F10.5)
AK(I)=(1.+AK(I)*(1.-SQRT(TR(I))))**2
A(I,I)=AK(I)*A(I,I)
30 FORMAT(1X,'TR,PR,A(I,I),B',5F13.4,X)
149 CONTINUE
1 CONTINUE
DO 2 I=1,NCOMP
DO 2 J=1,NCOMP
IF(Y(J).EQ..0) GO TO 145
IF(Y(I).EQ..0) GO TO 145
A(I,J)=(1.-CG(I,J))*SQRT(A(I,I)*A(J,J))
81 FORMAT(1X,2(I2,X),F15.5)
145 CONTINUE
2 CONTINUE
DO 4 I=1,NCOMP
IF(Y(I).LE..0) GO TO 41
41 CONTINUE
BM=BM+B(I)*Y(I)
4 CONTINUE
DO 75 I=1,NCOMP
AK(I)=.0
75 CONTINUE

```

```
DO 3 J=1,NCOMP
DO 3 I=1,NCOMP
IF(Y(I).EQ..0) GO TO 148
IF(Y(J).EQ..0) GO TO 148
AK(J)=Y(I)*A(I,J)+AK(J)
148 CONTINUE
3 CONTINUE
DO 6 J=1,NCOMP
AK(J)=2.*AK(J)
85 FORMAT(1X,F15.4)
6 CONTINUE
DO 5 I=1,NCOMP
DO 5 J=1,NCOMP
AM=AM+Y(I)*Y(J)*A(I,J)
5 CONTINUE
40 FORMAT(1X,2F15.5,X)
CALL VCUBE(AM,BM,P,R,T,V,Z, ID)
83 FORMAT(1X,'Z',F10.5)
AB=AM*P/(R*T)**2
BB=BM*P/(R*T)
DO 62 I=1,NCOMP
IF(Y(I).EQ..0) GO TO 61
A1=B(I)*(Z-1.)/BM
A2=ALOG(Z-BB)
A3=AB/(2*SQRT(2.)*BB)
86 FORMAT(1X,4(F15.3,X))
A4=AK(I)/AM-B(I)/BM
A5=ALOG((Z+2.414*BB)/(Z-.414*BB))
84 FORMAT(1X,4(F10.4,X))
PHI(I)=A1-A2-A3*A4*A5
PHI(I)=EXP(PHI(I))
PHI(I)=PHI(I)*Y(I)*P
61 CONTINUE
62 CONTINUE
RETURN
END
```

```
SUBROUTINE VCUBE(A,B,P,R,T,V,Z, ID)
```

```
D=B-R*T/P
```

```
E=-(3.*B*B+2.*R*T*B/P-A/P)
```

```
F=B*B*B+(R*T*B*B-A*B)/P
```

```
G=(3.*E-D*D)/3.
```

```
H=-(9.*D*E-27.*F-2.*D*D*D)/27.
```

```
IF(G**3./27.+H*H/4..LE.0.) GO TO 10
```

```
S=-H/2.+SQRT(G**3./27.+H*H/4.)
```

```
TT=-H/2.-SQRT(G**3./27.+H*H/4.)
```

```
IF(S)5,6,6
```

```
5 S=-((-S)**(1./3.))
```

```
GO TO 7
```

```
6 S=(S)**(1./3.)
```

```
7 IF(TT)8,9,9
```

```
8 TT=-(-TT)**(1./3.)
```

```
GO TO 15
```

```
9 TT=(TT)**(1./3.)
```

```
C SINGLE REAL ROOT
```

```
15 V=S+TT-D/3.
```

```
GO TO 40
```

```
10 THETA = (ACOS(-.5*H/SQRT(-G**3/27.)))/3.
```

```
V1=2.*SQRT(-G/3.)*CDS(THETA)
```

```
V2=2.*SQRT(-G/3.)*CDS(THETA+2.0944)
```

```
V3=2.*SQRT(-G/3.)*CDS(THETA+4.1888)
```

```
IF(ID)20,30,30
```

```
C TAKE LARGEST V FOR VAPOR
```

```
20 V=AMAX1(V1,V2,V3)-D/3.
```

```
GO TO 40
```

```
C TAKE SMALLEST V FOR LIQUID
```

```
30 V=AMIN1(V1,V2,V3)-D/3.
```

```
40 Z=P*V/(R*T)
```

```
RETURN
```

```
END
```



```
SUBROUTINE ACT(SO1,SO2,SO3,SO4,T,ACTI,NCOMP,Y)
DIMENSION SO1(10),SO2(10),SO3(10),SO4(10),X(10)
DIMENSION Y(10)
DO 1 I=1,NCOMP
IF(I.EQ.6) GO TO 2
X(I)=SO1(I)+SO2(I)/T+SO3(I)*ALOG(T)+SO4(I)*T
X(I)=EXP(X(I)/1.987)
IF(Y(I).EQ.0.0)X(I)=0.0
XSUM=XSUM+X(I)
2
1
8
Xλ=.0
CONTINUE
FORMAT(1X,F10.8)
Xw=1.-XSUM
ACTI=1.987*T*ALOG(Xw)
XSUM=.0
IF(T.LT.273.16) ACTI=.0
RETURN
END
```

C LIQE.FOR

```

      DIMENSION PHIL(10), EP(10),SIGP(10),CP(10),CB(4,10),SO1(10)
      DIMENSION CL(4,10),PHI(10),Y(10)
      1,SO2(10),SO3(10),SO4(10),TC(10),PC(10),VC(10),W(10)
      2,CG(100,100),X(10),VU(2),VL(2),D(2)
140  FORMAT(1X,4(F10.5,X))
      READ(4,10)NHY,NPT
      NCOMP=9
      DTINC=.01
      XSOM=.99398
      DO 21 I=1,NCOMP
      READ(15,10) EP(I),SIGP(I),CP(I)
304  FORMAT(1X,4(F10.5,X))
21  CONTINUE
      DO 3 I=1,NCOMP
      READ(15,10)CB(1,I),CB(2,I),CB(3,I),CB(4,I)
3  CONTINUE
      DO 4 I=1,NCOMP
      READ(15,10) SO1(I),SO2(I),SO3(I),SO4(I)
4  CONTINUE
      DO 6 I=1,NCOMP
      READ(15,10)TC(I),PC(I),VC(I),W(I)
6  CONTINUE
      CALL INI(NCOMP)
      DO 1 INPT=1,NPT
      READ(09,10)T,P,X(1),X(2),X(3),X(4),X(5),X(6),X(7),X(8),X(9)
      DO 811 JJ=1,NCOMP
      Y(JJ)=.0
811 CONTINUE
      TEX=T
      PEX=P
      P=P/14.696
      T=(T-32.)*5./9.+273.15
111 CONTINUE
      DO 660 K=1,2
      CALL LANG(T,CL,EP,SIGP,CP,NCOMP,CB)
      CL(4,4)=4.040815/T*EXP(2687.9744/T)
      CL(4,5)=7.0466187/T*EXP(3083.9044/T)
      DO 861 IX=1,NCOMP
      Y(IX)=.0
      PHIL(IX)=.0
861 CONTINUE
      CALL PHASE2(T,P,NCOMP,X,Y,TC,PC,VC,W,PHI)
      CALL AMUC(T,P,NHY,AMU)
10  FORMAT(10G)
      IF(NHY.GT.1) GO TO 18
      DO 17 I=1,NCOMP
      CSML=CL(1,I)*PHI(I)
      CSMLS=CSMLS+CSML

```

```

      CLG=CL(2,1)*PHI(I)
      CLGS=CLG+CLGS
17    CONTINUE
      AM1=2.*ALOG(1.+CSMLS)/46.
      AM2=6.*ALOG(1.+CLGS)/46.
      CALL ACT(SO1,SO2,SO3,SO4,T,ACTI,NCOMP,Y)
      DMCAL=(AM1+AM2)*1.987*T+ACTI
      CSMLS=.0
      CLGS=.0
      GO TO 20
18    DO 19 I=1,NCOMP
335   FORMAT(1X,I1,3(F10.4,X))
      CSML=CL(3,1)*PHI(I)
      CSMLS=CSMLS+CSML
      CLG=CL(4,1)*PHI(I)
      CLGS=CLG+CLGS
19    CONTINUE
536   FORMAT(1X,'CSMLS,CLGS',2(F15.5,X))
      AM1=16.*ALOG(1.+CSMLS)/136.
      AM2=8.*ALOG(1.+CLGS)/136.
      DMCAL=(AM1+AM2)*1.987*T+ACTI
      CSMLS=.0
819   FORMAT(1X,F10.5)
      CLGS=.0
332   FORMAT(1X,'CAL,EXP',2(F20.3,X))
20    DEL=AMU-DMCAL
16    FORMAT(1X,2(F15.3,X),I5)
      D(K)=DEL
      IF(NR.EQ.1) GO TO 664
      IF(K.GT.1) GO TO 662
      N=DEL/ABS(DEL)
41    FORMAT(1X,'N,NC1',2(I5,X))
      NC1=NC1+N
      IF(NC1.EQ.0) GO TO 664
      NC1=N
662   DPS=ABS(DEL)*100./AMU
      IF(DPS.LT..1) GO TO 80
      T=T+DTINC
660   CONTINUE
      TS=T
      T=T-DEL/((D(2)-D(1))/DTINC)
      K=0
      DS=DEL
      GO TO 111

664   DEL=AMU-DMCAL
      DPS=ABS(DEL)*100./AMU
      IF(NR.EQ.1) GO TO 51
      IF(ABS(DEL-DSAVE).GT..0) GO TO 80
51    IF(DPS.LT..1) GO TO 80
      DSAVE=DEL

```

```
NR=1
NRC=1+NRC
IF(NRC.GT.1) GO TO 668
U1=DEL
U2=DS
U3=T
U4=TS
44  FORMAT(1X,4(F10.5,X))
    GO TO 690
668  U2=DEL
    U4=T
    NUM=DEL/ABS(DEL)
    IF(NUM)670,672,676
670  U1=AMAX1(VU(1),VU(2))
    GO TO 675
676  U1=AMIN1(VU(1),VU(2))
    GO TO 675
672  WRITE(4,681)
681  FORMAT(1X,'CHECK CONVERGENCE')
    STOP
675  CONTINUE
    DO 682 II=1,2
    IF(U1.EQ.VU(II)) U3=VL(II)
682  CONTINUE
690  T=(U1*U4-U2*U3)/(U1-U2)
    VU(1)=U1
    VU(2)=U2
    VL(1)=U3
    VL(2)=U4
49  FORMAT(1X,'VU & VL',4(F10.4,X))
    GO TO 111
80  T=(T-273.15)*9./5.+32.
    P=P*14.696
    DPSUM=DPSUM+ABS(PEX-P)
    DTSUM=DTSUM+ABS(TEX-T)
    K=0
    N=0
    NR=0
    NC1=0
    NR=0
    NU1=0
    NUM=0
    NU=0
    NRC=0
    U1=.0
    U2=.0
    U3=.0
    U4=.0
    VU(1)=.0
    VU(2)=.0
    VL(1)=.0
```

```
VL(2)=.0
TS=.0
DS=.0
DEL=.0
DSAVE=.0
DPS=.0
I=0
K=0
ACTI=.0
WRITE(4,43)T,P
DO 816          L=1, NCOMP
PHI(L)=.0
816 CONTINUE
WRITE(02,403)X(1),X(2),X(3),TEX,PEX,T,P
403 FORMAT(1X,3(F6.3,X),4(F7.2,X))
1 CONTINUE
PDMN=DPSUM/NPT
TDMN=DTSUM/NPT
WRITE(02,43)TDMN,PDMN
43 FORMAT(1X,2(F10.3,X))
STOP
END
```

```

SUBROUTINE AMUC(T,P,NHY,DMU2)
PR(X)=EXP(AR+BR/X+CR*ALOG(X))
C INPUT T IN DEG K, P IN MM HG, DTF IN DEG K
VINT=0.0
VINT1=0.0
VINT2=0.0
10 FORMAT(3F)
IF(NHY.GT.1) GO TO 20
C CALCULATE STRUCTURE I PROPERTIES
V=6./46.
AML=.001449
BML=4579.6
GO TO 30
C CALCULATE STRUCTURE II PROPERTIES
20 V=8./136.
AML=.013136
BML=4653.4
30 CML=AML/T*EXP(BML/T)
TC=397.8
TR=T/TC
W=.127
PC=54.23
R=82.056
B=(.083-.422/(TR**1.6)+W*(.139-.172/(TR**4.2)))*
1R*TC/PC
PHI=EXP((P*B)/(R*T))
C CALCULATE LN OF ACTIVITY
A=(-1436.3*DTF)/(1.987*273.15**2)
IF(NHY.GT.1) GO TO 60
C CALCULATE STRUCTURE I PROPERTIES
AR=-1212.2
BR=44344.0
CR=187.719
DV=4.598
DH=332.
DM=310.
GO TO 70
C CALCULATE STRUCTURE II PROPERTIES
60 AR=-1023.14
BR=34984.3
CR=159.923
DV=4.998
DH=245.
DM=224.
70 TU=273.15
C CALCULATE MUO/RTO AT PO,TO
DMUO=(DM+DV*PR(TO)*.0242152)/(1.987*TO)
C CALCULATE ENTHALPY INTEGRAL
HINT=(1./1.987)*(DH*(1./T-1./TO)+2616.398*(1./T-
11./TO)+20.6166*ALOG(T/TO)-.021163*(T-TO))
IF(T.LT.273.15) HINT=1.*DH*(1./T-1./273.15)/1.987

```

```
C      CALCULATE VOLUME INTEGRAL
      N=ABS(273.15-T)
      DO 40 I=1,N+1
      DT=1.
      TI=TI+DT
      IF(I.EQ.1)TI=TO
      DPRDT=((-BR/TI+CR)/TI)*PR(TI)
      VINT1=(DPRDT/TI)*(DV/82.056)
      VINT=.5*(VINT1+VINT2)+DT*VINT
      VINT2=VINT1
40     CONTINUE
      DMPR=(DMUO+HINT+VINT)*1.987*T
115    FORMAT(1X,F15.2)
      DMU2=DMPR+DV*.0242152*(P-PR(T))
      RETURN
      END
```

```

SUBROUTINE LANG(T,CL,EP,SIGP,CP,NCOMP,CB)
DIMENSION A(4),Z(4),CB(4,10),KS(10),CL(4,10),
1X(20),WT(20),SIGP(10),EP(10),CP(10)

```

```

NPT=10

```

```

NP=5

```

```

DATA(X(J),WT(J),J=6,10)/.1488743389,.29552422147,
1.4333953941,.2692667193,.6794095683,.2190
2863625,.86506336627,.1494513492,.9739065285,
3.0666713443/

```

```

DATA (A(I),Z(I),I=1,4)/3.95,20.,4.3,24.,3.91,20.,4.73,
128./

```

```

DATA PI,BK/3.1416,1.3804E-16/

```

```

DO 22 J=1,NP

```

```

X(J)=-X(NPT-J+1)

```

```

WT(J)=WT(NPT-J+1)

```

```

22 CONTINUE

```

```

KBLOW=0

```

```

DO 5 J=1,NCOMP

```

```

DO 1 I=1,4

```

```

1 CL(I,J)=.0

```

```

C=CP(J)

```

```

EK=EP(J)

```

```

EC=EP(J)*BK

```

```

RC=SIGP(J)*1.122462

```

```

DO 5 I=1,4

```

```

IF (CB(I,J).LT.1.) GO TO 5

```

```

RCA=RC/A(I)

```

```

CA=C/A(I)

```

```

C NEWTON RAPSON METHOD FOR FINDING LIMITS , YL

```

```

C FIRST GUESS S=.4

```

```

S=.4

```

```

RCA6=RCA**6

```

```

RCA12=RCA**12

```

```

DO 2 N=1,20

```

```

IF (S.GT.1.0.OR.S.LE.0.0) GO TO 6

```

```

UM=1./(1.-S-CA)

```

```

UP=1./(1.+S-CA)

```

```

UM5=UM**5

```

```

UP5=UP**5

```

```

DA4=UM5+UP5

```

```

DA5=UM5*UM+UP5*UP

```

```

DB6=DA4+CA*DA5

```

```

UM11=UM**11

```

```

UP11=UP**11

```

```

DA10=UM11+UP11

```

```

DA11=UM11*UM+UP11*UP

```

```

DB12=DA10+CA*DA11

```

```

DB=RCA12*DB12-2.*RCA6*DB6

```

```

A10=UM11/UM-UP11/UP

```



```

A11=UM11-UP11
B12=(.1*A10+CA*A11/11.0)
A4=UM5/UM-UP5/UP
A5=UM5-UP5
B6=A4/4.+CA*A5/5.
B=RCA12*B12-2.*RCA6*B6
W=Z(I)*EK/(2.*S*T)*B
DWY=-W/S+Z(I)*EK*DB/(2.*S*T)
DS=S-(W-10.)/DWY
IF(ABS((DS-S)/DS).LT.0.01) GO TO 3
2  S=DS
3  YL=S
C  GAUSSIAN INTEGRATION
P=2.*PI*A(I)**3/(T*136.2)*YL
SQ=.0
DO 4 N=1,NPT
Y=YL*(X(N)+1.)/2.
UP=1./(1.+Y-CA)
UM=1./(1.-Y-CA)
UP5=UP**5
UM5=UM**5
A4=UM5/UM-UP5/UP
A5=UM5-UP5
B6=A4/4.+CA*A5/5.
UP11=UP**11
UM11=UM**11
A10=UM11/UM-UP11/UP
A11=UM11-UP11
B12=(.1*A10+CA*A11/11.)
B=RCA12*B12-2.*RCA6*B6
W=Z(I)*EK/(2.*Y*T)*B
4  SQ=SQ+EXP(-W)*Y**2*WT(N)
270 CL(I,J)=P*SQ
5  FORMAT(1X,4(F10.5,X))
6  CONTINUE
7  RETURN
KBL0W=2
WRITE(4,7)
FORMAT(1X,'PROBLEM BLOW UP')
RETURN
END

```

```

SUBROUTINE PENG(T,P,NCOMP,Y,PHI,TC,PC,VC,W,ID)
DIMENSION TC(10),PC(10),W(10),B(10),PHI(10),VC(10),AK(10)
1,A(100,100),Y(10),TR(10),PR(10),CG(100,100)
DATA CG(1,7),CG(1,8),CG(1,9),CG(2,7),CG(2,8),CG(2,9),
1CG(3,7),CG(3,8),CG(3,9),CG(4,7),CG(4,8),CG(4,9),
2CG(5,7),CG(5,8),CG(5,9),CG(6,7),CG(6,8),CG(6,9),
3CG(7,8),CG(7,9),CG(8,9)/.036,.1,.085,.05,.13,.084,
4.08,.135,.075,.09,.13,.06,.095,.13,.05,.095,.125,.065,
5-.02,.18,.1/
R=82.056
DO 97 I=1,NCOMP
DO 97 J=1,NCOMP
A(I,J)=.0
CG(J,1)=CG(I,J)
AM=.0
BM=.0
R(I)=.0
AK(I)=.0
TR(I)=.0
PR(I)=.0
PHI(I)=.0
97 CONTINUE
10 FORMAT(10G)
DO 1 I=1,NCOMP
TR(I)=T/TC(I)
IF(Y(I).EQ..0) GO TO 149
PR(I)=P/PC(I)
A(I,I)=.45724*(R*TC(I))**2/PC(I)
B(I)=.0778*R*TC(I)/PC(I)
103 FORMAT(1X,'I,A(I)',I2,X,F15.3)
AK(I)=.37464+1.54226*W(I)-.26992*W(I)**2
102 FORMAT(1X,'I,K',I2,X,F10.5)
AK(I)=(1.+AK(I)*(1.-SQRT(TR(I))))**2
A(I,I)=AK(I)*A(I,I)
30 FORMAT(1X,'TR,PR,A(I,I),B',5F13.4,X)
149 CONTINUE
1 CONTINUE
DO 2 I=1,NCOMP
DO 2 J=1,NCOMP
IF(Y(J).EQ..0) GO TO 145
IF(Y(I).EQ..0) GO TO 145
A(I,J)=(1.-CG(I,J))*SQRT(A(I,I)*A(J,J))
81 FORMAT(1X,2(I2,X),F15.5)
145 CONTINUE
2 CONTINUE
DO 4 I=1,NCOMP
IF(Y(I).LE..0) GO TO 41
41 CONTINUE
BM=BM+B(I)*Y(I)
4 CONTINUE
DO 75 I=1,NCOMP

```

```

75      AK(I)=.0
        CONTINUE
        DO 3 J=1, NCOMP
        DO 3 I=1, NCOMP
        IF(Y(I).EQ..0) GO TO 148
        IF(Y(J).EQ..0) GO TO 148
        AK(J)=Y(I)*A(I,J)+AK(J)
148     CONTINUE
3       CONTINUE
        DO 6 J=1, NCOMP
        AK(J)=2.*AK(J)
35      FORMAT(1X, F15.4)
6       CONTINUE
        DO 5 I=1, NCOMP
        DO 5 J=1, NCOMP
        AM=AM+Y(I)*Y(J)*A(I,J)
5       CONTINUE
40      FORMAT(1X, 2F15.5, X)
        CALL VCUBE(AM, BM, P, R, T, V, Z, ID)
33      FORMAT(1X, 'Z', F10.5)
        AB=AM*P/(R*T)**2
        BB=BM*P/(R*T)
        DO 62 I=1, NCOMP
        IF(Y(I).EQ..0) GO TO 61
        A1=B(I)*(Z-1.)/BM
        A2=ALOG(Z-BB)
        A3=AB/(2*SQRT(2.)*BB)
86      FORMAT(1X, 4(F15.3, X))
        A4=AK(I)/AM-B(I)/BM
        A5=ALOG((Z+2.414*BB)/(Z-.414*BB))
34      FORMAT(1X, 4(F10.4, X))
        PHI(I)=A1-A2-A3*A4*A5
        PHI(I)=EXP(PHI(I))
        PHI(I)=PHI(I)*Y(I)*P
61      CONTINUE
62      CONTINUE
        RETURN
        END
```

```

SUBROUTINE VCUBE(A,B,P,R,T,V,Z,LD)
D=B-R*T/P
E=-(3.*B*B+2.*R*T*B/P-A/P)
F=B*B*B+(R*T*B*B-A*B)/P
G=(3.*E-D*D)/3.
H=-(9.*D*E-27.*F-2.*D*D*D)/27.
IF(G**3./27.+H*H/4..LE.0.) GO TO 10
S=-H/2.+SQRT(G**3./27.+H*H/4.)
TT=-H/2.-SQRT(G**3./27.+H*H/4.)
IF(S)5,6,6
5 S=-((-S)**(1./3.))
GO TO 7
6 S=(S)**(1./3.)
7 IF(TT)8,9,9
8 TT=-(-TT)**(1./3.)
GO TO 15
9 TT=(TT)**(1./3.)
C SINGLE REAL ROOT
15 V=S+TT-D/3.
GO TO 40
10 THETA = (ACOS(-.5*H/SQRT(-G**3/27.)))/3.
V1=2.*SQRT(-G/3.)*COS(THETA)
V2=2.*SQRT(-G/3.)*COS(THETA+2.0944)
V3=2.*SQRT(-G/3.)*COS(THETA+4.1888)
IF(LD)20,30,30
C TAKE LARGEST V FOR VAPOR
20 V=AMAX1(V1,V2,V3)-D/3.
GO TO 40
C TAKE SMALLEST V FOR LIQUID
30 V=AMIN1(V1,V2,V3)-D/3.
40 Z=P*V/(R*T)
RETURN
END

```

```
2  
1  
8  
SUBROUTINE ACT(SO1,SO2,SO3,SO4,T,ACTI,NCOMP,Y)  
DIMENSION SO1(10),SO2(10),SO3(10),SO4(10),X(10)  
DIMENSION Y(10)  
DO 1 I=1,NCOMP  
IF(I.EQ.6) GO TO 2  
X(I)=SO1(I)+SO2(I)/T+SO3(I)*ALOG(T)+SO4(I)*T  
X(I)=EXP(X(I)/1.987)  
IF(Y(I).EQ.0.0)X(I)=0.0  
XSUM=XSUM+X(I)  
XX=.0  
CONTINUE  
FORMAT(1X,F10.8)  
XW=1.-XSUM  
ACTI=1.987*T*ALOG(XW)  
XSUM=.0  
IF(T.LT.273.16) ACTI=.0  
RETURN  
END
```

```

SUBROUTINE PHASE2(T,P,NCOMP,X,Y,TC,PC,VC,W,PHI)
DIMENSION Y(10),X(10),YY(10),PHI(10),PHIL(10)
DIMENSION TC(10),PC(10),VC(10),W(10)
DIMENSION RATIO(10),AK(10)
SUMY=.0
K=0
IV=-1
IL=1
KI=0
6 CONTINUE
CALL PENG(T,P,NCOMP,X,PHIL,TC,PC,VC,W,IL)
123 FORMAT(1X,'THIRTEEN')
DO 2 I=1,NCOMP
SUMY=SUMY+PHIL(I)
21 FORMAT(1X,F10.5,'PHI')

2 CONTINUE
DO 3 I=1,NCOMP
IF(PHIL(I).LE..0) GO TO 3
Y(I)=PHIL(I)/SUMY
23 FORMAT(1X,'PNEW,POLD',2(F10.2))
3 CONTINUE
13 CONTINUE
SUMY=.0
POLD=P

CALL PENG(T,P,NCOMP,Y,PHI,TC,PC,VC,W,IV)
DO 4 I=1,NCOMP
IF(PHIL(I).LE..0) GO TO 4
RATIO(I)=PHIL(I)/PHI(I)
Y(I)=RATIO(I)*Y(I)
SUMY=SUMY+Y(I)
4 CONTINUE
DO 5 I=1,NCOMP
Y(I)=Y(I)/SUMY
5 CONTINUE
P=P*SUMY
K=K+1
DO 28 I=1,NCOMP
RT=RT+RATIO(I)

28 CONTINUE
RT=.0
29 FORMAT(1X,F10.5)
DO 33 I=1,NCOMP
34 FORMAT(1X,3(F10.3,X))
33 CONTINUE
IF(ABS(P-POLD).GT.1.0E-2) GO TO 12
DO 19 I=1,NCOMP
42 FORMAT(1X,F10.5)

```

```
IF(RATIO(I).LE..0) GO TO 19
IF(ABS(RATIO(I)-1.0).GE.1.0E-4) GO TO 13
19 CONTINUE
RETURN

12 CALL PENG(T,P,NCOMP,X,PHIL,TC,PC,VC,W,IL)
124 FORMAT(1X,"CON.AF.13")
GO TO 13
127 FORMAT(1X,"PASS 13")
98 KI=1
K=K-1
99 CONTINUE
Vw=.0
DO 22 I=1,NCOMP
AK(I)=Y(I)/X(I)
YY(I)=Y(I)

22 CONTINUE
RETURN
END
```

```
SUBROUTINE IN1(NCOMP)
  DIMENSION TC(10),PC(10),W(10),B(10),PHI(10),VC(10),AK(10)
1, A(100,100),Y(10),TR(10),PR(10),CG(100,100)
  DIMENSION YY(10),X(1),PHIL(1)
  DIMENSION RATIO(10)
  DO 1 I=1,NCOMP
    B(I)=.0
    AK(I)=.0
    TR(I)=.0
    PR(I)=.0
    B(I)=.0
    PHI(I)=.0
    RATIO(I)=.0
    AK(I)=.0
    YY(I)=.0
    Y(I)=.0
    X(I)=.0
1  CONTINUE
    AB=.0
    BB=.0
    A1=.0
    A2=.0
    A3=.0
    A4=.0
    A5=.0
    K=0
    KI=0
    SUMY=0
    POLD=0
    RT=.0
    DO 2 I=1,NCOMP
      DO 2 J=1,NCOMP
2  A(I,J)=.0
    CONTINUE
    RETURN
  END
```


C W.FOR

C DETERMINATION OF THE WATER CONTENTY IN THE VAPOUR
C PHASE IN EQUILIBRIUM WITH THE HYDRATE PHASE.
C

```

DIMENSION TR(10),PR(10),W(10),PC(10),AL(10),A(10),VC(10),
1YL(10),B(10),ALA(20,20),CG(20,20),Y(10),
3PHICOE(10),TC(10),PHI(10),CL(4,10),YY(10)
READ(4,10)NPT
DU 620 I=1,9
620 READ(02,10)TC(I),PC(I),VC(I),W(I)
CONTINUE
DU 2 I=1,NPT
READ(01,10)T,P,WEX
P=P/14.696
CALL LANG(T,CL)
YEX=WEX*2.10555*10.**(-5.)
10 DATA YY(2),YY(3),YY(4),YV(5)/1.,.0,.0,.0/
FORMAT(10G)
Y(1)=YEX
1 Y(2)=1.-Y(1)
CALL PENG(T,P,Y,PHICOE,PHI,TC,PC,VC,W)
650 FORMAT(1X,'CL',2(F10.5,X))
A1=ALOG(1.+CL(1,1)*PHI(2))*2./46.
A2=ALOG(1.+CL(2,1)*PHI(2))*6./46.
AMUTP=- (A1+A2)
VICE=(1.069989-.249933*10.**(-4.))*T+.371606*10.
1**(-6.)*T**2)*18
PICE=EXP(17.37039-6140.8148/T)
VHYD=VICE+3.
PMT=EXP(17.440445-5003.9245/T)
X1=EXP(AMUTP+VHYD*(P-PMT)/(82.057*T))
YW=PMT*X1/(PHICOE(1)*P)
S=YW-Y(1)
IF(ABS(S).LT.1.*10.**(-7)) GO TO 20
Y(1)=YW
GO TO 1
20 WI=YW/(2.10555*10.**(-5.))
T=(T-273.15)*9./5.+32.
P=P*14.696
YEX=YEX*1000000.
YW=YW*1000000.
30 WRITE(07,30)T,P,YEX,YW
FORMAT(1X,F8.2,X,F7.2,X,2(F10.2,X))
YSUM=YEX-YW+YSUM
YASUM=ABS(YEX-YW)+YASUM
2 CONTINUE
YASUM=YASUM/NPT
YMN=YSUM/NPT
WRITE(07,40)YMN,YASUM

```

```
40  FORMAT(1X,2(F15.2,X))  
    STOP  
    END
```

```

SUBROUTINE LANG(T,CL)
  DIMENSION A(4),Z(4),CB(4,10),KS(10),CL(4,10),
  IX(20),WT(20),SIGP(10),EP(10),CP(10)
  SIGP(1)=3.2
  EP(1)=156.72
  CP(1)=.383359375
  CB(1,1)=20.
  CB(2,1)=20.
  CB(3,1)=20.
  CB(4,1)=20.
  NPT=10
  NP=5
  DATA(X(J),WT(J),J=6,10)/.1488743389,.29552422147,
  1.4333953941,.2692667193,.6794095683,.2190
  2863625,.86506336627,.1494513492,.9739065285,
  3.0666713443/
  DATA (A(I),Z(I),I=1,4)/3.95,20.,4.3,24.,3.91,20.,4.73,
  128./
  DATA PI,BK/3.1416,1.3804E-16/
  DO 22 J=1,NP
  X(J)=-X(NPT-J+1)
  WT(J)=WT(NPT-J+1)
22 CONTINUE

```

```

KBLUW=0
DO 5 J=1,1
DO 1 I=1,4
1 CL(I,J)=.0
C=CP(J)
EK=EP(J)
EC=EP(J)*BK
RC=SIGP(J)*1.122462
DO 5 I=1,4
IF (CB(I,J).LT.1.) GO TO 5
RCA=RC/A(I)
  CA=C/A(I)
C NEWTON RAPSON METHOD FOR FINDING LIMITS , YL
C FIRST GUESS S=.4
S=.4
RCA6=RCA**6
RCA12=RCA**12
DO 2 N=1,20
IF (S.GT.1.0.OR.S.LE.0.0) GO TO 6
UM=1./(1.-S-CA)
UP=1./(1.+S-CA)
UM5=UM**5
UP5=UP**5
DA4=UM5+UP5
DA5=UM5*UM+UP5*UP
DB6=DA4+CA*DA5
UM11=UM**11

```

```

UP11=UP**11
DA10=UM11+UP11
DA11=UM11*UM+UP11*UP
DB12=DA10+CA*DA11
DB=RCA12*DB12-2.*RCA6*DB6
A10=UM11/UM-UP11/UP
A11=UM11-UP11
B12=(.1*A10+CA*A11/11.0)
A4=UM5/UM-UP5/UP
A5=UM5-UP5
B6=A4/4.+CA*A5/5.
B=RCA12*B12-2.*RCA6*B6
W=Z(I)*EK/(2.*S*T)*B
DW=-w/S+Z(I)*EK*DB/(2.*S*T)
DS=S-(W-10.)/DWY
IF(ABS((DS-S)/DS).LT.0.01) GO TO 3
2 S=DS
3 YL=S
C GAUSSIAN INTEGRATION
P=2.*PI*A(I)**3/(T*136.2)*YL
SQ=.0
DO 4 N=1,NPT
Y=YL*(X(N)+1.)/2.
UP=1./(1.+Y-CA)
UM=1./(1.-Y-CA)
UP5=UP**5
UM5=UM**5
A4=UM5/UM-UP5/UP
A5=UM5-UP5
B6=A4/4.+CA*A5/5.
UP11=UP**11
UM11=UM**11
A10=UM11/UM-UP11/UP
A11=UM11-UP11
B12=(.1*A10+CA*A11/11.)
B=RCA12*B12-2.*RCA6*B6
W=Z(I)*EK/(2.*Y*T)*B
4 SQ=SQ+EXP(-w)*Y**2*WT(N)
5 CL(I,J)=P*SQ
CONTINUE
RETURN
6 KBLOW=2
WRITE(4,7)
7 FORMAT(1X,'PROBLEM BLOW UP')
RETURN
END

```

```

SUBROUTINE PENG(T,P,Y,PHICOE,PHI,TC,PC,VC,W)
  DIMENSION TC(10),PC(10),W(10),B(10),PHI(10),VC(10),AK(10)
  1,A(100,100),Y(10),TR(10),PR(10),PHICOE(10),CG(100,100)
  DATA CG(1,7),CG(1,8),CG(1,9),CG(2,7),CG(2,8),CG(2,9),
  1CG(3,7),CG(3,8),CG(3,9),CG(4,7),CG(4,8),CG(4,9),
  2CG(5,7),CG(5,8),CG(5,9),CG(6,7),CG(6,8),CG(6,9),
  3CG(7,8),CG(7,9),CG(8,9)/.036,.1,.085,.05,.13,.084,
  4.08,.135,.075,.09,.13,.06,.095,.13,.05,.095,.125,.065,
  5-.02,.18,.1/
  NCOMP=9
  DATA CG(1,2),CG(2,1)/.5,.5/
  R=82.056
  DO 97 I=1,NCOMP
  DO 97      J=1,NCOMP
  A(I,J)=.0
  AM=.0
  BM=.0
  B(I)=.0
  AK(I)=.0
  TR(I)=.0
  PR(I)=.0
  PHI(I)=.0
97  CONTINUE
10  FORMAT(10G)
  DO 1 I=1,NCOMP
  TR(I)=T/TC(I)
  IF(Y(I).EQ..0) GO TO 149
  PR(I)=P/PC(I)
  A(I,I)=.45724*(R*TC(I))**2/PC(I)
  B(I)=.0778*R*TC(I)/PC(I)
103  FORMAT(1X,'I,A(I)',I2,X,F15.3)
  AK(I)=.37464+1.54226*W(I)-.26992*W(I)**2
102  FORMAT(1X,'I,K',I2,X,F10.5)
  AK(I)=(1.+AK(I)*(1.-SQRT(TR(I))))**2
  A(I,I)=AK(I)*A(I,I)
30  FORMAT(1X,'TR,PR,A(I,I),B',5F13.4,X)
149  CONTINUE
1  CONTINUE
  DO 2 I=1,NCOMP
  DO 2 J=1,NCOMP
  IF(Y(J).EQ..0) GO TO 145
  IF(Y(I).EQ..0) GO TO 145
  A(I,J)=(1.-CG(I,J))*SQRT(A(I,I)*A(J,J))
81  FORMAT(1X,2(I2,X),F15.5)
145  CONTINUE
2  CONTINUE
  DO 4 I=1,NCOMP
  IF(Y(I).LE..0) GO TO 41
41  CONTINUE
  BM=BM+B(I)*Y(I)
4  CONTINUE

```

```
      DO 75      I=1, NCOMP
      AK(I)=.0
75     CONTINUE
      DO 3 J=1, NCOMP
      DO 3 I=1, NCOMP
      IF(Y(I).EQ..0) GO TO 148
      IF(Y(J).EQ..0) GO TO 148
      AK(J)=Y(I)*A(I,J)+AK(J)
148    CONTINUE
3      CONTINUE
      DO 6 J=1, NCOMP
      AK(J)=2.*AK(J)
85     FORMAT(1X, F15.4)
6      CONTINUE
      DO 5 I=1, NCOMP
      DO 5 J=1, NCOMP
      AM=AM+Y(I)*Y(J)*A(I,J)
5      CONTINUE
40     FORMAT(1X, 2F15.5, X)
      CALL VCUBE(AM, BM, P, R, T, V, Z, ID)
83     FORMAT(1X, 'Z', F10.5)
      AB=AM*P/(R*T)**2
      BB=BM*P/(R*T)
      DO 62      I=1, NCOMP
      IF(Y(I).EQ..0) GO TO 61
      A1=B(I)*(Z-1.)/BM
      A2=ALOG(Z-BB)
      A3=AB/(2*SQRT(2.)*BB)
86     FORMAT(1X, 4(F15.3, X))
      A4=AK(I)/AM-B(I)/BM
      A5=ALOG((Z+2.414*BB)/(Z-.414*BB))
94     FORMAT(1X, 4(F10.4, X))
      PHI(I)=A1-A2-A3*A4*A5
      PHICOE(I)=EXP(PHI(I))
      PHI(I)=PHICOE(I)*Y(I)*P
61     CONTINUE
62     CONTINUE
      RETURN
      END
```

```

SUBROUTINE VCUBE(A,B,P,R,T,V,Z, ID)
D=B-R*T/P
E=-(3.*B*B+2.*R*T*B/P-A/P)
F=B*B*B+(R*T*B*B-A*B)/P
G=(3.*E-D*D)/3.
H=-(9.*D*E-27.*F-2.*D*D*D)/27.
IF(G**3./27.+H*H/4..LE.0.) GO TO 10
S=-H/2.+SQRT(G**3./27.+H*H/4.)
TT=-H/2.-SQRT(G**3./27.+H*H/4.)
IF(S)5,6,6
5 S=-((-S)**(1./3.))
GO TO 7
6 S=(S)**(1./3.)
7 IF(TT)8,9,9
8 TT=-(-TT)**(1./3.)
GO TO 15
9 TT=(TT)**(1./3.)
C SINGLE REAL ROOT
15 V=S+TT-D/3.
GO TO 40
10 THETA = (ACOS(-.5*H/SQRT(-G**3/27.)))/3.
V1=2.*SQRT(-G/3.)*CJS(THETA)
V2=2.*SQRT(-G/3.)*CJS(THETA+2.0944)
V3=2.*SQRT(-G/3.)*CJS(THETA+4.1888)
IF(ID)20,30,30
C TAKE LARGEST V FOR VAPOR
20 V=AMAX1(V1,V2,V3)-D/3.
GO TO 40
C TAKE SMALLEST V FOR LIQUID
30 V=AMIN1(V1,V2,V3)-D/3.
40 Z=P*V/(R*T)
RETURN
END

```

C WICE.FOR

C DETERMINATION OF THE WATER CONTENTY IN THE VAPOUR
C PHASE IN EQUILIBRIUM WITH THE HYDRATE PHASE.
C

```

DIMENSION TR(10),PR(10),W(10),PC(10),AL(10),A(10),VC(10),
1YL(10),B(10),ALA(20,20),CG(20,20),Y(10),
3PHICOE(10),TC(10),PHI(10),CL(4,10),YY(10)
READ(4,10)NPT
DO 620 I=1,9
620 READ(02,10)TC(I),PC(I),VC(I),W(I)
CONTINUE
DO 2 I=1,NPT
READ(01,10)T,P,WEX
P=P/14.696
CALL LANG(T,CL)
YEX=WEX*2.105555*10.**(-5.)
DATA YY(2),YY(3),YY(4),YY(5)/1.,.0,.0,.0/
10 FORMAT(10G)
Y(1)=YEX
1 Y(2)=1.-Y(1)
CALL PENG(T,P,Y,PHICOE,PHI,TC,PC,VC,W)
650 FORMAT(1X,'CL',2(F10.5,X))
A1=ALOG(1.+CL(1,1)*PHI(2))*2./46.
A2=ALOG(1.+CL(2,1)*PHI(2))*6./46.
AMUTP=-(A1+A2)
VICE=(1.069989-.249933*10.**(-4.))*T+.371606*10.
1**(-6.)*T**2)*18
PICE=EXP(17.37039-5140.3148/T)
VHYD=VICE+3.
A1=3.*(P-PICE)/(82.056*T)
A2=-((332.*(1./T-1./273.15)))/1.987
A3=310./(1.987*T)
YW=(EXP(AMUTP+A1+A2+A3)*PICE)/(PHICOE(1)*P)
61 FORMAT(1X,F10.8)
S=YW-Y(1)
62 FORMAT(1X,3(F15.8,X))
IF(ABS(S).LT.1.*10.**(-7)) GO TO 20
Y(1)=YW
GO TO 1
20 WT=YW/(2.10555*10.**(-5.))
T=(T-273.15)*9./5.+32.
P=P*14.696
YEX=YEX*1000000.
YW=YW*1000000.
WRITE(07,30)T,P,YEX,YW
30 FORMAT(1X,F8.2,X,F7.2,X,2(F10.2,X))
YSUM=YEX-YW+YSUM
YASUM=ABS(YEX-YW)+YASUM
2 CONTINUE

```



```
YASUM=YASUM/NPT
YMN=YSUM/NPT
40 WRITE(07,40)YMN,YASUM
   FORMAT(1X,2(F15.2,X))
   STOP
   END
```

```

SUBROUTINE LANG(T,CL)
  DIMENSION A(4),Z(4),CB(4,10),KS(10),CL(4,10),
1X(20),WT(20),SIGP(10),EP(10),CP(10)
  SIGP(1)=3.2
  EP(1)=156.72
  CP(1)=.383359375
  CB(1,1)=20.
  CB(2,1)=20.
  CB(3,1)=20.
  CB(4,1)=20.
  NPT=10
  NP=5
  DATA(X(J),WT(J),J=6,10)/.1488743389,.29552422147,
1.4333953941,.2692667193,.6794095683,.2190
2863625,.86506336627,.1494513492,.9739065285,
3.0666713443/
  DATA (A(I),Z(I),I=1,4)/3.95,20.,4.3,24.,3.91,20.,4.73,
128./
  DATA PI,BK/3.1416,1.3804E-16/
  DO 22 J=1,NP
  X(J)=-X(NPT-J+1)
  WT(J)=WT(NPT-J+1)
22 CONTINUE

  KBLOW=0
  DO 5 J=1,1
  DO 1 I=1,4
1 CL(I,J)=.0
  C=CP(J)
  EK=EP(J)
  EC=EP(J)*BK
  RC=SIGP(J)*1.122462
  DO 5 I=1,4
  IF (CB(I,J).LT.1.) GO TO 5
  RCA=RC/A(I)
  CA=C/A(I)
C NEWTON RAPSON METHOD FOR FINDING LIMITS , YL
C FIRST GUESS S=.4
  S=.4
  RCA0=RCA**6
  RCA12=RCA**12
  DO 2 N=1,20
  IF (S.GT.1.0.OR.S.LE.0.0) GO TO 6
  UM=1./(1.-S-CA)
  UP=1./(1.+S-CA)
  UM5=UM**5
  UP5=UP**5
  DA4=UM5+UP5
  DA5=UM5*UM+UP5*UP
  DB6=DA4+CA*DA5
  UM11=UM**11

```

```

UP11=UP**11
DA10=UM11+UP11
DA11=UM11*UM+UP11*UP
DB12=DA10+CA*DA11
DB=RCA12*DB12-2.*RCA6*DB6
A10=UM11/UM-UP11/UP
A11=UM11-UP11
B12=(.1*A10+CA*A11/11.0)
A4=UM5/UM-UP5/UP
A5=UM5-UP5
B6=A4/4.+CA*A5/5.
B=RCA12*B12-2.*RCA6*B6
W=Z(I)*EK/(2.*S*T)*B
DWY=-W/S+Z(I)*EK*DB/(2.*S*T)
DS=S-(W-10.)/DWY
IF(ABS((DS-S)/DS).LT.0.01) GO TO 3
2  S=DS
3  YL=S
C  GAUSSIAN INTEGRATION
P=2.*PI*A(I)**3/(T*136.2)*YL
SQ=.0
DD 4  N=1,NPT
Y=YL*(X(N)+1.)/2.
UP=1./(1.+Y-CA)
UM=1./(1.-Y-CA)
UP5=UP**5
UM5=UM**5
A4=UM5/UM-UP5/UP
A5=UM5-UP5
B6=A4/4.+CA*A5/5.
UP11=UP**11
UM11=UM**11
A10=UM11/UM-UP11/UP
A11=UM11-UP11
B12=(.1*A10+CA*A11/11.)
B=RCA12*B12-2.*RCA6*B6
W=Z(I)*EK/(2.*Y*T)*B
4  SQ=SQ+EXP(-W)*Y**2*WT(N)
5  CL(I,J)=P*SQ
6  CONTINUE
7  RETURN
KBLW=2
WRITE(4,7)
FORMAT(1X,'PROBLEM BLOW UP')
RETURN
END

```

```

SUBROUTINE PENG(T,P,Y,PHICOE,PHI,TC,PC,VC,W)
DIMENSION TC(10),PC(10),W(10),B(10),PHI(10),VC(10),AK(10)
1,A(100,100),Y(10),TR(10),PR(10),PHICOE(10),CG(100,100)
DATA CG(1,7),CG(1,8),CG(1,9),CG(2,7),CG(2,8),CG(2,9),
1CG(3,7),CG(3,8),CG(3,9),CG(4,7),CG(4,8),CG(4,9),
2CG(5,7),CG(5,8),CG(5,9),CG(6,7),CG(6,8),CG(6,9),
3CG(7,8),CG(7,9),CG(8,9)/.036,.1,.085,.05,.13,.084,
4.08,.135,.075,.09,.13,.06,.095,.13,.05,.095,.125,.065,
5-.02,.18,.1/
NCOMP=9
DATA CG(1,2),CG(2,1)/.5,.5/
R=82.056
DO 97 I=1,NCOMP
DO 97 J=1,NCOMP
A(I,J)=.0
AM=.0
BM=.0
B(I)=.0
AK(I)=.0
TR(I)=.0
PR(I)=.0
PHI(I)=.0
97 CONTINUE
10 FORMAT(10G)
DO 1 I=1,NCOMP
TR(I)=T/TC(I)
IF(Y(I).EQ..0) GO TO 149
PR(I)=P/PC(I)
A(I,I)=.45724*(R*TC(I))**2/PC(I)
B(I)=.0778*R*TC(I)/PC(I)
103 FORMAT(1X,'1,A(I)',I2,X,F15.3)
AK(I)=.37464+1.54225*W(I)-.26992*W(I)**2
102 FORMAT(1X,'I,K',I2,X,F10.5)
AK(I)=(1.+AK(I)*(1.-SQRT(TR(I))))**2
A(I,I)=AK(I)*A(I,I)
30 FORMAT(1X,'TR,PR,A(I,I),B',5F13.4,X)
149 CONTINUE
1 CONTINUE
DO 2 I=1,NCOMP
DO 2 J=1,NCOMP
IF(Y(J).EQ..0) GO TO 145
IF(Y(I).EQ..0) GO TO 145
A(I,J)=(1.-CG(I,J))*SQRT(A(I,I)*A(J,J))
81 FORMAT(1X,2(I2,X),F15.5)
145 CONTINUE
2 CONTINUE
DO 4 I=1,NCOMP
IF(Y(I).LE..0) GO TO 41
41 CONTINUE
BM=BM+B(I)*Y(I)
4 CONTINUE

```

```

DO 75      I=1, NCOMP
AK(I)=.0
75 CONTINUE
DO 3 J=1, NCOMP
DO 3 I=1, NCOMP
IF(Y(I).EQ..0) GO TO 148
IF(Y(J).EQ..0) GO TO 148
AK(J)=Y(I)*A(I,J)+AK(J)
148 CONTINUE
3 CONTINUE
DO 6 J=1, NCOMP
AK(J)=2.*AK(J)
85 FORMAT(1X, F15.4)
6 CONTINUE
DO 5 I=1, NCOMP
DO 5 J=1, NCOMP
AM=AM+Y(I)*Y(J)*A(I,J)
5 CONTINUE
40 FORMAT(1X, 2F15.5, X)
CALL VCUBE(AM, BM, P, R, T, V, Z, ID)
83 FORMAT(1X, 'Z', F10.5)
AB=AM*P/(R*T)**2
BB=BM*P/(R*T)
DO 62      I=1, NCOMP
IF(Y(I).EQ..0) GO TO 61
A1=B(I)*(Z-1.)/BM
A2=ALOG(Z-BB)
A3=AB/(2*SQRT(2.)*BB)
86 FORMAT(1X, 4(F15.3, X))
A4=AK(I)/AM-B(I)/BM
A5=ALOG((Z+2.414*BB)/(Z-.414*BB))
34 FORMAT(1X, 4(F10.4, X))
PHI(I)=A1-A2-A3*A4*A5
PHICOE(I)=EXP(PHI(I))
PHI(I)=PHICOE(I)*Y(I)*P
61 CONTINUE
62 CONTINUE
RETURN
END

```

```

SUBROUTINE VCUBE(A,B,P,R,T,V,Z,LD)
D=B-R*T/P
E=-(3.*B*B+2.*R*T*B/P-A/P)
F=B*B*B+(R*T*B*B-A*B)/P
G=(3.*E-D*D)/3.
H=-(9.*D*E-27.*F-2.*D*D*D)/27.
IF(G**3./27.+H*H/4..LE.0.) GO TO 10
S=-H/2.+SQRT(G**3./27.+H*H/4.)
TT=-H/2.-SQRT(G**3./27.+H*H/4.)
IF(S)5,6,6
5 S=-((-S)**(1./3.))
GO TO 7
6 S=(S)**(1./3.)
7 IF(TT)8,9,9
8 TT=-(-TT)**(1./3.)
GO TO 15
9 TT=(TT)**(1./3.)
C SINGLE REAL ROOT
15 V=S+TT-D/3.
GO TO 40
10 THETA = (ACOS(-.5*H/SQRT(-G**3/27.)))/3.
V1=2.*SQRT(-G/3.)*COS(THETA)
V2=2.*SQRT(-G/3.)*CJS(THETA+2.0944)
V3=2.*SQRT(-G/3.)*CJS(THETA+4.1888)
IF(ID)20,30,30
C TAKE LARGEST V FOR VAPOR
20 V=AMAX1(V1,V2,V3)-D/3.
GO TO 40
C TAKE SMALLEST V FOR LIQUID
30 V=AMIN1(V1,V2,V3)-D/3.
40 Z=P*V/(R*T)
RETURN
END

```